THE ASTROPHYSICAL JOURNAL

AN INTERNATIONAL REVIEW OF SPECTROSCOPY AND ASTRONOMICAL PHYSICS

VOLUME 87 APRIL 1938 NUMBER 3

THE TOTAL LIGHT AND COLOR OF THE SOLAR CORONA OF JUNE 8, 1937

JOEL STEBBINS AND A. E. WHITFORD

ABSTRACT

The total light of the corona was measured with a photoelectric cell and portable amplifier at Cerro de Pasco, Peru, altitude 14,500 feet. The corona was referred to a set of standard lamps, which were later compared with the full moon. The atmospheric extinction for altitude 5°40′ at mid-totality was determined by measures of the sun on the same day before and after the eclipse. The ratio of corona to full moon was 0.47, in good agreement with determinations at previous eclipses. There is no evidence of a large variation of the light of the corona in different years.

The color of the corona was found to be the same as that of the sun. Since there is no Rayleigh scattering, the light must come either from electrons or from particles too large to produce such scattering.

The eclipse of June 8, 1937, did not promise much for observations from the end of the track on the west coast of South America. In the mountains of Peru the altitude of the setting sun was about 5°, and an air mass of nearly ten times that at the zenith would make the extinction so large that only rough photometric results could be expected. Nevertheless, as Mr. Stebbins had in mind a personal trip to Peru, he decided to take along a simple photometer and repeat the photoelectric measures of the corona made by Kunz and Stebbins[1] at the eclipses of 1918 and 1925. The incidental nature of the proposed observations was gradually forgotten in the course of the preparations, and every advance precaution was taken to get as good a set of measures as possible.

At the previous eclipses a photoelectric cell was mounted at the lower end of a blank tube 4 feet long and 4 inches in diameter, with a

[1] *Ap. J.*, **49**, 137, 1919; **62**, 114, 1925.

diaphragm at the upper end giving a clear field of 3° about the sun. Exposure to the corona gave a deflection from a sensitive galvanometer. This time, by using an amplifier, the galvanometer and its necessary solid support were eliminated, and the apparatus was much more compact. As the amplifying tube cost about a dollar, and the other commercial parts were in proportion, we give some details of the outfit, which makes a useful laboratory instrument.

All the parts of the photometer, excepting the meter but including the batteries, were contained in a light-tight sheet-steel box 10 × 10 × 7 inches (see Pl. VI). The light of the corona was re-

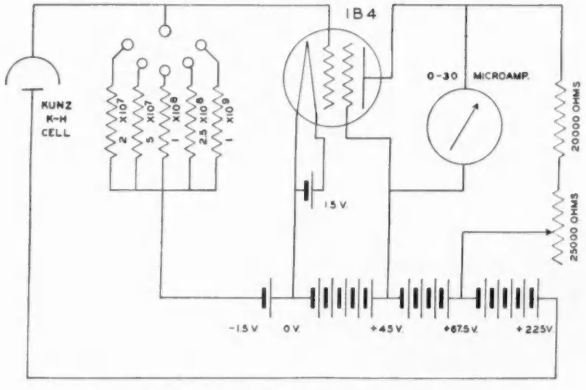

FIG. 1.—Diagram of circuit for amplifier

ceived by an achromatic lens of 20 mm aperture and 180 mm focal length. The field of view was limited to 3° by a diaphragm of 10 mm in the focal plane, and the sensitive cathode of the photocell was about 60 mm beyond this plane. A Kunz potassium hydride cell in a pyrex bulb was used. For measuring colors, a yellow and a blue filter could be swung over the objective by means of a turrethead mounted on the front of the photometer box. The spectral sensitivity of the cell and filters closely approximates that given for the photometer used in measuring the colors of the globular clusters.[2] The current from the photocell was amplified by a Sylvania 1B4 tube, and the output was read on a small microammeter.

A conventional direct-current amplifier circuit was used, with the connections as shown in Figure 1. The 1B4 tube was chosen because

[2] *Mt. Wilson Contr.*, No. 547; *Ap. J.*, **84**, 132, 1936.

PLATE VI

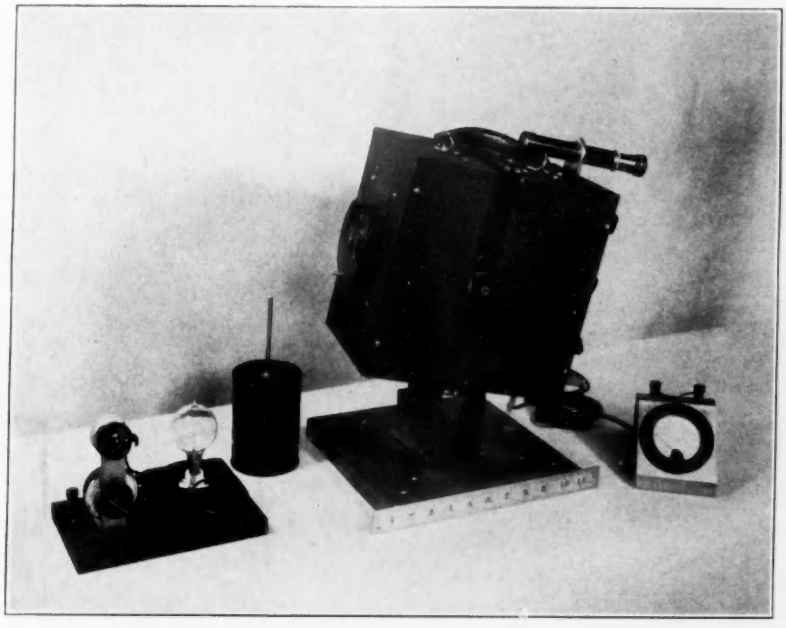

PORTABLE ECLIPSE PHOTOMETER

UNIV. OF MICH.

of its low filament-power requirements and its low grid current. The filament was run by a single No. 6 dry battery. With 45 volts on plate and screen, the grid current was less than 10^{-10} ampere, and the input resistance was greater than 10^{11} ohms. The normal plate current was 0.7 miliampere, and the mutual conductance was 420 microamperes per volt. The sensitivity was varied by changing the grid resistor. With the highest resistance, 10^9 ohms, in the circuit, one division on the meter, or 0.5 microampere, corresponded to a photocurrent of 1.2×10^{-12} ampere, a current amplification of 400,000. The meter needle was very steady.

For measures of the sun we used a "reducer" which was essentially a compound microscope with a 4-mm objective and a 6-mm eyepiece separated by 10 cm. When this combination was pointed at the sun, the effective aperture was limited by the diaphragm in front of the photocell. The reduction made the sun's light about equal to that of the full moon. The filters could be used either with the reducer or with the 20-mm objective.

The photometer was furnished with a simple altazimuth mounting constructed by Mr. E. J. Bernet. By stops in the azimuth motion the instrument could be turned just 6° for alternate pointings at the sun and at the sky during totality.

The entire outfit, assembled and tested by Whitford, weighed about forty pounds, and was taken as hand luggage by Stebbins to Peru and return. Inasmuch as, after the preparations in Madison, Wisconsin, the expedition was contracted to one observer and a suitcase, the account may be shifted to the first person singular.

The site at Cerro de Pasco was selected in advance by my son-in-law, Mr. Theodore A. Dodge, who interested officials of the Cerro de Pasco Copper Corporation in our plans. In fact, this company, through their local superintendent, Mr. R. C. Philpott, simply took charge of the general arrangements for the eclipse. They provided a portable house, which was shared with the party from the Hayden Planetarium, Mr. W. H. Barton in charge, and together we were glad of the forethought which gave us comfortable shelter during the preparations in the cold mountain air. The station was on a knoll about two miles from the town, conveniently reached by motor car to the very door. The position was 10°41′ S, 76°15′ W, altitude

14,500 feet. Toward the west was a rolling plain leading to the main crest of the Andes some forty or fifty miles away. From our elevation, peaks of 17,000–20,000 feet were only a degree or so above the true horizon, and none was near the sun's altitude of 5°40′ at mid-totality.

With the house available, a window toward the west which could be left open or closed, and the photometer mounted on a plank for an optical bench, I was ready for the eclipse a few hours after arrival at the station. I had planned to measure the atmospheric extinction by observations of the setting sun on the two days before the eclipse, but this was a vain hope. Whether this was the favorable or unfavorable season in Peru, it could not have been much worse for the advance prospects. The sky had been almost continually cloudy for two weeks, and snow was falling on the afternoon of the day before the eclipse. At dawn of eclipse day a heavy frost had formed and a fog hung over Cerro, signs of a change in the weather, according to the local people.

During the morning the clouds were gradually dissipating; and by noon there were stretches of beautiful blue sky overhead, which, as they drifted westward, gave promise of a clear sky by sunset. About two o'clock there were many clear spaces, and the sun was measured for total light and color all afternoon, with increasingly favorable conditions. By an hour before totality, at 5:20 local time. the sky near the sun was practically cloudless, and remained so until 5:35, when the sun dipped into a line of clouds which had persisted over the Andes.

The measures with the sun-reducer during the period of several hours when the air mass increased from 2.0 to 18 gave an excellent determination of the extinction for air mass 9.5 at totality. The sky looked equal to the best I have ever seen. The measured light of the partial phase was, of course, reduced to the full sun.

During totality Mr. Dodge kept the photometer pointed first at the sun and then at the sky 6° distant, while I operated the shutter and filters and read the microammeter. The steps of sensitivity, Nos. 7, 8, and 9, were in the approximate ratios 1:2.5:10, and from previous results my guess was that No. 8 would be the proper choice. I was prepared for the corona to be ten times fainter or one hundred

times brighter than the estimate. After the last Bailey's bead had gone, I opened the shutter slowly for No. 7, and then shifted to No. 8; the deflection of 10.5 divisions was so near the advance estimate that I forgot that there had been any doubt about it. The readings were begun at about 10 seconds after second contact and were continued until we heard the count of 120 from the Hayden party. By that time I had all the measures needed, and I devoted the remaining 25 seconds to a general view of the corona in its spectacular setting above the clouds and distant mountains.

It turned out that within the interval of 110 seconds I had taken 26 individual scale readings for the zeros and deflections for light and color of the corona and sky. During the measures I felt that I was spending most of the time in making sure of the whole divisions on the scale. In fact, this matter of avoiding a mistake in a whole division was a veritable obsession, since, with everything else working mechanically, that was the only thing left to think about. It is here that photographic recording would be advantageous; and another time I would arrange to photograph the meter, as well as to read it visually. The reading of a scale during totality seems easy enough at the time; but when it is over, one finds himself in such a state of concentration that he cannot recover in time to appreciate the corona.

As the Hefner lamp, used at previous eclipses, would have been useless with the barometer reading 16 inches, the corona was referred to a set of four pyrometer lamps, which were intercompared before and after totality. Then the amplifier was brought back safely to Mount Wilson and set up on the night of July 22 for measures of the full moon. It could not have been foreseen that the standard lamps would turn out to be superfluous. The scale deflection for a lamp at fixed voltage and standard distance had changed only 1 per cent in the six weeks after the eclipse. We could have exposed the cell to the corona and then six weeks later to the full moon, and the ratio of the deflections would have been within 1 per cent of what we obtained by way of the standard lamps.

The transparency was apparently below average during the night on Mount Wilson; but we felt that the measures of the moon over several hours, from rising at dusk up to altitude 38°, gave a better

value than anything obtainable for the corona in the two minutes of totality. But after all, the important item was the correction for extinction in Peru. We return to the observations in detail.

In Table 1 are the measures of the sun and corona on eclipse day. Each measure comprises two deflections before and during totality, but only one deflection after totality, when the air mass was changing rapidly. In column 1 is given the Greenwich Civil Time; in

TABLE 1

MEASURES OF SUN, JUNE 8, 1937

G.C.T. (1)	z (2)	$F(z)$ (3)	Observed log d (4)	Reduction to Full Sun (5)	Corrected log d (6)	Color Index (7)	Remarks
19^h23^m5...	48°0	1.49	1.678	.....	1.678	−0.14	
19 30.2...	49.1	1.53	1.690	.....	1.690	− .12	
19 35.8...	50.2	1.56	1.690	.....	1.690	− .14	
20 56.8...	66.5	2.50	1.533	.....	1.533	− .08	
20 59.8...	66.8	2.53	1.548	.....	1.548	− .10	
21 15.0...	70.0	2.90	1.526	.....	1.526	− .05	
21 43.5...	76.1	4.10	1.347	0.155	1.502	.00	
21 46.0...	76.6	4.25	1.278	0.190	1.468	− .06	
21 50.8...	77.6	4.61	1.161	0.269	1.430	.00	
21 56.0...	78.8	5.04	1.069	0.365	1.434	+ .02	
22 4.2...	80.6	5.90	0.785	0.612	1.397	+ .07	
22 19.8...	84.22	9.18	0.931	.....	0.931	+ .17	Corona
22 20.8...	84.44	9.51	0.895	.....	0.895	+ .10	
22 28.8...	86.39	13.4	9.762	1.022	0.784	+ .31	
22 29.2...	86.48	13.7	9.883	0.983	0.866	+ .30	
22 30.2...	86.72	14.4	9.889	0.910	0.799	+ .28	
22 31.3...	86.94	15.1	9.908	0.845	0.753	+ .34	
22 33.0...	87.31	16.6	9.987	0.752	0.739	+ .40	
22 34.3...	87.58	17.7	9.955	0.690	0.645	+0.40	

column 2, the true zenith distance z of the sun or of the centroid of the apparent crescent. The air mass $F(z)$ in column 3 was taken from Bemporad's table.[3] The log deflection in column 4 has been reduced to the sensitivity of step No. 8 by the addition of +0.456 to each of the first seven values and −0.636 to each of the last six. These constants were determined from measurements on a standard lamp.

The reduction of the deflection from partial to full sun in column 5 was determined graphically. On a circle of 10 cm radius for the sun were marked on ten concentric rings, of mid-radii r, the relative

[3] *Handbuch der Astrophysik*, 2, No. 1, 268.

values of the intensity I on the solar disk given by Abbot[4] for 4500 A. Other circles of radius 10.57 cm for the moon were then drawn in the computed positions, at intervals of ten minutes before and of five minutes after totality. The relative lights from the unobscured portions of the rings were then added and the log reduction to full sun was determined and tabulated. This correction was then interpolated for the proper time, and the value in column 5 of Table 1 was added to log d in column 4 to get the corrected log d in column 6. The color index in column 7 was measured according to our custom-

TABLE 2

MEASURES OF CORONA, JUNE 8, 1937

	R	d	Sky	Corona	R	d	Sky	Corona	R	d	Sky	Corona
Dark	5	.....	.....	.....	5	.....	.....	.....	5	.....	.....	.....
Clear	15.5	10.5	1.5	9.0	14.5	9.5	1.4	8.1	6.2	1.2	1.2	.....
Yellow	11	6.0	0.5	5.5	10.5	5.5	0.47	5.03	.....	.....	.....	.....
Blue	9.5	4.5	0.5	4.0	10.5	5.5	0.47	5.03	.....	.....	.....	.....
Dark	5	.....	.....	.....	5	.....	.....	.....	5	.....	.....	.....
Dark	5	.....	.....	.....	5	.....	.....	.....	5	.....	.....	.....
Clear	6.5	1.5	1.5	.....	14.2	9.2	1.3	7.9	14	9.0	1.2	7.8
Yellow	5.5	0.5	0.5	.....	10.6	5.6	0.43	5.17	10.5	5.5	0.4	5.1
Blue	5.5	0.5	0.5	.....	10.2	5.2	0.43	4.77	10	5.0	0.4	4.6
Dark	5	.....	.....	.....	5	.....	.....	.....	5	.....	.....	.....

ary procedure for stars. The exposures were in the order: dark, clear, yellow, blue, dark, and gave the ratio of yellow to blue, with a check by the clear. This ratio was reduced to magnitude and is on the same scale as our color system C_2, but the zero point is arbitrary for the eclipse installation.

In Table 2 are the readings during totality. The order of the sets, reading down in each column, was: corona, sky, corona twice, sky, and corona. For each set the first column gives the scale reading R and the second column the resulting deflection d for corona plus sky. The zero reading at 5 did not shift perceptibly during the measures. The third column gives the adopted deflection for the sky, which, subtracted from the deflection for corona plus sky, gives the net

[4] *The Sun*, p. 107.

value for the corona in the last column. From these measures the means for the corona in Table 1 were derived, and from the residuals probable errors for the mean results of ± 1 per cent in d and $\pm 0^m.05$ in the color index.

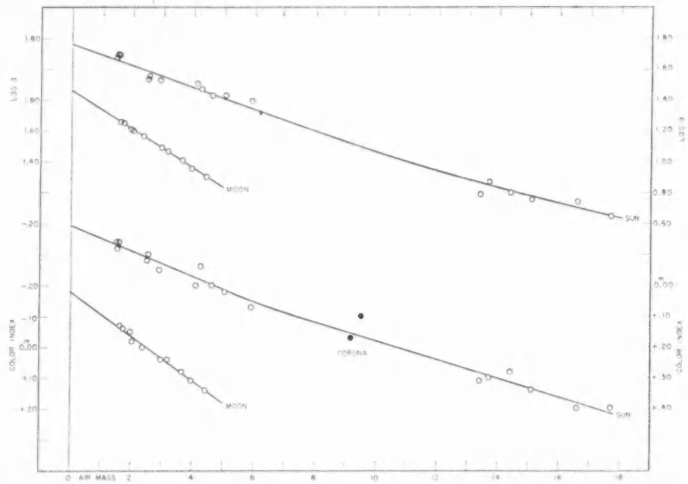

FIG. 2.—Observed total light and color of sun, corona, and moon, for different air masses.

The correction for extinction for the corona is derived from the measures of the sun in Figure 2. From the curve is read the log reduction to no atmosphere, which is applied as follows,

Air mass, $F(z)$	9.18	9.51
Extinction	0.640	0.664
Log d, observed	0.931	0.895
Log d, no atmosphere	1.571	1.559
Mean	1.565	
Reduction to mean distance	0.013	
Corona, log d_o	1.578	

Similarly for the color index we have,

Corona, observed	$+0^m.135$
Sun from curve	+ .162
Corona *minus* Sun	− .027
Sun, no atmosphere	− .194
Corona, no atmosphere	−0.22

The corona was found to be of the same color as the sun within the probable error of the determination.

The observations of the moon on Mount Wilson are given in Table 3. Again each measure is the mean of two deflections. The air mass was taken from Bemporad's table, and the reduction to no

TABLE 3

MEASURES OF THE MOON, JULY 23, 1937

G.C.T.	z	$F(z)$	log d	Color Index
3^h42^m	77.2	4.42	1.305	$+0^m14$
3 51	75.6	3.96	1.356	+ .11
4 0	74.2	3.64	1.406	+ .08
4 16	71.8	3.17	1.464	+ .04
4 25	70.4	2.96	1.489	+ .04
5 0	65.2	2.37	1.564	.00
5 36	60.5	2.02	1.600	− .02
5 45	59.5	1.97	1.610	− .05
7 46	52.1	1.62	1.658	− .07
8 59	54.7	1.73	1.649	−0.06

atmosphere is found from Figure 2. The reduction to standard conditions is as follows:

Moon, log d, no atmosphere	1.862
Reduction to mean distance of moon and sun	+0.037
Correction for lamp comparison	+0.005
Moon, log d_0	1.904
Corona, log d_0	1.578
Log (Corona/Moon)	9.674
Corona/Moon	0.47

The ratio of the corona to the full moon as measured with a photoelectric cell at this and two previous eclipses was, then,

1918 June 8	0.50
1925 January 24	.44
1937 June 8	0.47

The coronas of 1918 and 1925 were referred to the moon at 3° from the antisolar point; in 1937 the moon was 4° from the same. At opposition the moon may be as much as 5° from strictly full, and about 1°.5 is as close to full as it can get without touching the earth's shadow. The variation of the moon's light at these phases has never been well determined; but the difference between 3° and 4° is probably not more than 1 or 2 per cent, and it may be less. Of more importance is the amount of the bright inner corona obscured by the

moon at different eclipses, and on this account the close agreement of the results at the three eclipses is accidental.

If we assume Becker's law for the variation of the intensity of the corona along the radius,

$$J = \frac{A_1}{(r - 0.720)^4},$$

then from a previous paper[5] the total light for the moon's radius, $r = 1.057$ in 1937, can be reduced to $r = 1.024$ in 1918 by dividing by 0.79. Hence 0.47/0.79 = 0.60 moon in 1937 is comparable with 0.50 in 1918. We do not consider the difference to be significant.

The transparency of the atmosphere on eclipse day in Peru is shown by the curves in Figure 2. At moderate zenith distances the extinction is represented by $0^m176\ F(z)$ as against $0^m316\ F(z)$ for the night at Mount Wilson. Similarly, the differential extinction for the filters was $0^m042\ F(z)$ as against $0^m072\ F(z)$. The effect of the air at 14,500 feet was only six-tenths that at 5700 though the transparency at Mount Wilson was apparently below normal on the night in question. At the three eclipses the actual corrections applied to the observed total lights of the corona and moon to reduce them to no atmosphere were, expressed in magnitude:

	Corona	Moon
1918	0^m60	0^m95
1925	1.30	.....
1937	1.63	0.54

Despite the low altitude in 1937 the extinction was probably better determined than at the previous eclipses, and the value for the light of the corona is probably the best of the three.

It is sufficient to call the corona about half as bright as the full moon; and from the measures here presented, there is no evidence of a variation over the years. We have seen popular accounts of results making the corona much brighter—as much as fifty times as bright as the full moon at the Siberian eclipse of 1936—but until

[5] *Ap. J.*, **62**, 123, 1925.

these observations are published in detail, it is useless to attempt to account for the discrepancy. The mean of all determinations of the total light of the corona, listed by Dyson and Woolley,[6] is about half of that of the full moon, with no discordance greater than by a factor of 2. In deciding upon the reliability of any determination of the light of corona in terms of the full moon, it is well to examine whether (1) the effect of the sky background has been eliminated, (2) the atmospheric extinction has been allowed for, and (3) the moon has been actually measured in the same fashion as the corona. In some published results the sky has been included, the extinction has been ignored, and the light of the moon has been taken from a book.

It may be noted that whether an eclipse is a "bright" or a "dark" one has little to do with the intensity of the corona, since most of the general illumination comes from the sky. In Peru a 3° circle of the sky gave one-sixth as much light as the corona. Hence, a 7° or 8° circle would equal the corona, and it is the whole hemisphere of the sky that determines the illumination of the landscape. The brightness of the sky at the three eclipses can be determined from the readings during totality. Reducing the areas to a circle $\frac{1}{2}$° in diameter, and taking as unit the light of the full moon with no atmosphere, the values are:

1918	0.0020
1925	.0034
1937	0.0019

The sky was measured 8° from the sun in the first two and 6° in the last. The eclipse of 1925 was known as a bright one, and our measures of all three are reasonably consistent.

The color index of the full moon from Figure 2, reduced to no atmosphere, is $-0^m.18$ on our scale. We have, then, for the three color indices:

Sun	$-0^m.19$
Corona	.22
Moon	−0.18

The sun was measured through the lenses of the reducer, but the corona and moon were taken with the same 20-mm objective. The

[6] *Eclipses of the Sun and Moon*, p. 125.

difference in the absorption by the glass in the two cases was undoubtedly small; and we can call the sun, moon, and corona all the same color, within the error of measurement.

The photoelectric measures should have detected any Rayleigh scattering in the corona, as the instrument is very sensitive to the blue color of the sky. In our regular observations with the reflectors at Mount Wilson we are continually measuring the intensity and color of the sky background for the corrections to be applied to measures of stars or nebulae taken with large focal diaphragms. When the crescent moon is above the horizon, the sky is always bluer than when the moon is down.

Our measures of the corona confirm the previous results of Ludendorff[7] and of Grotian[8] that the corona is essentially the same color as the sun. Therefore the continuous and the Fraunhofer spectrum can be produced by electrons or by large dust particles, but not by atoms, molecules, or other particles of the size that would produce Rayleigh scattering. Any satisfactory theory of the nature of the corona must take into account the fact that over a considerable range of wave lengths the intensity distributions for the sun and the corona are the same.

The conclusions from the present work are that the total light of the corona is about half that of the full moon, there is no great variation in this light over the years, and the corona is of very nearly the same color as the sun.

We are much indebted to officials of the Cerro de Pasco Copper Corporation, particularly to Mr. R. C. Philpott and Mr. John Moses, for assistance and hospitality during the stay in Cerro. We also thank the trustees of the Watson and Draper funds of the National Academy of Sciences for grants in support of previous expeditions, from which the present work has naturally followed.

Washburn Observatory
University of Wisconsin
November 1937

[7] *Sitzungsber. d. Preuss. Akad. d. Wiss.*, **5**, 83, 1925.

[8] *Zs. f. Ap.*, **2**, 199, 1931.

THE MAGNITUDES OF THE THIRTY BRIGHTEST STARS IN THE NORTH POLAR SEQUENCE*

JOEL STEBBINS[1] AND A. E. WHITFORD

ABSTRACT

The magnitudes and colors of stars of the North Polar Sequence down to magnitude 11.6 have been measured with a photoelectric cell attached to the 60-inch reflector.

The measured colors of these stars are in good agreement with the colors of the international system, and confirm the result of Seares that the polar region is one of moderate obscuration and selective absorption.

Special treatment is given to the known variable Polaris; the phase and amplitude of the light-variation of this star agree well with the prediction from recent photoelectric measures by Meyer.

The photoelectric magnitudes have the usual small accidental errors, and the scale has been tested over the range from magnitude 2.5 to 11.6. Laboratory measures of an artificial star, observations of stars with a neutral-shade glass, observations of the stars down to magnitude 9.2 with the 15-inch telescope at Madison, and independent measures of 13 stars with an ultraviolet cell on the 60-inch, all agree in giving the same scale of magnitudes.

There are serious differences between the photoelectric and the international photographic magnitudes, especially from the fifth to the ninth magnitude, where the two systems diverge by nearly 0.20 mag. The possibility that this divergence is due to strong hydrogen absorption is discussed by Seares in *Mt. W. Contr.*, No. 587.

Formulae are given for the reduction of photoelectric or photographic magnitudes to our suggested revision of the international scale.

In a study of the brightness and color of extragalactic nebulae with the photoelectric photometer, our scale of magnitudes has been based upon the Harvard visual system. Owing to the time consumed in picking up and identifying faint objects with the large reflectors, the comparison stars selected for the nebulae are usually of the sixth or seventh magnitude, those which have been observed photometrically at Harvard. The photoelectric scale can be carried down to magnitude 12 or 13, presumably without introducing additional errors larger than already exist in the visual magnitudes. It has seemed advisable, however, to check our photoelectric magnitudes with the photographic magnitudes of the North Polar Sequence, so that the magnitudes of the nebulae can be reduced to the international scale.

* *Contributions from the Mount Wilson Observatory, Carnegie Institution of Washington*, No. 586.

[1] Research Associate of the Mount Wilson Observatory, Carnegie Institution of Washington.

Accordingly, several groups of our standard stars were compared with a few polar stars; and, after this start had been made, on the suggestion of Dr. F. H. Seares, we decided to reobserve with the photocell all the stars of the North Polar Sequence bright enough to be measured easily and accurately with the amplifier in its present form. Since the 100-inch reflector cannot be pointed at the pole, the observations were made with the 60-inch. The program included the 30 stars down to No. 16, which is of magnitude 11.6, photographic. For stars much fainter than this the errors increase until the photocell has no special advantage over the photographic plate. By a laborious procedure involving photographic registration of the galvanometer deflections we have carried photoelectric standards in some Selected Areas down to magnitude 16.0, with the internal probable error of an observation less than ± 0.1 mag. When sixteenth magnitude with the 100-inch and fifteenth magnitude with the 60-inch are possible limits, the stars brighter than twelfth magnitude are all relatively easy to observe. In fact, with the amplifier working properly, the precision for bright stars is set not by the instrument but by the quality of the sky.

In work on variable stars with the photocell it is usually possible to find comparison stars of nearly the same brightness; if not, the objects can be equalized by means of shade glasses, rotating sectors, or different apertures, and the scale of brightness need be correct over only a magnitude or so. For the Polar Sequence, however, we have a range of nine magnitudes in the stars observed, from 2.5 to 11.6, and the problem is obviously to get the correct scale rather than to make the accidental errors very small. The order of presentation here will follow somewhat the way in which the work was done. The photoelectric observations were made, and the preliminary magnitudes were compared with the international photographic magnitudes of the same stars. When discrepancies were found between the two scales of magnitude, we made a serious effort to check our scale by several independent tests.

The installation on the 60-inch is the same that we have used at Mount Wilson for the past several years.[2] The potassium hydride cell by Kunz, our number QK 31-2, has a color sensitivity giving

[2] Stebbins and Whitford, *Mt. W. Contr.*, No. 547; *Ap. J.*, **84**, 132, 1936.

magnitudes as near the standard photographic scale as do many combinations of photographic telescopes and plates. The cell and amplifying tube are mounted in a brass tank at the Newtonian focus; one observer operates the photometer while the other reads the galvanometer mounted below in the clock room at the junction of the main pier and the iron column of the mounting. With the night assistant making the settings we have three men carrying on the measures; but much time is still spent in mere manipulation of the telescope. After a star has been picked up and centered in the guiding eyepiece, its total light and color can be measured in 5 minutes or less, but 5–10 minutes more are required to set on the next star. Four or five stars per hour is a good rate; and because of their large range in right ascension, the polar stars do not go faster than other stars in limited regions of the sky. Compensating for the slow operation is the advantage that one or two readings with the amplifier give results correct to the hundredth of a magnitude. If the sky holds good, the resulting magnitudes should be of this order of precision. Fortunately, at Mount Wilson we can turn to a check star about once an hour and assume that conditions have remained the same during the interval.

The observations with the 60-inch are in Table 1. The zero point of the photoelectric magnitudes was chosen temporarily from a group of southern stars; it can be changed later to conform with the international system.

The color index C_2 for each star was measured with a pair of blue and yellow filters, the same as used on the nebulae and globular clusters.[2] The color equation Ao − Ko is 0.44 mag.; for the B stars, which are nearly all brighter than tenth magnitude, the heavier filters in our system C_1 give Ao − Ko = 0.74 mag.

The probable errors of one observation shown in Table 2 have been computed from the residuals. The errors increase for the fainter stars, but the probable error of the mean of two observations is still less than 0.01 mag. Since the color measures with the filters were made differentially at intervals of 20 seconds, while the stars were taken 10 or 15 minutes apart, we should expect the colors to agree better than the magnitudes; but the errors run about the same. The internal probable error of an observed color computed

TABLE 1

PHOTOELECTRIC OBSERVATIONS OF THE NORTH POLAR SEQUENCE

NPS	Mag.	Residuals in $0^m.01$								Color Index C_2	Residuals in $0^m.01$					
		(1)	(2)	(3)	(4)	(5)	(6)	(7)	(8)		(1)	(2)	(3)	(4)	(5)	(6)
1S	2.51	...	...	...	...	...	...	...	...	$+0^m.01$	...	...	*1*	1	...	*1*
1	4.39	...	...	...	*2*	0	*1*	*2*	...	− .20	...	...	...	1	*1*	...
2	5.23	...	...	...	*1*	1	1	...	...	− .24	...	...	...	*1*	0	...
3	5.75	0	*2*	0	*2*	...	1	...	...	− .17	0	*2*	1	..	...	...
4	5.96	...	...	1	*1*	...	0	0	...	− .15	...	...	*1*	2	...	...
5	6.53	0	*1*	0	0	...	0	...	0	− .19	*2*	*3*	1	3	...	...
2S	6.57	...	...	*1*	1	...	1	...	...	− .13	...	...	1	*1*	...	...
3S	6.71	...	...	3	0	...	*2*	...	...	− .10	...	...	0	0	...	...
1r	6.45	1	2	...	*2*	...	...	*2*	...	+ .38	0	*1*	...	1	...	...
6	7.22	...	...	...	0	0	...	...	...	− .18	...	...	...	*1*	0	...
7	7.52	...	...	*1*	0	...	...	...	...	− .25	...	...	0	0	...	...
2r	7.73	2	...	*2*	...	...	...	1	...	+ .36	*1*	...	1	...	...	...
8	8.41	*1*	...	0	1	...	...	0	...	− .11	0	...	1	0	...	...
9	9.07	...	...	...	2	(6)	...	*1*	*1*	− .13	...	...	...	0	1	...
3r	8.74	...	...	0	*1*	...	...	...	...	+ .34	...	...	0	0	...	...
10	9.25	0	1	...	*1*	...	...	...	...	− .15	2	...	...	*1*	...	...
4r	9.13	...	...	*1*	...	...	1	...	...	+ .20	...	...	*1*	...	1	*1*
11	9.86	...	...	0	*1*	...	...	...	...	− .14	...	...	1	*1*	...	...
12	10.12	...	...	0	0	...	...	...	...	− .07	...	...	*2*	1	...	...
5r	9.99	...	...	*1*	1	...	...	...	...	+ .39	...	...	0	0	...	...
4S	10.32	...	...	...	1	...	*1*	...	...	− .03	...	...	...	*1*	0	0
13	10.59	...	...	2	...	0	...	*1*	...	− .16	...	...	*2*	...	2	...
6r	10.36	...	...	...	*1*	...	2	...	...	+ .27	...	...	...	1	*1*	*1*
14	10.90	*3*	2	1	0	...	...	...	...	− .09	1	...	*2*	1	...	...
7r	10.84	...	...	1	...	0	...	...	...	+ .21	...	...	0	...	1	...
5S	10.94	...	...	2	*2*	...	*1*	...	...	+ .20	...	...	1	*3*	...	1
15	11.30	...	...	...	1	...	*2*	...	...	− .09	...	...	...	*2*	*2*	*1*
6S	11.35	...	...	0	2	...	*2*	...	...	+ .07	...	...	*3*	*4*	...	0
8r	11.34	...	...	0	...	*1*	...	...	...	+ .14	...	...	0	...	0	...
16	11.60	*2*	...	1	...	...	...	...	...	−0.12	...	...	2	...	*2*	...

NOTES ON TABLE 1

Dates: 1935, (1) September 3, (2) September 4; 1936, (3) June 23, (4) June 24, (5) July 22, (6) August 20, (7) September 9, (8) September 10.

First 8 stars taken with reduced voltage on date (6).

No. 1S, see special discussion of Polaris.

No. 9, measure known to be defective on date (5).

from the residuals from the first 10 stars brighter than seventh magnitude on a certain night was ±0.0017 mag.; whereas the external probable error derived from a comparison of the colors of the same stars on different nights was ±0.011 mag., an increase of more than sixfold. We are inclined to think that the differences from night to night are probably due to variations in the sky, but we have found no well-established case of a noticeable systematic deviation of all the stars on a single night.

Since the correctness of the scale of the photoelectric magnitudes depends upon the linearity of response of both the photocell and the amplifying tube, we have made various tests to be sure that no avoidable error has been introduced. First of all, the scale of the

TABLE 2

Magnitudes	Probable Error of One Observation		No. of Stars
	Magnitude	Color	
2.51– 7.22	±0^{m}009	±0^{m}011	9, 10
7.52–10.12	.009	.008	10
10.32–11.60	±0.014	±0.014	10

galvanometer was tested at the beginning of each run with the telescope, and an orientation of the coil was found where the deflection for an applied voltage was constant at different parts of the scale to less than 1 per cent; the differential error between deflections from the same zero reading was much less. This precaution is necessary because, even with a good galvanometer, the magnetic field may be sufficiently nonuniform to cause variation in sensitivity of as much as 10 per cent from one end of the scale to the other.

Another source of error was the possibility that the sensitivity of the amplifier might change with different inclinations to the vertical or to the earth's magnetic field. Such an error would show up in varying magnitudes of the same star at different hour angles, an effect which, however, has not been noted. With measures on an artificial star, the tank containing cell and tube was rotated 90° and

180°, both vertically and horizontally; and no discordance as large as 1 per cent was found in any position.

The shunts for the galvanometer have the approximate values of 1/100, 1/10, and 1/3; full sensitivity was not used. The ratios of the successive steps were measured with probable errors of a few tenths of 1 per cent. Here, again, the check measures are easily made with a standard light or a fixed voltage.

With these ordinary precautions against systematic error out of the way, we could test the overall agreement of the magnitudes with a correct scale by laboratory measures of an artificial star. The photometric tank with cell and tube was set up on the ground floor of the 60-inch dome with cable connection to the galvanometer in its regular location in the clock room. In front of the cell was placed a lens of 1-inch aperture and focal ratio $f:5$ to simulate the beam of light from the large mirror. The image of an artificial star was centered in the same optical system as was used on the telescope, the extra-focal image covering the same area on the cell that was effective in the stellar observations. The artificial star was formed by a small controllable electric lamp in front of which was an opal glass and a small aperture which could be changed in size. The opal glass was quite necessary to insure that there would be no directional variations in intensity from the lamp. Measures of the star from different azimuths showed that the cross-section of the light beam from the star was effectively uniform, and that we could depend upon the simple law of the inverse square for the resulting intensity of the star at different distances.

The star at a definite brightness was measured at positions laid out to give intervals of exactly half a stellar magnitude. The distances ranged from 3.828 to 15.240 meters, measured from the principal plane of the 1-inch lens. This arrangement gave a variation of 3 mag. with the same light and aperture for the star. Distances less than 3.8 meters would have been feasible but would have required more care in their measurement.

In Table 3 are the laboratory tests on the artificial star. The first column gives for each run the approximate equivalent magnitudes on the stellar scale; the intervals computed from the law of inverse square are correct within one or two thousandths of a magnitude;

hence the difference between successive log deflections in the second column should be 0.200, and the last two figures should be the same for each deflection. The third column gives the residuals in the logarithms, which should be multiplied by 2.5 to get magnitudes.

TABLE 3

TEST OF SCALE BY LAW OF INVERSE SQUARE

Mag.	log d	Resid.	Mag.	log d	Resid.	Mag.	log d	Resid.	Mag.	log d	Resid.
2.8	2.366	−0.001	5.3	2.324	−0.001	7.5	2.406	+0.002	9.7	1.997	+0.001
3.3	2.167	.000	5.8	2.125	− .001	8.0	2.204	.000	10.2	1.791	− .006
3.8	1.967	.000	6.3	1.930	+ .003	8.5	2.003	− .002	10.7	1.605	+ .007
4.3	1.769	+ .001	6.8	1.730	+ .002	9.0	1.805	− .001	11.2	1.396	−0.003
4.8	1.568	.000	7.3	1.528	− .001	9.5	1.605	− .001	11.2	1.974	+0.003
5.3	1.371	+ .003	7.8	1.330	.000	10.0	1.407	.000	11.7	1.766	− .006
5.8	1.165	−0.003	8.3	1.130	−0.001	10.5	1.209	+0.002	12.2	1.577	+ .004
									12.7	1.373	−0.001
PE 1 obs. in log		±0.0011			±0.0013			±0.0011			±0.0033
PE 1 obs. in mag.		±0.003			±0.003			±0.003			±0.008

As any deviation from linearity of response may be due to either the photocell or the amplifying tube, a test was made, by applying fixed potentials to the tube, to simulate the case where the greatest current from the star was produced. It was found that for the ex-

TABLE 4

CORRECTION FOR NONLINEAR RESPONSE OF TUBE

Magnitude	Observed log d	Correction for Tube	Corrected log d	Residual
5.3	2.324	+0.006	2.330	0.000
5.8	2.125	.004	2.129	− .001
6.3	1.930	.002	1.932	+ .002
6.8	1.730	.001	1.731	+ .001
7.3	1.528	.001	1.529	− .001
7.8	1.330	+ .001	1.331	+ .001
8.3	1.130	0.000	1.130	0.000

treme case, where the change in grid voltage was as much as 0.15 volt, the tube did run off from linearity; and the second series could then be corrected as in Table 4. For the brighter star in the first series the potential on the photocell was reduced, and the tube was not operated over a range in voltage large enough to cause ap-

preciable nonlinearity. The corrected log d in the fourth column of Table 4 measures the true response of the photocell; the residuals in the fifth column are from the mean of the last two figures of the log d's. The average deviation of ± 0.0009 in the logarithms, or ± 0.0023 in magnitude, indicates that over this range the response of the cell is practically linear.

The errors of the tube go into the correction for scale, which we proceed to determine. From the different series in Table 3 solutions were made for the correction $\Delta \log d$ in the form

$$\Delta \log d = a - b(m - m_0) . \qquad (1)$$

After the numerical solutions were made, the constant a could be discarded, and the results for the four series were expressed in magnitude. Δm is the correction to an observed magnitude on account of scale.

$$\left.\begin{aligned} \Delta m &= (+0.0011 \pm 0.0011)(m - 2.8) \\ \Delta m &= (+0.0047 \pm 0.0013)(m - 5.3) \\ \Delta m &= (+0.0031 \pm 0.0011)(m - 7.5) \\ \Delta m &= (+0.0048 \pm 0.0052)(m - 9.7) \end{aligned}\right\} \qquad (2)$$

In the first equation the correction is too small to bother with; in the last, it is uncertain by its whole amount. We have, therefore, averaged the correction from the second and third equations, and we adopt the approximate values:

$$\left.\begin{aligned} &\text{From magnitude } 2.5 \text{ to } 6.0 \ldots . \quad \Delta m = 0.00 , \\ &\text{From magnitude } 6.0 \text{ to } 11.6 \ldots \quad \Delta m = +0.0039\,(m - 6.0) . \end{aligned}\right\} \qquad (3)$$

In nine magnitudes the correction from (3) runs up to $+0.02$ mag., a value which could have been neglected; but we have duly applied the correction in Table 7.

Another test at the telescope was to observe stars with and without a neutral-shade glass having an absorbing-power of about three magnitudes. White stars of the Polar Sequence and other stars of spectrum A were selected; also, two red polar stars, 1r and 2r, to check the color of the shade glass. It was known from many observations in past years that this shade glass is nearly neutral and that it

has a constant value over a wide range of magnitude, but only the recent measures in connection with the polar stars are given here in Table 5. The first two stars were observed with reduced voltage on the cell. The values for the third and fourth stars have been corrected by +0.03 mag. to allow for the nonlinearity of the tube, determined in the manner shown in Table 4. The remaining deviations from a constant scale seem to be accidental, and we thus have another independent check on the photoelectric magnitudes.

TABLE 5

TEST OF SCALE WITH NEUTRAL-SHADE GLASS

Star	Visual Magnitude	Absorption	AD	No.
HD 47105	1.93	$3^{m}02$	.....	1
HD 58715	3.09	3.05	.....	1
NPS 1	4.39	3.04	±0.01	3
HD 1280	4.44	3.04	.....	1
NPS 2	5.23	3.06	.00	2
HD 8374	5.53	3.03	.....	1
NPS 4	5.96	3.04	.....	1
NPS 1r	6.45	(2.96)	.....	1
HD 5066	6.48	3.06	.....	1
NPS 5	6.53	3.04	.01	2
NPS 6	7.22	3.04	.00	2
HD 59333	7.40	3.07	.....	1
NPS 2r	7.73	(2.97)	.....	1
NPS 8	8.41	3.03	.01	2
HD 3361	9.0	3.04	.....	1
NPS 9	9.07	3.02	±0.02	4

Finally, we have made a completely independent series of measures of the brighter stars with the 15-inch refractor at Madison. As the telescope, photocell, and amplifying tube were all different, we should expect any systematic errors to be varied. The observations were made on four nights in October and November, 1936, with additional measures of Polaris on other nights. The sensitivity of the installation at Madison is about the same as at Mount Wilson, so that with the smaller telescope the stars are shifted to three magnitudes fainter. With the 15-inch we were able to get satisfactory measures of seventeen stars down to No. 10, magnitude 9.24. We did not attempt measures of color at Madison, the determinations at Mount Wilson being sufficient.

We begin with Polaris, No. 15 of the sequence. To measure this bright star with the 60-inch it was necessary to reduce the voltage on the photocell; with the 15-inch a small correction for large deflections was determined and applied. The known variation of Polaris in a period of four days makes the star a poor standard of magnitude, unless the phase is well determined. At first we did not intend to observe Polaris carefully, and the measures on three nights at Mount Wilson were rather perfunctory; but at Madison we made enough measures to get a satisfactory mean magnitude. At both stations Polaris was referred to several other stars of the Polar Sequence, at Madison particularly to Nos. 1 and 5.

In Table 6 the Julian date gives the average time of the observation. The phase is computed from Meyer's elements,[3]

$$\text{Max.} = \text{JD } 2427689.13 + 3^{d}9685E\,. \qquad (4)$$

In the fourth column the Mount Wilson magnitudes are given as observed; those obtained at Madison have been corrected by +0.04 mag. for differential color effect between the two systems.

TABLE 6

OBSERVATIONS OF POLARIS

	JD	Phase	Observed Magnitude	Corrected Magnitude	Residual	Sets
Mount Wilson	2420000+					
	8343.983	$0^{p}013$	2.43	2.425	$-0^{m}010$	1
	8344.682	.189	2.48	2.475	− .007	2
	8401.988	0.629	2.58	2.575	+0.013	3
Madison	8449.774	0.670	2.53	2.539	−0.007	2
	8460.803	.450	2.57	2.579	− .002	3
	8481.581	.685	2.53	2.539	− .001	3
	8482.767	.984	2.44	2.449	+ .014	5
	8483.606	0.196	2.47	2.479	−0.006	6

On the assumption of a simple sine curve for the light variation, two solutions have been made for the relation between the magnitude m and the phase θ,

$$\text{Mount Wilson} \ldots\ldots \quad m = 2.515 - 0.082 \cos\theta\,,$$
$$\text{Madison} \ldots\ldots\ldots \quad m = 2.501 - 0.068 \cos\theta\,.$$

[3] *A.N.*, **256**, 425, 1935.

We adopt for the mean,

$$m = 2.51 - 0.075 \cos \theta , \qquad (5)$$

and apply −0.005 mag. and +0.009 mag., respectively, to the magnitudes of the two series to reduce them to a common zero point. These corrected magnitudes are given in the fifth column of Table 6; the residuals in the next column are based on equation (5).

The slightly greater amplitude indicated at Mount Wilson, 0.164 mag. as compared with 0.136 mag. at Madison, is in the direction to be expected from the greater violet sensitivity of the reflector.

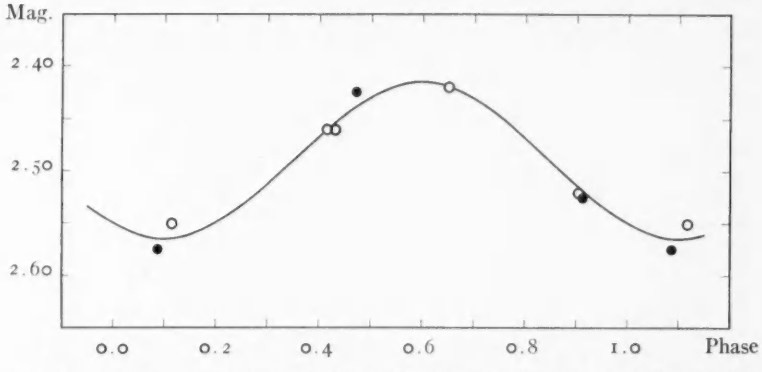

FIG. 1.—Light-curve of Polaris. Solid circles, Mount Wilson; open circles, Madison

Meyer's amplitude is 0.136 mag. The observations and light-curve are shown in Figure 1, where there is a satisfactory agreement with the predicted phase. The mean photoelectric magnitude of Polaris is adopted as 2.51 on the system of the 60-inch.

With Polaris out of the way, we may consider the other stars of the sequence which are brought together in Table 7. The first four columns give the star, the magnitude observed at Madison, the average deviation, and the number of observations. As the aluminum mirrors of the 60-inch make the installation at Mount Wilson more sensitive to the violet, the redder stars are measured brighter at Madison. The small color correction required to reduce the Madison observations to the system of the 60-inch is in the fifth column and is computed from the relation

$$\text{Correction} = +0.20(C_2 + 0.21) , \qquad (6)$$

where C_2 is the photoelectric color index in Table 1.

The corrected Madison magnitude in the sixth column is to be combined with the Mount Wilson magnitude in the seventh, giving

TABLE 7

PHOTOELECTRIC MAGNITUDES OF THE NORTH POLAR SEQUENCE

NPS	MADISON					MOUNT WILSON		MEAN Pe
	Obs. Mag.	AD	No. Obs.	Color Corr.	Corr. Mag.	Obs. Mag.	Scale Corr.	
1S	2.46	.....	19	+0m04	2.50	2.51	0m00	2.51
1	4.38	±0m00	3	.00	4.38	4.39	.00	4.38
2	5.25	.01	3	− .01	5.24	5.23	.00	5.23
3	5.76	.01	3	+ .01	5.77	5.75	.00	5.76
4	5.96	.02	3	+ .01	5.97	5.96	.00	5.96
5	6.53	.00	3	.00	6.53	6.53	.00	6.53
2S	6.57	.00	2	+ .02	6.59	6.57	.00	6.58
3S	6.70	.00	3	+ .02	6.72	6.71	.00	6.71
1r	6.36	.01	3	+ .12	6.48	6.45	.00	6.46
6*	7.23	.03	3	+ .01	7.24	7.22	.00	7.23
7	7.49	.02	4	− .01	7.48	7.52	+ .01	7.52
2r	7.62	.02	4	+ .11	7.73	7.73	.01	7.74
8	8.40	.02	4	+ .02	8.42	8.41	.01	8.42
9	9.06	.01	5	+ .02	9.08	9.07	.01	9.08
3r	8.60	.04	5	+ .11	8.71	8.74	.01	8.74
10	9.22	.05	5	+ .01	9.23	9.25	.01	9.25
4r	9.05	±0.05	5	+0.08	9.13	9.13	.01	9.14
11	.....	.....	.....	.....	.....	9.86	.02	9.88
12	.....	.....	.....	.....	.....	10.12	.02	10.14
5r	.....	.....	.....	.....	.....	9.99	.02	10.01
4S	.....	.....	.....	.....	.....	10.32	.02	10.34
13	.....	.....	.....	.....	.....	10.59	.02	10.61
6r	.....	.....	.....	.....	.....	10.36	.02	10.38
14	.....	.....	.....	.....	.....	10.90	.02	10.92
7r	.....	.....	.....	.....	.....	10.84	.02	10.86
5S	.....	.....	.....	.....	.....	10.94	.02	10.96
15	.....	.....	.....	.....	.....	11.30	.02	11.32
6S	.....	.....	.....	.....	.....	11.35	.02	11.37
8r	.....	.....	.....	.....	.....	11.34	.02	11.36
16	.....	.....	.....	.....	.....	11.60	+0.02	11.62

* One observation rejected as possibly defective.

double weight to the latter. To this weighted mean the correction for scale in the eighth column, derived from equation (3), is applied to get the adopted photoelectric magnitude. Thus the Mount Wil-

son correction for scale has been applied also to the Madison measures, since only about 0.01 mag. is involved.

The last column of Table 7 gives the final photoelectric magnitude, which we designate as Pe. The effect of the Madison measures

TABLE 8

FINAL MAGNITUDES AND COLORS OF THE NORTH POLAR SEQUENCE

NPS	Pe	Pg_p	Pg_r	$Pg_p - Pg_r$	C_2	C_p	C_r	$C_p - C_r$
1S....	2.51	2.58	2.55	+0.03	+0.01	+0.58	+0.47	+0.11
1.....	4.38	4.34	4.39	− .05	− .20	+0.03	0.00	+ .03
2.....	5.23	5.16	5.22	− .06	− .24	−0.08	−0.08	.00
3.....	5.76	5.73	5.76	− .03	− .17	+0.10	+0.18	− .08
4.....	5.96	5.94	5.95	− .01	− .15	+0.16	+0.13	+ .03
5.....	6.53	6.49	6.46	+ .03	− .19	+0.05	0.00	+ .05
2S....	6.58	6.57	6.50	+ .07	− .13	+0.21	+0.20	+ .01
3S....	6.71	6.72	6.64	+ .08	− .10	+0.29	+0.31	− .02
1r....	6.46	6.72	6.67	+ .05	+ .38	+1.55	+1.59	− .04
6.....	7.23	7.20	7.15	+ .05	− .18	+0.08	+0.07	+ .01
7.....	7.52	7.45	7.37	+ .08	− .25	−0.10	−0.19	+ .09
2r....	7.74	7.99	7.92	+ .07	+ .36	+1.49	+1.57	− .08
8.....	8.42	8.42	8.30	+ .12	− .11	+0.26	+0.17	+ .09
9.....	9.08	9.07	8.93	+ .14	− .13	+0.21	+0.09	+ .12
3r....	8.74	8.98	8.92	+ .06	+ .34	+1.44	+1.38	+ .06
10.....	9.25	9.23	9.15	+ .08	− .15	+0.16	+0.10	+ .06
4r....	9.14	9.31	9.18	+ .13	+ .20	+1.07	+0.90	+ .17
11.....	9.88	9.87	9.77	+ .10	− .14	+0.18	+0.20	− .02
12.....	10.14	10.16	10.08	+ .08	− .07	+0.37	+0.29	+ .08
5r....	10.01	10.28	10.18	+ .10	+ .39	+1.57	+1.55	+ .02
4S....	10.34	10.39	10.31	+ .08	− .03	+0.47	+0.49	− .02
13.....	10.61	10.59	10.55	+ .04	− .16	+0.13	+0.20	− .07
6r....	10.38	10.58	10.51	+ .07	+ .27	+1.26	+1.26	.00
14.....	10.92	10.93	10.94	− .01	− .09	+0.31	+0.41	− .10
7r....	10.86	11.03	10.98	+ .05	+ .21	+1.10	+1.12	− .02
5S....	10.96	11.13	11.07	+ .06	+ .20	+1.07	+1.01	+ .06
15.....	11.32	11.33	11.28	+ .05	− .09	+0.31	+0.38	− .07
6S....	11.37	11.47	11.37	+ .10	+ .07	+0.73	+0.67	+ .06
8r....	11.36	11.50	11.44	+ .06	+ .14	+0.92	+0.98	− .06
16.....	11.62	11.62	11.58	+0.04	−0.12	+0.24	+0.36	−0.12

has been to change some of the Mount Wilson values by 0.01 mag. at most. We have gained nothing but an additional check on the essential correctness of the Mount Wilson scale.

We are now ready for the comparison with the international scale, which, of course, we made tentatively from time to time during the course of the work. In Table 8 the columns give, respectively, the

number of the star, the photoelectric magnitude Pe, the photographic magnitude Pg_p computed from Pe by means of equation (8), the international photographic magnitude Pg_r, and the difference $Pg_p - Pg_r$. Similarly for the colors, the columns contain, respectively, the photoelectric color index C_2, the color index C_p computed from C_2 by equation (7), the international color index C_r, and the difference $C_p - C_r$. The values of Pg_r and C_r are the latest unpublished results kindly furnished by Seares. They correspond to the values designated as Pg and C_m in the *Rome Report* on the Polar Sequence.[4]

We begin with a discussion of the colors. It should be remembered that our photoelectric color index C_2 is derived from alternate measures of a star through blue and yellow filters and is not dependent upon the photoelectric magnitude Pe. The international color index C_r is the difference between the photographic and photovisual magnitudes, $Pg_r - Pv_r$. We have grouped the values of C_2 and C_r into six normals, and then from a least-squares solution have derived the relation

$$C_p = \underset{\pm 0.04}{2.62}(C_2 + \underset{\pm 0.003}{0.21}) . \qquad (7)$$

The values of C_p and the difference $C_p - C_r$ for each star are in Table 8. The average difference is ± 0.06 mag. on the scale of C_p, or ± 0.023 mag. on the scale of C_2. There seem to be no outstanding cases of discordance among the stars, but we might expect some of the red ones to vary in both magnitude and color over the years.

From many stars in other parts of the sky we have found the color index of an Ao star on our scale to be $C_2 = -0.27$ mag. Substituting this value in (7), we get for an Ao star, $C_p = -0.16$ mag. on the international scale. Thus we confirm the result, recently noted by Seares,[5] that there is obscuration and space reddening in the region about the pole. When the international scale was established, it was intended to make IC = 0.00 mag. for stars of spectrum Ao, but Seares now finds IC = −0.14 mag. for Ao stars in nonobscured

[4] *Trans. I.A.U.*, **1**, 71, 1922.

[5] *Mt. Wilson Comm.*, No. 119; *Proc. Nat. Acad. Sci.*, **22**, 327, 1936.

regions, which is equivalent to a mean color excess of +0.14 mag. for the pole, where our value is +0.16 mag. on the same scale.

Our colors of stars of class A, so far as the spectra are known, are given in Table 9. The first seven spectra are from Harvard or Mount Wilson, the last three from Schwassmann. The color excess in the column E_2 is the difference between the observed C_2 and the standard color for the spectral class. The distance modulus $m - M$ is derived by comparing Pg_p with the assumed mean absolute magnitude. The spectroscopic parallaxes for three stars are taken from the Yale Catalogue.

TABLE 9

COLORS OF A STARS IN THE POLAR SEQUENCE

NPS	Pg_p	Spectrum	C_2	E_2	$m - M$	Spec. π
1	4.34	A0	−0^m.20	+0^m.07	3.4	0".018
2	5.16	A0	.24	.03	4.3	.012
3	5.73	A2	.17	.07	4.0	.....
4	5.94	A3	.15	.08	3.8	0.014
5	6.49	A2	.19	.05	4.8	.....
6	7.20	A0	.18	.09	6.3	.....
7	7.45	B8	.25	.04	7.6	.....
10	9.23	A5p	.15	.05	6.7	.....
12	10.16	A3	.07	.16	8.1	.....
13	10.59	A3	−0.16	+0.07	8.5	.....

For the first five stars in Table 9 the means are $E_2 = +0.06$ mag., $m - M = 4.1$, distance $R = 66$ parsecs; the mean of three spectroscopic parallaxes, $\pi = 0''.015$, also gives $R = 67$ parsecs. Reduction to the scale of the B stars gives $E_1 = 1.68 \times E_2 = +0.10$ mag. We then have a selective absorption of (+0.10 mag./0.067) = 1.5 mag. per kiloparsec, which is several times as large as that shown by the B stars along the galactic equator.[6] This figure for the space reddening certainly looks excessive, but there can be no doubt that there is absorption about the pole. The obscuring material must be relatively near to affect stars at distances less than 100 parsecs; and since there is little change in the color excess with an increase of five magnitudes in the modulus, we are probably dealing with a local obscuration which does not extend far in the line of sight.

[6] *Pub. Washburn Obs.*, **15**, 248, 1934.

Returning to the magnitudes in Table 8, we have still to reduce our photoelectric magnitudes Pe to the system of Pg_r. After various approximations we have adopted the relation,

$$Pg_p = Pe - 0.05 + 0.53(C_2 + 0.21) . \qquad (8)$$

The constant term −0.05 mag. brings the zero point into agreement with Pg_r at magnitude 6.0, the mean for the five stars, Nos. 2, 3, 4, 5, and 2s. The coefficient 0.53 was found to bring the red stars into

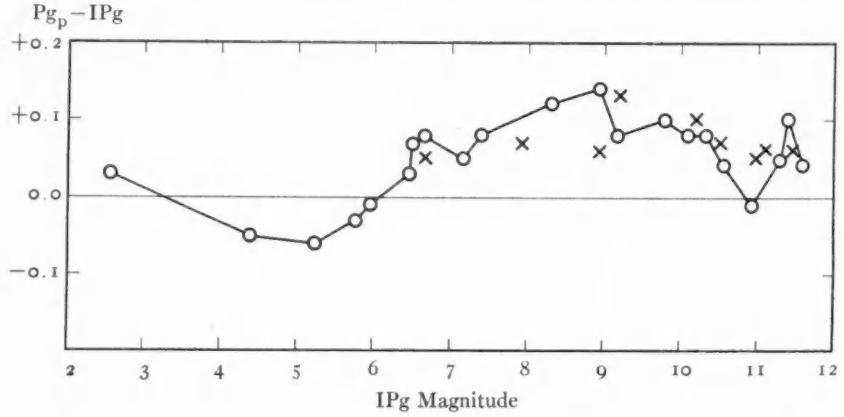

FIG. 2.—Differences in the magnitudes of the North Polar Sequence. Red stars are indicated by ×.

substantial agreement with the white ones. The last constant, +0.21 mag., was taken from equation (7), which shows that (8) may also be written

$$Pg_p = Pe - 0.05 + 0.20\,C_r . \qquad (9)$$

The values of Pg_p computed from (8) are in the third column of Table 8, and the differences $Pg_p - Pg_r$ in the fifth column give the definitive comparison of our measures with the international scale.

The values of $Pg_p - Pg_r$ are shown in Figure 2, and here we find differences in scale for which we were quite unprepared. If the first and last stars alone are taken, the agreement is within 0.01 mag. over the range of nine magnitudes, but from magnitudes 5.0 to 9.0 the two scales diverge by nearly 0.2 mag., or by at least ten times

the amount of error that we had thought could possibly be in the photoelectric series. Any one of our three independent checks should be sufficient to show that the photoelectric scale is incontestably correct within small limits, but in view of the disagreement with the international scale it is worth while to review these checks.

Let us suppose for the moment that the scale of Pg_r is quite correct, and see where that leads us. The photoelectric measures then run off more than 0.15 mag. in the interval of three magnitudes from 5.3 to 8.3, whereas the tests with the artificial star gave an error of only 0.01 mag. in this range, and this error was in the other direction. Similarly, according to Figure 2, the neutral-shade glass should have given a value differing about 0.25 mag. at magnitude 9 from the value at magnitude 5; actually, the difference was less than a tenth of this amount. Likewise, the results with the 15-inch and the 60-inch are practically the same from magnitudes 2.5 to 9.2, but the intensities on the cell were much less with the smaller telescope. It is inconceivable that the errors in scale for one cell and tube could be so nicely duplicated at three magnitudes fainter with the other combination.

The foregoing results on the Polar Sequence were held about a year in the hope of finding a satisfactory explanation of the difference between the photoelectric and photographic magnitudes. Finally, in September, 1937, we made still another test with a photocell sensitive to the ultraviolet. This sodium cell, kindly loaned to us by Dr. John Strong, was constructed by Dr. R. C. Burt and is of the vacuum type in a quartz bulb. We have only a rough test of its color sensitivity, made with a quartz monochromator and a tungsten filament for a source. The color-curve, reduced to an equal-energy spectrum, shows a maximum sensitivity at about 4300 A, with a gradual decrease to zero at 3000 A. The curve covers a much broader range of wave lengths than the ordinary Kunz potassium hydride cell. On the 60-inch with the aluminum mirrors and a quartz window in the cell-container, the combination had an effective sensitivity considerably to the violet of the ordinary photographic plate. There was still some sensitivity at the limit of the hydrogen series at 3646 A.

The sky on the one night available was poor on the Mount Wilson

standard, and this ultraviolet cell was especially sensitive to variations of transparency when the sky looked all right to the eye. In the worst set of several stars the check back on the first one was off by 0.06 mag. in an hour, and we had to assume a uniform change during that interval. We would ordinarily reject such measures, but these are probably worth something.

In Table 10 the magnitudes with the ultraviolet cell are labeled Pe_3. The new colors C_3, in the third column, were determined with

TABLE 10

OBSERVATIONS WITH THE ULTRAVIOLET CELL

NPS	Pe_3	C_3	Pg_{p3}	Pg_p	$Pg_p - Pg_{p3}$	Means
1	4.35	-0^m37	4.34	4.34	0^m00	
2	5.14	− .44	5.14	5.16	+ .02	0^m00
3	5.77	− .30	5.75	5.73	− .02	
4	5.96	− .31	5.94	5.94	.00	
5	6.52	− .38	6.51	6.49	− .02	
2s	6.56	− .35	6.55	6.57	+ .02	+0.01
3s	6.71	− .31	6.69	6.72	+ .03	
1r	6.92	+ .70	6.69	6.72	+ .03	
6	7.23	− .32	7.21	7.20	− .01	
7	7.44	− .42	7.44	7.45	+ .01	0.00
2r	8.21	+ .56	8.01	7.99	− .02	(6, 7, 8)
8	8.43	− .37	8.42	8.42	.00	
3r	9.21	+0.69	9.00	8.98	−0.02	

two filters of Jena glass, BG_3, 1 mm, and GG_3, 2 mm. The colors are quite independent of the previous colors, C_2, and the scale is more open. The approximate relation is

$$C_3 + 0.41 = 1.78\,(C_2 + 0.21)\,. \qquad (10)$$

The computed photographic magnitude Pg_{p3} in the fourth column is derived from

$$Pg_{p3} = Pe_3 - 0.21\,(C_3 + 0.41)\,, \qquad (11)$$

which is compared in the last two columns with Pg_p from equation (8) and the third column of Table 8. The zero point of Pe_3 was

taken so that Pg_{p3} would agree with Pg_p and Pg_r for the mean of the five stars 2–2s without requiring an extra constant term in (11).

The agreement of Pg_{p3} and Pg_p in Table 10 is too good to be anything but accidental, but there seems to be no way of changing our scale for the bright stars of the Polar Sequence. The magnitudes have now been measured with two cells on the 60-inch and with a third cell on the 15-inch, while the scale has been checked by the law of the inverse square and by measures with a neutral filter on the telescope.

We have had many conferences with Dr. Seares in the course of this work, and we have all been puzzled over the nonagreement with the international scale. The photographic magnitudes are the mean results from six observatories and a dozen or more telescopes. The average deviation of a magnitude at one observatory from the mean of all is about ± 0.03 mag. for the 30 stars concerned. The scale values of the different series were determined in many ways, and our scale is confirmed by only one or two series of low weight. There seems to remain only the possibility that the photographic and photoelectric magnitudes are affected differently by spectral peculiarities. At first we rejected the idea that strong hydrogen absorption in the brighter stars could cause the discrepancy; but when this suggestion was advanced by Seares, we considered it more carefully.

The arguments for the influence of hydrogen absorption are clearly stated by Seares in the following paper.[7] From the outset we have agreed with him that there ought to be some such effect. The potassium cell stops at about 4000 A, while the photographic plate continues to be sensitive for the higher members of the Balmer series and the continuous hydrogen absorption beginning at 3646 A. Therefore the stars with stronger hydrogen absorption will be relatively fainter in the photographic series, and that is the direction of the discrepancy. Nevertheless, our results with the ultraviolet cell seem to weaken this argument. This cell, with a quartz optical system and the aluminized mirrors, certainly takes in much of the hydrogen absorption, and the over-all sensitivity is to the violet of that of the combination of photographic plate and the silvered

[7] *Mt. W. Contr.*, No. 587; *Ap. J.*, **87**, 257, 1938.

mirrors of the 60-inch. A complete and satisfactory solution of the problem would require a fundamental determination of the color sensitivity of every installation as well as the spectral-intensity curves of the stars in question.

After all, the magnitudes of the first half-dozen stars of the Polar Sequence are not very important for faint standards, but a final word may be given on our corrections to the international scale. Our revised magnitudes, reduced to the photographic system, are in the column headed "Pg_p" in Table 8. The zero point agrees with Pg_r at magnitude 6.0. Connection with this or any other zero point can be made with the differences in the column "$Pg_p - Pg_r$." For our own photoelectric magnitudes, we expect to use the zero point of the Pe in Table 8 and then reduce to the photographic system by means of equation (8) or (9), depending upon whether the color index C_2 or IC is available.

This investigation has been supported in part by grants from the Alumni Research Foundation of the University of Wisconsin and from the California Institute of Technology, the latter in connection with plans for the 200-inch reflector.

CARNEGIE INSTITUTION OF WASHINGTON
MOUNT WILSON OBSERVATORY,
UNIVERSITY OF WISCONSIN
WASHBURN OBSERVATORY
November 1937

PHOTOELECTRIC MAGNITUDES AND THE INTERNATIONAL STANDARDS*

FREDERICK H. SEARES

ABSTRACT

Comparison of scales.—When international color indices are used with a linear formula for the reduction, a comparison of the photoelectric measures by Stebbins and Whitford of the North Polar Sequence with standard photographic magnitudes shows satisfactory agreement in scale for the interval 6.5–11.6, including the 24 stars 2s–16. The average difference is ±0.017. To obtain an independent set of differences for a photovisual comparison, photoelectric colors must be used, giving an average of ±0.030 mag. (Table 3). A scale divergence for stars 1–5, which reaches a maximum of 0.13 mag. and cannot be explained wholly by errors in either the photoelectric measures or the standards, possibly represents the influence of hydrogen absorption on the photographic standards. The photoelectric magnitudes are not appreciably affected by this absorption.

Characteristics of color indices.—Owing to the short spectral interval covered by the photoelectric measures of color, the color indices C_2 are not directly comparable with the standard color indices C_r. For the polar region the values of C_2, reduced to the scale of C_r, show an excess dispersion of ±0.033 mag. not accounted for by observational error. Systematic differences are also present. This lack of comparability is attributed to departures from black-body radiation, originating, possibly, in the star and certainly to some extent in the absorbing cloud known to affect the light of some of the polar stars. The relatively large average difference found from the photovisual comparison (preceding paragraph) arises from the excess dispersion in C_2.

Revision of standards.—Table 1 gives revised photographic and photovisual magnitudes and color indices for the 30 brightest stars of the Polar Sequence. The revision includes data accumulated since the *Rome Report* of 1922 was prepared. The international scales and color system remain unchanged; only the accidental errors are affected.

The photoelectric observations of stars of the North Polar Sequence presented by Stebbins and Whitford in the preceding *Contribution*[1] represent a new order of precision in the measurement of these fundamental standards of brightness. Comment is in order, however, on several points. Since Stebbins and Whitford have compared their results, not with the international standards of the *Rome Report*,[2] but with certain unpublished revisions, the origin of these revisions should be explained. Second, the photoelectric color indices present certain characteristics which require attention in comparisons with other measurements. Finally, the scale diver-

* *Contributions from the Mount Wilson Observatory, Carnegie Institution of Washington*, No. 587.

[1] *Mt. W. Contr.*, No. 586; *Ap. J.*, **87**, 237, 1938.

[2] *Trans. I.A.U.*, **1**, 70, 1922.

gence, which is serious for stars 1, 2, 3, and 4, should be examined with care. That any large part of this discrepancy should be the result of observational error seems improbable. A possible explanation lies in an influence of spectral peculiarities, which must be allowed for if the full precision of the photoelectric measures is to be utilized.

1. REVISION OF INTERNATIONAL STANDARDS

The revision is concerned only with the accidental errors affecting the standards; the scale and the color system remain unchanged. The new data include photographic and photovisual magnitudes by Seares, Ross, and Joyner at Mount Wilson[3] and by de Sitter at Leiden,[4] and color indices from exposure ratios by Malmquist at Lund.[5] De Sitter's results (10 brightest stars) are utilized in the form of color indices.

The deviations of the recent Mount Wilson magnitudes from the international standards appear in columns 4 and 5 of Table 1, following the standards themselves in columns 2 and 3. The scales, color system, and accidental errors are such that the two series of magnitudes might be combined directly with equal weights. The differences Pg − Pv in the resulting means would not, however, agree exactly with the best values of the color index; slight adjustments are therefore necessary to obtain consistent results.

The data for color index are:

IPg − IPv	$= C_m$	*Rome Report*[2]
	C_e	*Rome Report*, exposure ratios
MWPg − MWPv	$= C_{MW}$	*Mount Wilson Catalogue of Polar Stars*[3]
LPg − LPv	$= C_L$	De Sitter, Leiden,[4] reduced to international system by *Mount Wilson Contribution* No. 588, Table 1
	C_M	Malmquist,[5] exposure ratios

[3] *Magnitudes and Colors of Stars North of +80°*, mimeograph edition, Pasadena, 1935. The photographic magnitudes of the Polar Sequence stars included in this catalogue are complete. Some of the photovisual magnitudes used in the present discussion were obtained since the catalogue was published.

[4] *Fotovisueele fotometrie van sterren tot 8^m.0 benoorden +80° declinatie* (dissertation), Leiden, 1936. A comparison of this catalogue with the recent Mount Wilson results appears in the following *Contribution*, No. 588; *Ap. J.*, **87**, 280, 1938. The two series of measures are in close agreement.

[5] *Meddelande från Lunds Astronomiska Observatorium*, Ser. II, No. 37, p. 21, 1927.

TABLE 1

REVISION OF POLAR STANDARDS

NPS Group		International		Int.—MW*		Revised			Revised *minus*		C_r *minus*			
		Pg	Pv	Pg	Pv	Pg_r	Pv_r	C_r	IPg	IPv	C_m	C_e	C_{MW}	$C_{L,M}$
	(1)	(2)	(3)	(4)	(5)	(6)	(7)	(8)	(9)	(10)	(11)	(12)	(13)	(14)
	1S	2.55	2.08	....	....	2.56	2.07	0.49	+1	−1	+2	− 2	...	...
(1)	1	4.40	4.37	+1	−1	4.39	4.39	0.00	−1	+2	−3	+ 1	−1	+3
	2	5.24	5.28	+4	−2	5.22	5.30	−0.08	−2	+2	−4	+10	+2	−3
	3	5.78	5.56	+4	−2	5.76	5.58	0.18	−2	+2	−4	+ 4	+2	0
	4	5.91	5.84	−5	+2	5.95	5.82	0.13	+4	−2	+6	− 8	−1	−1
(2)	5	6.46	6.45	−3	−1	6.46	6.46	0.00	0	+1	−1	− 2	−3	+5
	2S	6.47	6.30	−5	0	6.50	6.30	0.20	+3	0	+3	+ 2	−2	−3
	3S	6.64	6.35	0	+3	6.64	6.33	0.31	0	−2	+2	+ 8	−1	−4
	1R	6.69	5.09	+2	+3	6.67	5.08	1.59	−2	−1	−1	+ 5	−2	−1
(3)	6	7.12	7.06	−6	−2	7.15	7.08	0.07	+3	+2	+1	+ 2	−3	+1
	7	7.38	7.55	+3	−2	7.37	7.56	−0.19	−1	+1	−2	− 3	+3	+2
	2R	7.93	6.32	+3	−5	7.92	6.35	1.57	−1	+3	−4	+ 2	+4	...
	8	8.32	8.13	+4	−1	8.30	8.13	0.17	−2	0	−2	(−14)	+3	...
(4)	9	8.93	8.83	0	−2	8.93	8.84	0.09	0	+1	−1	(−15)	+1	...
	3R	8.96	7.57	+9	+5	8.92	7.54	1.38	−4	−3	−1	− 5	+3	...
	10	9.11	9.06	−4	0	9.15	9.05	0.10	+4	−1	+5	− 9	+1	−1
	4R	9.18	8.27	−1	−2	9.18	8.28	0.90	0	+1	−1	(−20)	0	...
(5)	11	9.77	9.56	+1	−3	9.77	9.57	0.20	0	+1	−1	− 6	+3	−1
	12	10.08	9.77	+1	−4	10.08	9.79	0.29	0	+2	−2	− 2	+3	−1
	5R	10.16	8.63	−4	0	10.18	8.63	1.55	+2	0	+2	....	−2	...
	4S	10.31	9.83	−1	+1	10.31	9.82	0.49	0	−1	+1	− 3	−1	+2
(6)	13	10.52	10.37	−3	−2	10.55	10.35	0.20	+3	−2	+5	− 9	+4	−5
	6R	10.53	9.24	0	+2	10.51	9.25	1.26	−2	+1	−3	+ 2	−5	+6
	14	10.92	10.56	+1	+1	10.94	10.53	0.41	+2	−3	+5	− 7	+5	−5
	7R	10.96	9.87	−4	+2	10.98	9.86	1.12	+2	−1	+3	− 1	−3	+1
(7)	5S	11.07	10.06	....	....	11.09	10.04	1.05	+2	−2	+4	− 5	...	...
	15	11.27	10.88	−3	−4	11.28	10.90	0.38	+1	+2	−1	+ 1	0	+1
	6S	11.36	10.72	+1	+2	11.37	10.70	0.67	+1	−2	+3	− 4	+2	−3
	8R	11.44	10.46	−2	+1	11.44	10.46	0.98	0	0	0	+ 1	−3	+2
	16	11.58	11.22	−2	+5	11.58	11.22	0.36	0	0	0	+ 1	...	0
	SD	.....	.....	-0^3	-0^2	.....	.....	.....	$+0^4$	0^0	$+0^4$	-1^0	$+0^3$	-0^2
	AD	.....	.....	$\pm 2^8$	$\pm 2^1$	.....	.....	.....	$\pm 1^5$	$\pm 1^4$	$\pm 2^4$	$\pm 4^0$	$\pm 2^3$	$\pm 2^3$

* Unit for differences, 0.01 mag.

The internal agreement shows that all five series are of the same precision except C_e, which has half the weight of the others. Means formed with the weights thus indicated are the adopted color indices, C_r, given in column 8 of Table 1. For stars 8, 9, and 4r, however, C_e was rejected altogether because of low weight and exceptional discordance.[6] For 1s and 5s, on the other hand, C_e depends on many observations and is given the same weight as C_m. The residuals for the five determinations of color are given in the last four columns of Table 1. The first ten values in column 14 refer to de Sitter's measures; the others, to Malmquist's.

The adjustments made to obtain the revised magnitudes in columns 6 and 7 are indicated by the treatment for star 1. The means of the international and Mount Wilson results are: Pg, 4.39^5; Pv, 4.37^5. The corresponding color index is +0.02; the adopted color, C_r, is, however, 0.00. The adjustment corrections are −0.01 and +0.01, respectively, giving 4.38^5 for both Pg_r and Pv_r, which is rounded off to 4.39. The largest correction applied to any magnitude is 0.03, occurring once; 0.02 was used for only 7 of the 56 magnitudes.

The differences, revised standards *minus* international, are in columns 9 and 10. The maximum change made in IPg is 0.04 (stars 4, 3r, 10); in IPv, 0.03 (2r, 3r, 14). The average change is ±0.015 mag.

2. OBSERVATIONAL BASIS FOR COMPARISONS

For comparison with the revised photographic standards, Pg_r, Stebbins and Whitford have reduced their photoelectric magnitudes, Pe, to the international color system by means of the formula[7]

$$Pg_p = Pe - 0.05 + 0.53\,(C_2 + 0.21)\,. \qquad (1)$$

Their colors, C_2, have also been reduced to the standard system, with the aid of

$$C_p = 2.62\,(C_2 + 0.21)\,. \qquad (2)$$

[6] In spite of low weight, the values of C_e for these stars agree with the photoelectric colors better than do the corresponding values of C_m. See Table 2; also *Trans. I.A.U.*, 1, 81, 1922.

[7] A subscript "p" designates results on the international system which have been derived from the photoelectric measures.

The reduced magnitudes and colors and the differences $Pg_p - Pg_r$ and $C_p - C_r$ are given in the third and the seventh, and the fifth and the last columns, respectively, of Table 8 of *Mount Wilson Contribution* No. 586. For convenience some of these results are reprinted here in Table 2, columns 2, 3, and 5, the last of which shows the all-important scale differences.

Additional data bearing on the question of scale divergence are the differences $Pv_p - Pv_r$ and Pv_p — Potsdam, in columns 6 and 7 of Table 2. Pv_p (col. 4) is the photoelectric magnitude reduced to the photovisual system by subtracting C_p from Pg_p; Pv_r is the revised photovisual standard (Table 1, col. 7); and "Potsdam," the Potsdam visual magnitude, reduced to the international color system, as given in column 8 of Table III, *Mount Wilson Contribution* No. 431.[8]

Table 2 also gives, in columns 8–11, comparisons of C_p with the component series of color indices included in C_r, with which Stebbins and Whitford have already compared their results. Various group means and systematic and average deviations are collected at the bottom of the table.

The group means for the scale difference $Pg_p - Pg_r$, column 5, show essentially what appears in the plot, Figure 2, by Stebbins and Whitford, namely, a marked discordance for the four stars in group 1 and, for the other groups, a fluctuation, with an amplitude of approximately 0.04, about the mean difference of +0.07 mag. Since the average difference relative to this mean is only ±0.025, the accidental errors are small.

The similar comparisons based on Pv_r and Potsdam, columns 6 and 7, both show the discordance for group 1 but do not suggest any important systematic effects for groups 2–7. Here, however, the large average differences, ±0.046 and ±0.051, respectively, render judgment less certain. Incidentally, the large value of AD for the Pv_r comparison, which is twice that for Pg_r, is noteworthy. The precision of the standards is such that the AD's for these two comparisons should be approximately the same.

[8] *Ap. J.*, **74**, 138, 1931.

TABLE 2

COMPARISON OF MAGNITUDES AND COLORS

NPS Group	Reduced Pe			Red. Pe *minus*			C_p *minus*				$C'_p - C_p$
	Pg_p	C_p	Pv_p	Pg_r	Pv_r	Potsd.	C_m	C_e	C_{MW}	$C_{L,M}$	
	(1)	(2)	(3)	(4)	(5)	(6)	(7)	(8)	(9)	(10)	(11)	(12)
	1S....	2.58	0.58	2.00	+ 2	− 7	− 1	+11	+ 7	....	....	...
(1)	1.....	4.34	0.03	4.31	− 5	− 8	−16	0	+ 4	+ 2	+ 6	0
	2.....	5.16	−0.08	5.24	− 6	− 6	+ 7	− 4	+10	+ 2	− 3	0
	3.....	5.73	0.10	5.63	− 3	+ 5	+ 5	−12	− 4	− 6	− 8	+1
	4.....	5.94	0.16	5.78	− 1	− 4	−10	+ 9	− 5	+ 2	+ 2	0
(2)	5.....	6.49	0.05	6.44	+ 3	− 2	− 6	+ 4	+ 3	+ 2	+10	−2
	2S....	6.57	0.21	6.36	+ 7	+ 6	+12	+ 4	+ 3	− 1	− 2	−2
	3S....	6.72	0.29	6.43	+ 8	+10	+16	0	+ 6	− 3	− 6	−2
	1R....	6.72	1.55	5.17	+ 5	+ 9	+12	− 5	+ 1	− 6	− 5	+4
(3)	6.....	7.20	0.08	7.12	+ 5	+ 4	+ 4	+ 2	+ 3	− 2	+ 2	−5
	7.....	7.45	−0.10	7.55	+ 8	− 1	+ 9	+ 7	+ 6	+12	+11	−6
	2R....	7.99	1.49	6.50	+ 7	+15	+15	−12	− 6	− 4	....	+1
	8.....	8.42	0.26	8.16	+12	+ 3	+15	+ 7	− 5	+12	....	−4
(4)	9.....	9.07	0.21	8.86	+14	+ 2	− 1	+11	− 3	+13	....	−8
	3R....	8.98	1.44	7.54	+ 6	0	+ 8	+ 5	+ 1	+ 9	....	−4
	10.....	9.23	0.16	9.07	+ 8	+ 2	+ 9	+11	− 3	+ 7	+ 5	−8
	4R....	9.31	1.07	8.24	+13	− 4	+ 2	+16	− 3	+17	....	−5
(5)	11.....	9.87	0.18	9.69	+10	+12	− 1	− 3	− 8	+ 1	− 3	−2
	12.....	10.16	0.37	9.79	+ 8	0	− 7	+ 6	+ 6	+11	+ 7	−3
	5R....	10.28	1.57	8.71	+10	+ 8	+ 5	+ 4	....	0	....	−2
	4S....	10.39	0.47	9.92	+ 8	+10	+ 7	− 1	− 5	− 3	0	−2
(6)	13.....	10.59	0.13	10.46	+ 4	+11	+ 9	− 2	−16	− 3	−13	+5
	6R....	10.58	1.26	9.32	+ 7	+ 7	+ 8	− 3	+ 2	− 5	+ 6	−1
	14.....	10.93	0.31	10.62	− 1	+ 9	(+34)	− 5	−17	− 5	−15	+4
	7R....	11.03	1.10	9.93	+ 5	+ 7	+ 1	+ 1	− 3	− 5	− 1	0
(7)	5S....	11.13	1.07	10.06	+ 4	+ 2	+ 6	+ 6	− 3	....	....	+1
	15.....	11.33	0.31	11.02	+ 5	+12	+16	− 8	− 6	− 7	− 6	+9
	6S....	11.47	0.73	10.74	+10	+ 4	+ 4	+ 9	+ 2	+ 8	+ 3	+5
	8R....	11.50	0.92	10.58	+ 6	+12	+ 4	− 6	− 5	− 9	− 4	+2
	16.....	11.62	0.24	11.38	+ 4	+16	+12	−12	−11	−19	−12	+9
(1)					− 4	− 3	− 4	− 1	+ 1	0	− 1	0
(2)					+ 6	+ 6	+ 8	+ 1	+ 3	− 2	− 1	-0^5
(3)					+ 8	+ 5	+11	+ 1	0	+ 4	+ 6	-3^5
(4)	.....	Group means			+10	0	+ 4	+11	− 2	+12	+ 5	−6
(5)					+ 9	+ 8	+ 1	+ 2	− 2	+ 2	+ 1	−2
(6)					+ 4	+ 8	+ 6	− 2	− 8	− 4	− 6	+2
(7)					+ 6	+ 9	+ 9	− 2	− 5	− 7	− 5	+5
Means (for scale, groups 2–7) ...					+ 7	+ 6	+ 7	+ 1	− 2	+ 1	− 1	-0^5
AD					± 2^5	± 4^6	± 5^1	± 6^2	± 5^4	± 6^3	± 5^9	$\pm 3^3$

3. CHARACTERISTICS OF COLOR INDICES

Any examination of the differences between the standards and the photoelectric results may well begin with a study of the measurements of color, and, first of all, with a test of the simple linear formula (2) used for the transformation of C_2 into C_p. The differences $C_p - C_r$ (Stebbins and Whitford, last column Table 8) have the algebraic mean values shown in line (3), where the grouping of

Group	1	2	3	4	5	6	7	
Mean $C_p - C_r$	0.00	0.00	+0.03	+0.10	+0.02	−0.05	−0.03	(3)
Mean $C'_p - C_r$	0.00	−0.00[5]	−0.01	+0.04	−0.01	−0.03	+0.02	(4)

the stars is that indicated in column 1, Table 2. If C_2 for each star be plotted against the corresponding C_r, after the latter has been corrected by the mean difference for its group as given by (3) (in order to eliminate any systematic effects originating in the magnitude scales), the points do, in fact, define a linear relation with a coefficient exactly that given in (2). There is, however, indication of a dependence of slope on magnitude, the red stars for groups 2 and 3 deviating in one direction, those for groups 6 and 7 in the opposite direction.

Separate solutions for each group, with a slight smoothing, lead to formulae (5), in which the coefficient 2.75 for Group 1 is an extrapolation.

$$\left.\begin{array}{rl} \text{Group 1} & C'_p = 2.75\,(C_2 + 0.21) \\ 2 & = 2.74\,(C_2 + 0.20) \\ 3 & = 2.73\,(C_2 + 0.19) \\ 4 & = 2.69\,(C_2 + 0.18) \\ 5 & = 2.62\,(C_2 + 0.20) \\ 6 & = 2.50\,(C_2 + 0.23) \\ 7 & = 2.35\,(C_2 + 0.26) \end{array}\right\} \qquad (5)$$

The changes $C'_p - C_p$ produced by using (5) in place of (2) are shown in column 12, Table 2.

The mean of the differences $C'_p - C_r$ (col. 9, Table 3) obtained

TABLE 3

FINAL COMPARISON

	NPS Group	Pe	C'_p	C_r	Reduced Pe		Red. Pe *minus*		$C'_p - C_r$
					Pg''_p	Pv'_p	Pg_r	Pv_r	
	(1)	(2)	(3)	(4)	(5)	(6)	(7)	(8)	(9)
	1S	2.51	0.60	0.49	2.49	1.91	− 7	−16	+11
(1)	1	4.38	0.03	0.00	4.26	4.24	−13	−15	+ 3
	2	5.23	−0.08	−0.08	5.09	5.17	−13	−13	0
	3	5.76	0.11	0.18	5.68	5.55	− 8	− 3	− 7
	4	5.96	0.16	0.13	5.87	5.71	− 8	−11	+ 3
(2)	5	6.53	0.03	0.00	6.41	6.39	− 5	− 7	+ 3
	2S	6.58	0.19	0.20	6.50	6.31	0	+ 1	− 1
	3S	6.71	0.27	0.31	6.65	6.37	+ 1	+ 4	− 4
	1r	6.46	1.59	1.59	6.66	5.07	− 1	− 1	0
(3)	6	7.23	0.03	0.07	7.12	7.09	− 3	+ 1	− 4
	7	7.52	−0.16	−0.19	7.36	7.53	− 1	− 3	+ 3
	2r	7.74	1.50	1.57	7.93	6.42	+ 1	+ 7	− 7
	8	8.42	0.22	0.17	8.33	8.12	+ 3	− 1	+ 5
(4)	9	9.08	0.13	0.09	8.98	8.86	+ 5	+ 2	+ 4
	3r	8.74	1.40	1.38	8.90	7.50	− 2	− 4	+ 2
	10	9.25	0.08	0.10	9.15	9.07	0	+ 2	− 2
	4r	9.14	1.02	0.90	9.20	8.20	+ 2	− 8	+12
(5)	11	9.88	0.16	0.20	9.80	9.63	+ 3	+ 6	− 4
	12	10.14	0.34	0.29	10.08	9.75	0	− 4	+ 5
	5r	10.01	1.55	1.55	10.20	8.65	+ 2	+ 2	0
	4S	10.34	0.45	0.49	10.32	9.86	+ 1	+ 4	− 4
6)	13	10.61	0.18	0.20	10.53	10.35	− 2	0	− 2
	6r	10.38	1.25*	1.26	10.51	9.26	0	+ 1	− 1
	14	10.92	0.35	0.41	10.88	10.52	− 6	− 1	− 6
	7r	10.86	1.10	1.12	10.96	9.86	− 2	0	− 2
(7)	5S	10.96	1.08	1.05	11.05	9.98	− 4	− 6	+ 3
	15	11.32	0.40	0.38	11.28	10.88	0	− 2	+ 2
	6S	11.37	0.78	0.67	11.38	10.63	+ 1	− 7	+11
	8r	11.36	0.94	0.98	11.44	10.49	0	+ 3	− 4
	16	11.62	0.33	0.36	11.57	11.24	− 1	+ 2	− 3
(1)							-10^5	-10^5	-0^2
(2)*							0^0	-0^8	-0^5
(3)							0^0	$+1^0$	-0^8
(4)	Group means						$+1^2$	-2^0	$+4^0$
(5)							$+1^5$	$+2^0$	-0^8
(6)							-2^5	0^0	-2^8
(7)							-0^8	-2^0	$+1^8$
Means							-0^1	-0^1	$+0^2$
AD							$\pm 1^7$	$\pm 3^0$	$\pm 3^7$

* Star 5, which belongs with the discordant stars in group 1, is excluded from the group means in cols. (7) and (8).

with (5) is ± 0.037, as against ± 0.057 for the mean of $C_p - C_r$; the group means are shown in line (4). Further, the average differences for columns 8–11 of Table 2 are reduced to

	$C'_p - C_m$	$C'_p - C_e$	$C'_p - C_{MW}$	$C'_p - C_{L,M}$	
AD.....	± 0.041	± 0.052	± 0.046	± 0.045	(6)

The agreement is, of course, necessarily improved by this procedure; but the regular variation in the coefficients of (5) suggests that the improvement is not simply a representation of errors of observation. The coefficients of C_2, for example, are unaffected by errors in the scales for Pg_r and Pv_r; and if their variation is illusory, the distribution of accidental errors must be one that has little probability.

If we accept the variation as real, it follows that either C_2 or C_r, and perhaps both, must depend on magnitude. To test this point, consider the coefficient of C_2 in (1) and of C_r in the similar relation

$$Pg_p = Pe + a + bC_r . \qquad (7)$$

For groups 2–7 the respective values of these coefficients are shown in lines (8) and (9). For these calculations star 5 was excluded, since

Group.....	2	3	4	5	6	7	
Coeff. C_2.....	0.60	0.58	0.54	0.50	0.46	0.52	(8)
Coeff. C_r.....	0.21	0.19	0.21	0.19	0.19	0.22[5]	(9)

it obviously belongs with the discordant group 1; and also star 14, because the difference $Pe - Pg_r$, as measured by the precision of the other differences, is abnormal.

The effective wave-length of the radiation measured by the photoelectric cell does not depend on the intensity of the radiation. On the other hand, there is no direct evidence that the international color system is homogeneous, that is, independent of magnitude. The marked progression in line (8) and the essential constancy of the values in (9) are therefore noteworthy. Again the results cannot be explained by accidental errors without doing violence to the probabilities.

We turn now to a peculiarity affecting both C_p and C'_p, the reduced colors obtained by (2) and (5), respectively. Consider first the differences between C_p and the component series of color indices which enter into C_r (cols. 8–11, Table 2). Disregard for a moment, however, the values of $C_p - C_{MW}$, since these differences include any systematic errors affecting the series $C_p - C_m$. The three remaining series are, in the main, independent in respect to systematic, as well as accidental, errors; and yet for 12 of the 22 stars occurring in all three series the algebraic sign of the difference is the same in each series. If column 10 is used in place of 8, the result is the same; and, finally, if the mean of 8 and 10 be compared with 9 and 11, the sign remains unchanged for 13 of the 22 stars.

This persistence in algebraic sign implies the presence of either a systematic difference or a dispersion in C_p which is large relative to that of the other series of color indices. Systematic effects, however, may be eliminated by using the values of C'_p from equations (5) in place of C_p; but the persistence of sign is just as pronounced in the differences $C'_p - C_m$, etc., as in those shown in Table 2. The alternative seems, therefore, to be an unexpectedly large dispersion in C_p and C'_p, relative to C_r, which cannot be accounted for by observational errors in C_2.

The relative excess dispersion σ_E in C'_p may be calculated from the total dispersion σ in the differences $C'_p - C_m$, etc., by means of the relation

$$\sigma^2 = \sigma_E^2 + \sigma_p^2 + \sigma_C^2 , \qquad (10)$$

in which σ_p and σ_C are, respectively, the dispersions corresponding to the accidental errors in C'_p and in the various color indices C_m, etc. We may also obtain σ_E by applying (10) to the dispersion in $C'_p - C_r$; in that case, however, the dispersion used for the last term must be that of the mean color indices C_r.

The average probable error of observation for a single value of C_2 is ± 0.011 mag. (Stebbins and Whitford, Table 2), and in the mean for a star, ± 0.0071 mag. (average, 2.4 observations). The corresponding accidental mean error in C_p or C'_p (σ_p) is ± 0.028 mag.

Further, from the differences in Table 1, columns 11, 13, and 14,

the low-weight series in 12 being disregarded, we find (unit, 0.01 mag.) line (11); and from $C'_p - C_m$, etc., line (12). Line (13) then follows from equation (10).

	C_m	C_{MW}	$C_{L,M}$	C_r	
σ_C	3.5	3.3	3.4	1.9	(11)
σ	5.4	5.7	5.3	4.6	(12)
σ_E	3.1	3.8	3.0	3.2	(13)

The mean of the first three values of σ_E in (13) should equal the last, as it does, sensibly. The unexplained excess dispersion in C'_p is therefore ± 0.033 mag.; and when the accidental errors are included, the total dispersion in C'_p, relative to the C_r system, becomes ± 0.043 mag.

These values take into account the systematic deviations of C_m, etc., from C_r, but assume that C_r and C'_p differ only accidentally. Any residual systematic effects not cared for by equations (5) must be very small, however, and quite incapable of accounting for the excess dispersion in C'_p.

The explanation of this peculiar result is undoubtedly the same as that proposed by Baade[9] to account for the lack of proportionality between the values of color excess derived from photoelectric measures and those obtained by him from ordinary color indices. The mean effective wave lengths for the sensitivity-curves of the cell and filter combinations used in obtaining values of C_2 are 4340 and 4670 A, which differ by only 330 A.[10] Those for the plate-curves corresponding to standard colors are 4250 and approximately 5550 A, with a difference of 1300 A. Color gradients derived from these two intervals will agree only if the radiation is of the black-body type. On the scale of C_2 the excess dispersion is only 0.033/2.62, or ± 0.013 mag. Examination of color-temperature curves suggests that departures of this order may occur even for stars unaffected by selec-

[9] An unpublished result which Dr. Baade kindly allows me to quote.

[10] Stebbins and Whitford, *Mt. Wilson Contr.*, No. 547; *Ap. J.*, **84**, 132, 1936. The published curves and wave lengths refer to silvered mirrors. Although the photoelectric measures of NPS stars were made with aluminium-coated mirrors, the general result remains the same.

tive absorption.[11] If absorption is present, as it is, to a moderate degree at least, in the polar region, the departures may be very much larger. Accidental fluctuations will certainly occur, and systematic effects may also be present.

The matter may be clarified by a reference to the expression for the gradient of the color-temperature curve, whose characteristics are reflected in the color index. For black-body radiation the color-temperature curve is a linear function of $1/\lambda$, its gradient Δg is constant, and $C_r = kC_2$, where k is a constant. But for a star affected by Rayleigh scattering, for example, the curve is not linear and its gradient relative to a black-body source is[12]

$$\Delta g'\left(\frac{1}{\lambda}\right) = \Delta g\left(\frac{1}{\lambda}\right) + \frac{4a}{\lambda^3}, \tag{14}$$

where a is the optical thickness of the scattering cloud. The variable term in λ increases the gradients corresponding to C_r and to C_2, but, owing to the values of λ involved, more for C_2 than for C_r. The color indices themselves are similarly increased (i.e., color excess appears) by disproportionate amounts, such that now $C_r = k'C_2$, where $k' < k$.

C'_p and C_r are therefore probably not strictly comparable. Theoretically, at least, both must be affected by departures from black-body radiation, irrespective of their origin; and the relative excess dispersion in C'_p presumably measures the differential effect. Owing to the relatively short wave-length interval covered in the determination of C_2, C'_p is disturbed more than C_r; further, the systematic differences between C_p and C_r which depend on magnitude probably originate largely in C_2 and suggest the influence of selective absorption. At any rate, the change in the coefficients of C_2 in (5) is in the right direction to be accounted for by the plausible supposition of a selective absorption which increases with the magnitude. This supposition would also explain the variation of the coefficient of C_2 shown in line (8). The constancy of the quantities in

[11] See, e.g., H. Strassl's spectral photometric measures of Pleiades stars: *Göttingen Veröffentl.*, Heft 29, 1932.

[12] Kienle, *Göttingen Veröffentl.*, Heft 11, 1930. For Rayleigh scattering, $\ln\psi$ in Kienle's formula (11) becomes $-a/\lambda^4$.

line (9), on the other hand, indicates that the color system defined by C_r is substantially independent of brightness.

4. REDUCTION TO STANDARD SYSTEM

Of the four series of color indices, C_2, C_p, C'_p, and C_r, which should be used for the reduction of the photoelectric magnitudes to the international system? Neither C_p nor C'_p is directly comparable with C_r; both include an excess dispersion which is larger than the total dispersion in C_r (see formula 19). C'_p agrees systematically with C_r; but C_r itself may be affected by systematic errors in the magnitude scales whose accuracy is to be tested. Stebbins and Whitford have used equation (1) involving C_2; but since the correlation coefficients involved are not far from unity, the combination of equations (1) and (2) shows that this procedure is practically equivalent to using C_p in the relation

$$Pg_p = Pe - 0.05 + 0.20C_p . \qquad (15)$$

On the other hand, a direct solution based on C_r gives

$$Pg''_p = Pe - 0.12 + 0.20C_r , \qquad (16)$$

in which the coefficient (mean for l. 9) does not vary progressively from group to group.

Because of the constancy of the coefficient of C_r, equation (16) is preferable to (15), although, as far as systematic effects are concerned, it is unimportant whether C_r or C'_p be used in (16). Practically, however, C_r is to be preferred, because the excess dispersion in C'_p increases the scatter in the differences between the reduced photoelectric magnitudes and the values of Pg_r on which judgment as to the accordance of the scales must be based.

For comparison with Pv_r, however, it is necessary to use C'_p; for, if C_r be subtracted from (16) and the result be used for the Pv comparison, the residual differences will be identical with those given by (16) when used to compare Pe with Pg_r. We therefore have

$$Pv'_p = Pe - 0.12 - 0.80C'_p . \qquad (17)$$

The adopted reduction formulae (16) and (17) require a further remark: Any relative scale error in Pg_r and Pv_r appears in C_r (and

to the same extent in C_p') and is carried over into the comparisons. Hence, only 0.8 of any error in the Pg_r scale will be revealed by the comparison based on (16); and this same divergence, i.e., 0.8 of the Pg_r error, will appear in the comparison made with (17) as a spurious error affecting the Pv_r scale, a circumstance which may aid in differentiating the residual effect of accidental errors from a real error in scale. In fact, this is the main advantage in using (17), since this formula can reveal only 0.2 of any error in the Pv_r scale.

The results obtained from (16) and (17) are given in columns 5 and 6 of Table 3, while the differences $Pg_p'' - Pg_r$ and $Pv_p' - Pv_r$, the final results of the comparison with the revised standards, are given in columns 7 and 8. For the 24 stars beginning with 2s, only three of the Pg differences exceed 0.03 mag., the maximum being −0.06; and, as far as can be judged from the group means at the bottom of the table, the fluctuation which shows in the differences in Table 2 has disappeared. In spite of the larger AD for column 8, the systematic agreement is good. From star 2s downward, therefore, the accordance of the Pg_r magnitudes with the photoelectric measures is all that could have been hoped for.

The values of AD for columns 7 and 8, together with formulae (16) and (17), give further information on the various errors involved. The mean error in Pe, according to the data of Stebbins and Whitford, is ±0.010; and for the total dispersion in C_p' we have already found 0.043. Equation (17) and the AD of 0.030 then lead to a mean error of 0.012 in Pv_r. On the other hand, (16) and the corresponding AD, 0.017, give 0.022 for the mean error of Pg_r and Pv_r (assumed to be equal). The average of these results may be adopted, whence

$$\text{ME of } Pg_r \text{ or } Pv_r = \pm\, 0.017\,, \tag{18}$$

$$\text{ME of } C_r = \pm\, 0.024\,. \tag{19}$$

These values include systematic, as well as accidental, errors (the scale of Pe is assumed to be free from systematic error) and are probably a reliable indication of the precision. The value (19) for C_r is to be preferred to that in (11), since in the present instance the influence of systematic error is more completely accounted for.

Finally, the use of (18) with (17) gives ± 0.040 for the total dispersion in C'_p, in close agreement with the adopted value ± 0.043. This quantity, it will be recalled, includes the accidental error of observation, ± 0.028 (ME in C_2, ± 0.010[5]) and the relative excess dispersion of ± 0.033 attributed to spectral peculiarities.

5. SCALE DISCORDANCE FOR BRIGHT STARS

The scale divergence for group 1, with which star 5 is also to be included, remains practically as in Table 2. Error in the original Pe magnitudes is not seriously to be considered. An error in the Pg_r scale, as already mentioned, would not only affect the photographic comparison but, through C_r, would be carried over into the photovisual differences and there appear as a spurious error of the same amount. As a matter of fact, the mean divergence for group 1 (cols. 7 and 8, bottom of Table 3) is exactly the same for the two comparisons. On this basis, therefore, the discordance in the Pg differences accounts for the whole of the divergence in the photovisual comparison, and hence there is no real inconsistency between the Pv_r and the Pe scales, even for group 1.

As for the reliability of the Pg_r standards, Stebbins and Whitford have already commented on the consistency of the photographic data entering into the *Rome Report*. The essential results, however, should be shown in detail, especially as additional measures are now available and the visual and photovisual observations can also be utilized for the comparison.

Table 4 shows the differences relative to Pg_p for ten series of photographic measures and to $Pv_p = Pg_p - C_p$ for six visual and photovisual series. The photoelectric data used are such that these differences are directly comparable with those given by Stebbins and Whitford in the fifth column of their Table 8. Further, the group means at the bottom of Table 4 may be compared with those for column 5 of Table 2. The characteristic difference of about 0.1 mag. between groups 1 and 2 appears in every comparison except those in columns 6 and 16 of Table 4. Moreover, the approximate equality in the means for groups 2 and 3 is also generally evident. Since the average deviation for a group mean is usually one-half the value of AD for single differences given in the last line of Table 4,

TABLE 4

PHOTOELECTRIC COMPARED WITH INDIVIDUAL SERIES OF PHOTOGRAPHIC AND PHOTOVISUAL MAGNITUDES*

NPS GROUP	Pg_p *minus* INDIVIDUAL Pg										Pv_p *minus* Pv AND Vis					
	GAP	Gr13	H1	H5	HK	MW60	MW10	YPg	YPg1	LPg	IPv	PD	YPv	LPv	WPv	Hvis
(1)	(2)	(3)	(4)	(5)	(6)	(7)	(8)	(9)	(10)	(11)	(12)	(13)	(14)	(15)	(16)	(17)
(1) 1	− 7	− 4	−18	− 7	− 7	− 5	−12:	−12	− 4	− 5	− 6	−15	−16	−12	+ 6	−13
2	− 6	− 8	− 6	− 8	•−12	−14	.....	− 6	− 4	− 9	− 4	+10	− 6	− 7	− 3	−15
3	− 1	− 4	− 9	− 9	+ 7	−10	.....	+ 1	0	− 2	+ 7	+ 3	+ 2	+ 5	+ 3	+ 3
4	− 3	+ 7	+13	− 9	− 3	+ 3	−11:	− 6	− 9	− 1	− 6	−10	− 2	− 4	+ 3	− 6
(2) 5	− 2	+ 3	+ 8	+ 2	− 9	+ 4	+ 9	− 1	− 7	+ 1	− 1	− 4	− 7	−10	− 8	+ 1
2S	+13	+ 5	+ 8	+ 8	− 3	+12	+11	+15	+10	+ 5	+ 6	+ 6	+22	+ 6	+ 1	+10
3S	+ 9	+ 7	+ 8	+ 4	− 4	+ 8	+14	+14	+ 8	+ 4	+ 8	+14	+24	+ 9	+ 8	+13
1r	+15	0	.....	−12	− 4	+11	+ 2	+14	+ 6	+ 5	+ 8	+ 5	+10	+ 9	+ 5	+10
(3) 6	− 1	+10	.....	+ 8	+ 9	+ 9	+ 7	+ 6	− 4	+ 5	+ 6	+ 6	+10	+ 2	− 6	+12
7	+ 9	+10	.....	0	− 5	+ 4	+ 2	+15	+ 3	+ 9	0	+ 4	+ 5	− 3	− 5	+ 9
2r	+ 7	+ 8	.....	+ 4	− 8	+ 5	+ 6	+11	− 6	.....	+18	+10	+13	+11	+11	+15
8	.....	+13	.....	+ 3	+11	*+10	+ 7	.....	.....	.....	+ 3	.....	.....	.....	+ 5	+22
(1)	− 4	− 2	− 5	− 8	− 4	− 6	−11:	− 6	− 4	− 4	− 2	− 3	− 6	− 4	+ 2	− 8
(2)	+ 9	+ 4	+ 8	0	− 5	+ 9	+ 9	+10	+ 4	+ 4	+ 5	+ 5	+12	+ 4	+ 2	+ 8
(3)	+ 5	+10	.....	+ 4	+ 2	+ 7	+ 6	+11	− 2	+ 7	+ 7	+ 7	+ 9	+ 4	+ 1	+14
AD	± 3^8	± 2^8	± 5^1	± 3^8	± 4^3	± 3^9	± 2^5	± 4^2	± 3^9	± 2^0	± 4^1	± 5^8	± 6^7	± 5^3	± 5^1	± 4^8

* Unit for differences, 0.01 mag.

Col. NOTES TO TABLE 4

2. Göttingen = col. 8 *RR* (*Rome Report*), reduced to international color system by *Mt. W. Contr.*, No. 489, Table VII; *Ap. J.*, **79,** 210, 1934.
3. Greenwich 13-inch = col. 10 *RR*.
4, 5, 6. Harvard, three of the four component series of H2, col. 11 *RR*. The second series includes no observations on group 1, and hence does not appear here; the last series consists of King's measures with the 24-inch reflector.
7, 8. Mount Wilson = cols. 12, 13 *RR*.
9. *Yerkes Actinometry* = col. 15 *RR*. Reduction includes the 6 per cent scale correction proposed by Schwarzschild.
10. Same as col. 9 but reduced without Schwarzschild's correction.
11. Leiden, de Sitter's recent Pg measures (n. 4), reduced to international color system by *Mt. W. Contr.*, No. 588; *Ap. J.*, **87,** 280, 1938.
12. Mount Wilson Pv = col. 3 *RR;* differences essentially the same as in col. 6 of Table 2.
13. *Potsdam Durchmusterung*. Magnitudes included in the comparison in col. 7 of Table 2; differences essentially the same as in that column.
14. *Yerkes Actinometry*, reduced to international color system by *Mt. W. Contr.*, No. 472, Table I; *Ap. J.*, **78,** 148, 1933.
15 Leiden, de Sitter's recent Pv measures (n. 4), reduced to international color system by *Mt. W. Contr.*, No. 588; *Ap. J.*, **87,** 280, 1938
16. Warsaw, *Publications*, **9,** 1934; provisional measures by Rybka, reduced to the international zero point and color system by the correction +0.10 − 0.09C.
17. Harvard visual, reduced to international color system by *Mt. W. Contr.*, No. 288, Table I; *Ap. J.*, **61,** 286, 1925.

accidental errors can account for most of the fluctuations from series to series in the means for any group.

With the two exceptions mentioned, therefore, each of the sixteen series of measures shows the characteristic scale divergence revealed by the comparison with the photographic standards. Even the single star 5 almost invariably shows a difference which is algebraically less than the mean for its group, in agreement with the general comparison in Table 3.

The number and variety of instruments and methods used in obtaining the data summarized in Table 4 is such that the scale discordance affecting stars 1–5 can scarcely be observational error alone. The discrepancy probably therefore arises from some inherent lack of comparability in the Pg_p and Pg_r magnitudes for these stars, perhaps in an incomplete reduction of the photoelectric magnitudes to the international system of color. Since the spectral types of these five stars are all close to A0, the most promising explanation seems to lie in the influence of Balmer-line and hydrogen continuous absorption on the Pg_r magnitudes and the lack of any such influence on the Pe measures. Compare, for example, the sensitivity-curve for the photoelectric cell[10] with Yü's tracings of spectrograms of typical spectra photographed with the Crossley reflector.[13] Only a small percentage of the energy recorded by the cell lies to the violet of λ 4000, whereas the photographic plate, used with the reflector, reaches down to about λ 3300.

The differential effect of hydrogen absorption should be appreciable from B8 to A5 and conspicuous in the region A0–A2. The photovisual region is, of course, unaffected. The full amount of the absorption should therefore appear in the color indices C_r, as well as in the magnitudes. The photoelectric colors, on the other hand, are little affected, if at all.[10]

Assume for a moment that formula (16) and its alternative, with C'_p replacing C_r, have been derived from stars *outside* the narrow spectral range within which hydrogen absorption appears. For stars *within* this critical region the formulae will then require additional

[13] *Lick Obs. Bull.*, **15**, No. 422, 1, 1930.

terms; and if c is the differential effect upon Pe and Pg_r, we should expect, zero point being disregarded,

$$Pg'_p = Pe + 1.2c + 0.2C'_p , \tag{20}$$

$$Pg''_p = Pe + c + 0.2C_r . \tag{21}$$

The coefficient 1.2 in (20), instead of simply unity, compensates for the fact that in this case we should have for the stars in question,

$$C'_p = C_r - c .$$

For these stars, however, there is no systematic difference between C_r and the values of C'_p calculated by equations (5). It must be remembered, however, that formulae (5) were so established as to make these quantities agree as closely as possible, and that to some extent the equation for group 1 is an extrapolation. Nor do the faint stars with color indices so small as to suggest spectral types which would imply the presence of hydrogen absorption show conspicuous negative values for the differences $Pg''_p - Pg_r$ (col. 7, Table 3), as might be expected. Here careful observations of spectra indicate that the types are not really such as correspond to strong hydrogen absorption. Stars 9 and 10, for example,[14] according to Schwassmann, are F0 and A5p. Confirmatory observations kindly supplied by Dr. A. B. Wyse, of the Lick Observatory, are dF2 and dA7. All these values are outside the region of strongest absorption. Again, star 6, commonly listed as A0, is found, from special observations placed at my disposal by Dr. Adams, to be A2s. In this case the sharp-line spectrum would probably account for the small negative difference.

Finally, since both the photovisual and the photoelectric regions of the spectrum are unaffected by hydrogen absorption, the values of $Pv_p - Pv_r$ in column 8, Table 3, should differ from zero only by the amount of the spurious error introduced by using C_r for the calculation of Pv_p. As already remarked, these differences do, in fact, satisfy this condition. The test, however, is not final, since it can reveal only 0.2 of any divergence that might be present.

[14] *Bergedorfer Spektral-Durchmusterung*, 1, 1935.

In this connection it would appear safer, theoretically at least, to test the consistency of the Pe and the Pv_r scales by reducing Pe to the Pv_r system with the aid of C_2, which is free from hydrogen absorption. But since in this case the reduction coefficients depend on the magnitude, any real difference in the Pv_p and Pv_r scales goes over into the coefficients; and the comparison is likely to fail. Actual trial does show, however, that, with coefficients varying smoothly with the magnitude, there is no break between groups 1 and 2, a circumstance which confirms the conclusion already expressed.

In attempting to find direct evidence bearing on the hypothesis of hydrogen absorption, we may first test the grounds on which its presence is suspected by comparing the relation between spectral type and color index as determined with the reflector with the corresponding relation obtained with the photoelectric cell. Colors of excellent precision derived with the 60-inch reflector for stars in the Pleiades,[15] together with accurate spectral classifications, provide the first of these relations. For the photoelectric colors on the C_2 scale used for the Polar Sequence no similar relation is available at the moment of writing; but Stebbins and Huffer[16] have given one for the C_1 scale, based on stars of known type in unobscured regions. The sensitivity-curves involved are such that the effect sought for cannot be enhanced by substituting C_1 for C_2.

To reduce them to the standard scale (gKo − Ao = 1.12), the values of C_1 must be multiplied by 1.51. The differences in the two series of colors (unit, 0.01 mag.) are then:

Spectrum...	B7	B8	B9	Ao	A1	A2	A3	A5	A6	A7	F4	Ko
C_{Refl} − 1.51C_1...	0	+2	−3	+9	+16	+19	+11	+6	+8	+10	−2	+2
No. of stars..	3	3	1	1	7	3	1	1	1	1	3	3

(22)

For types B, F, and K the two series are in agreement. For the interval Ao to about A6 or A7 the influence of hydrogen absorption

[15] Hertzsprung, *Effective Wavelengths of Stars in the Pleiades*, Copenhagen, 1923; also unpublished Mount Wilson color indices derived from exposure ratios, agreeing closely with Hertzsprung's values.

[16] *Pub. Washburn Obs.*, **15**, Part V, 221, 1934.

is clearly in evidence, the maximum excess in C_{Refl} amounting to about 0.15 mag.

The spectral types used for the comparison are Mount Wilson values.[17] Harvard classifications[18] show a similar result, although slightly different in amount. In both cases the number of stars and the precision of the data are ample to insure the reality of the differential absorption.

Instructive examples of the effect of such absorption may also be found in Oosterhoff's[19] discussion of the double cluster in Perseus. Although not quantitatively applicable to the polar standards, these illustrations show that in special cases the differential effect may amount to half a magnitude.

There remains now the question whether the international standards, and especially the values of Pg_r and C_r, are really on the color system of the silvered reflector. In view of the amount of material obtained with refractors which enters into the standards, this question is important. The glass absorption of the objective undoubtedly tends to mask the influence of hydrogen absorption on measures made with such instruments; but unless the results give evidence of a large color equation relative to the standard system, the effect is likely to be only somewhat reduced. As a matter of fact, the color corrections applied to the component series of measures for the *Rome Report* were all small except for the Mount Wilson 10-inch Cooke triplet, which contributed practically nothing to the critical stars. Finally, as for the possibility of a disturbance of the color relations during the recent revision of the standards, columns 9 and 11 of Table 1 show that the maximum systematic change for group 1 is 0.01 mag.

We now proceed to a comparison of spectrum-color curves for the North Polar Sequence stars, similar to that just made for the Pleiades. In Table 5 are given the results for two series of spectral classifications, Harvard and Mount Wilson combined, and Schwassmann's results[14] from spectrograms of relatively low dispersion.

[17] From special spectrograms kindly supplied by Dr. Adams for the study of a related question.

[18] Shapley, *Harvard Bull.*, No. 764, 1922.

[19] *Ann. Sterrewacht te Leiden*, **17**, Part I, 13, 1937.

Since the photoelectric colors C_1 are for stars in unobscured regions, the most obvious result shown by the differences in the fourth and the last column of the table is the color excess of about 0.1 mag., now well established for stars in the polar region.[1,20] As

TABLE 5

COMPARISON OF STANDARD AND PHOTOELECTRIC COLOR INDICES (C_1 SCALE)

NPS	C_r	MW and H Sp	$C_r - 1.51C_1$	Schwassmann Sp	$C_r - 1.51C_1$
1S	0.49	cF7	+0.13	F8	+0.08
1	0.00	A0	.15		
2	−0.08	A0	.07		
3	0.18	A2	.25		
4	0.13	A3	.16		
5	0.00	A2	.07	A1p	+ .11
2S	0.20	F0	.06		
3S	0.31	F0	.17		
1r	1.59	M2	.11	d:: K8	
6	0.07	A0	.22	A2	+ .14
7	−0.19	B8	.01	B9	− .01
2r	1.57	M4	.09		
8	0.17			F2	− .02
9	0.09			F0	− .05
3r	1.38	gK2	+ 0.20	d:: K2	+ .26*
10	0.10			A5p	+ .05
11	0.20			F2	+ .01
12	0.29			A3	+ .32
5r	1.55			g K5	+ .19
13	0.20			A3	+ .23
14	0.41			F2	+ .22
16	0.36			F7	0.00
Means			+ 0.13		+0.11

* The star is treated as a giant.

usual, however, the excess varies from star to star. Number 7 apparently is unaffected; and the differences for 8, 9, 10, 11, and 16, on the basis of the present evidence, are probably also free from color excess. Others, for example, 3r and 12, show an amount considerably larger than the average.

From these data for the polar stars it is therefore impossible to

[20] Seares, *Mt. Wilson Comm.*, No. 119; *Proc. Nat. Acad. Sci.*, **22**, 327, 1936.

isolate any influence arising from hydrogen absorption. Most of the A stars which might be, and probably are, affected by such absorption show relatively large differences; but uncertainty as to the color excess prevents any quantitative estimate.

Some additional evidence is available through the co-operation of Dr. A. B. Wyse, who kindly obtained a series of exposures on stars 1–8 and 2s and 3s with the very efficient quartz spectrograph of the Lick Observatory. From Dr. Wyse's measures of relative spectral intensity between λ 3400 and λ 4700, supplemented by the reflection coefficients of the mirror, the atmospheric transmission, and the sensitivity-curves of the photographic plate and the photoelectric cell, I have calculated the effect of hydrogen absorption on the differences $Pg_p - Pg_r$ (col. 7, Table 3).

Two different methods of reduction both show an influence in the direction to be expected. The mean results are:

Stars	1–4	5–7	8, 2s, 3s
$Pg_p - Pg_r$, corrected	−0.03	+0.03	$+0.00^5$
$Pg_p - Pg_r$, Table 3	-0.10^5	−0.03	+0.01

Since the spectral photometric observations were intended only as a preliminary test of the influence of hydrogen absorption, the corrected differences are not to be regarded as final. The mean values are still rather large for groups of three or four stars, and there is still a discontinuity of 0.06 mag. between stars 1–4 and 5–7; but it is noteworthy that the systematic effect shown by the values in Table 3 has mostly disappeared. In particular, the difference for the discordant group (1), including stars 1–4, has been reduced to a value which can reasonably be accounted for by inherent uncertainties in the photographic standards and in the present discussion.

Unfortunately, however, the matter is not yet wholly settled, since the foregoing results and conclusions seem to be contradicted by the supplementary measures made by Stebbins and Whitford with another type of photocell which are described in the closing pages of their article.

CARNEGIE INSTITUTION OF WASHINGTON
MOUNT WILSON OBSERVATORY
January and December 1937

COMPARISON OF LEIDEN AND MOUNT WILSON MAGNITUDES FOR POLAR STARS*

FREDERICK H. SEARES

ABSTRACT

A comparison of recent Mount Wilson magnitudes for bright stars in the polar region with photographic and photovisual results by de Sitter shows excellent agreement. With the exception of a scale difference of 0.03 mag. for Pg magnitudes between 7.25 and 7.75 and a zero-point difference of the same amount for Pv data (of low weight) south of 83°0′, the accordance is complete. The average difference for a star, based on all Pg results and on the Pv magnitudes north of 83°0′, is ±0.03 mag. Owing to difficulties met in reducing the Mount Wilson measures to the international system, the result of the comparison is important.

The photographic and photovisual magnitudes derived by A. de Sitter[1] for the brighter stars north of about 80° declination provide a valuable check on certain Mount Wilson results, as yet only partially published.[2]

The magnitude scales of de Sitter were established independently by means of an objective grating; his zero points, however, depend on the international standards.[3] The Mount Wilson results, in scale, color system, and zero point, are based directly on these standards. Owing to difficulties in the reductions arising from the small number of the Polar Sequence standards and the rather large and complicated corrections for distance and color, the general confirmation afforded by the comparison with de Sitter's results is important.

The color corrections which reduce Leiden to Mount Wilson are given in Table 1.[4] The differences are regular, and there is no indica-

* *Contributions from the Mount Wilson Observatory, Carnegie Institution of Washington*, No. 588.

[1] *Fotovisueele fotometrie van sterren tot 8^{m}.0 benoorden +80° declinatie* (dissertation), Leiden, 1936.

[2] Seares, Ross, and Joyner, *Magnitudes and Colors of Stars North of +80°*, mimeograph edition, Pasadena, 1935. Except for minor corrections depending on revisions of the color indices, the photographic magnitudes are complete. The photovisual results are fragmentary and for most of the stars still unpublished.

[3] *Trans. I.A.U.*, 1, 70, 1922.

[4] That Mount Wilson is in agreement with the international color system may be seen by a reference to p. viii of the work cited in n. 2.

tion that they depend on magnitude. The scale and zero-point differences, formed after the correction of Leiden with the aid of Table 1, appear in Tables 2 and 3.

It should be noted that the Leiden magnitudes used here are those given in the second and fourth columns of de Sitter's catalogue.[1] The final Leiden photovisual magnitudes in the seventh column, although of higher weight, are based partly on existing

TABLE 1

COLOR CORRECTION, MW − L

MW C	Pg*			Pv†		
	Obsd.	No.	Adopted	Obsd.	No.	Adopted
−0.1	−0.01	34	−0.01	+0.02	19	+0.02
+0.1	+ .01	34	.00	.00	25	.00
+0.3	.00	24	+ .01	− .01	23	− .01
+0.5	+ .02	10	+ .03	− .01	20	− .01
+0.7	+ .06	5	+ .06			.00
+0.9	+ .08	14	+ .08	+ .01	21	+ .01
+1.1	+ .09	7	+ .09	+ .01	15	+ .02
+1.3	+ .11[5]	5	+ .11	+ .03	9	+ .03
+1.5	+ .11	4	+ .12	+ .07	12	+ .06
+1.7	+0.12[5]	2	+0.13	+0.07	2	+0.08
Total		139			146	

* Declinations +80°0′ to +90°0′.
† Declinations +83°0′ to +90°0′.

catalogues and hence to some extent on other determinations of the scale. In other words, the present comparison is with observational data by de Sitter himself.

The comparison of photographic scales shown in Table 2 includes all the stars observed in common, except a few objects in the 79° zone for which the Mount Wilson results are of low weight. Photovisual magnitudes (Table 3) north and south of 83°0′ are treated separately, however, since the errors in the lower declinations are much larger than those for stars closer to the pole. For this reason, also, the color corrections in Table 1 were based only on the stars north of 83°0′.

The systematic differences (SD) in Table 2 indicate a maximum

scale divergence of 0.03 mag. affecting the photographic magnitudes between 7.25 and 7.75. The mean zero-point difference of 0.01 mag. arises from this small divergence. For photovisual magnitudes north of 83°0′ (Table 3) the scales and zero points are identical; south of

TABLE 2

MWPg − LPg

LPg	SD	AD	No.
4.0 −5.0	0.000	.....	1
5.0 −6.0	− .014	±0.032	13
6.0 −6.5	− .003	.020	21
6.5 −7.0	+ .005	.016	26
7.0 −7.25	+ .018	.022	18
7.25−7.50	+ .029	.037	31
7.50−7.75	+ .029	.036	25
⩾7.75	−0.002	±0.038	4
All	+0.013	±0.028	139

TABLE 3

MWPv − LPv

LPv	Zones 79°–82°			Zones 83°–89°		
	SD	AD	No.	SD	AD	No.
4.0 −5.0	+0.048	±0.108	4	−0.033	±0.060	3
5.0 −6.0	− .074	.074	13	+ .004	.036	12
6.0 −6.5	− .011	.032	15	+ .011	.018	11
6.5 −7.0	+ .008	.035	26	− .003	.026	21
7.0 −7.5	− .021	.055	42	− .010	.030	42
7.5 −7.75	− .044	.070	31	+ .013	.027	22
7.75−8.0	− .037	.060	26	+ .011	.038	29
⩾8.0	−0.044	±0.067	9	−0.027	±0.043	6
All	−0.026	±0.057	166	0.000	±0.031	146

this limit the scale agreement is satisfactory, but a zero-point difference of about 0.03 mag. makes its appearance. The larger accidental error, ±0.057, as against ±0.031, for the average difference (AD) is also noteworthy and reflects the lower accuracy in these zones for both series of measures. A comparison with de Sitter's adopted magnitudes (Pv_{gem}) for stars in this region gives a slightly smaller zero-point difference and an average difference of ±0.047 mag.

For well-determined magnitudes, therefore, the scales and zero points of the Leiden and the Mount Wilson measures, both photographic and photovisual, are in substantial accordance. The average difference for a single star, including all errors in scales and zero points, is ± 0.03 mag., corresponding to an uncertainty of about 0.02 mag. in the individual results for each series.

CARNEGIE INSTITUTION OF WASHINGTON
MOUNT WILSON OBSERVATORY
January 1937

POLARIZATION OF THE SOLAR CORONA IN THE TOTAL ECLIPSES OF 1932 AND 1934

WILLI M. COHN

ABSTRACT

Polarigraphs of $35\frac{1}{4}$-inch and 60-inch focal lengths, equipped with Wollaston prisms and Wratten filters, were used. Intensity marks were printed on each coronal plate. The plates were measured with the Hartmann microphotometer of the Lick Observatory and the Zeiss microphotometer of the physics department of the University of California.

The polarization was determined as a function of the distance from the sun's limb and as a function of the wave length. The influence of skylight on the polarization of the corona was eliminated in the reduction. The skylight close to the corona was found to be unpolarized in the violet, blue, and red spectral regions investigated.

The shape of the coronal polarization curves for short and long wave lengths is different. The polarization in the integrated light, in the blue, and in the red increases steadily from the sun's limb toward the outer corona, whereas it reaches maxima in the violet and green and then decreases again. The polarization for short wave lengths is higher than that for long wave lengths in the inner corona; this ratio is reversed for distances of $>4'.5$ from the limb; the polarization is independent of the wave length at $4'.5$, resulting in the intersection of the polarization curves for short and long wave lengths at $4'.5$. The polarization at short wave lengths is, for a certain distance from the limb, smaller at the poles than at the equator. The difference in polarization between the polar and equatorial corona is less at long than at short wave lengths.

The influence of prominences on the polarization of the corona was investigated. The polarization values of the corona are greatly depressed close to strong prominences, and the entire polarization curve seems shifted to a greater distance from the limb. A rotation of the plane of polarization by some prominences was observed. The polarization of a well-defined streamer was determined in 1932. The polarization curves at short wave lengths seem shifted to greater distances from the limb, resulting in smaller polarization values than in corresponding parts of the corona. The red curve agrees with the coronal values. The plane of polarization of the corona is, as a rule, radial; deviations from radial polarization occur in several cases and are explained by the greater amount of polarization at the equator than at the poles and by the difference in brightness of different parts of the corona.

Visual determinations of the polarization were carried out in 1932 in integrated light and in the red.

Conclusions are drawn with regard to the distribution of particle sizes in the corona. The average particle size was found to increase from close to the limb toward the outer corona. The average diameter of a particle close to the limb amounts to less than 100 $m\mu$, and beyond $4'.5$, to less than 170 $m\mu$. The appearance of sharp Fraunhofer lines $5'$ from the limb is explained by reflection and diffraction of sunlight of short wave length by particles which are large compared with short wave lengths but are small compared with long wave lengths.

The emission proper of the 1934 corona was computed as a function of the distance from the limb and for the spectral regions investigated. The emission of the corona decreases, at all wave lengths, from the limb toward the middle corona. The emissions in the violet, blue, and green coincide very closely. The coronal emission at long wave lengths differs from that at short wave lengths. The emission proper of the corona close to the limb is relatively greater at short than at long wave lengths, this ratio being reversed farther away from the limb, indicating a coronal radiation of gradually de-

creasing temperature or a corresponding combination of temperature and luminescence radiation.

The polarization and the emission proper per volume element of the 1934 equatorial corona were computed for various distances from the limb in three spectral regions.

I. INTRODUCTION

An investigation of the polarization of the solar corona seems desirable as a means of solving problems connected with the constitution of the corona. Theoretical considerations require a knowledge of the polarization as a function of the distance from the sun's limb and as a function of the wave length. Only those observations which are obtained under perfect weather conditions are of value, because the presence of clouds or haze interferes seriously with this type of work.

The total eclipses of August, 1932, and of February, 1934, gave a chance to observe the minimum type of corona (1.3 years before and 0.2 years after the time of minimum of spots). The purpose of my 1932 expedition was to gather experience in this type of work and to decide about the methods best suited, whereas the 1934 expedition was undertaken to obtain more elaborate data.

Polarization measurements may be carried out visually, photographically, or by spectroscopic methods. Difficulties in visual polarization work are encountered because only a small number of coronal points can be measured during the short time of an eclipse, and because it is difficult to obtain the polarization as a function of the wave length. The advantages of photographic polarization work are obvious, and it is surprising that comparatively little photographic polarization work has been carried out successfully. Several attempts have been made to obtain polarization data as a function of the wave length, using various spectrographic devices. Difficulties in this work are caused by the additional polarization introduced by the prism and the lenses of the spectrograph, and by internal scattering in the instrument.

II. THE POLARIGRAPHS

The most promising approach to our program of obtaining the polarization of the corona both as a function of the distance from the sun's limb and as a function of the wave length seemed to be the use of polarigraphs equipped with color filters of narrow trans-

mission ranges. A photographic camera, lent by the A.A.V.S.O. through Professor L. Campbell, of the Harvard College Observatory, was equipped in 1932 with a quartz Wollaston double-image prism. The same camera was used in 1934 with a new quartz Wollaston prism (with optical contact) made by Halle Nachfolger of Berlin-Steglitz. Another polarigraph was built in 1934 from a camera lent by the Lick Observatory and equipped with another Halle Wollaston prism.

The advantage of the Wollaston against the Nicol prism is that the ordinary and extraordinary beams emerge at the same angle with the incident beam. Two pictures of the corona are obtained simultaneously which have the same distance from the optical axis. Quartz prisms were preferred, although their dispersion is smaller than that of calcite prisms. With quartz prisms the chromatism is greatly decreased, and the definition of the images is improved. The use of color filters makes the residual chromatism almost ineffective. The prisms were oriented so that the images fell in the north-south direction.

Wratten gelatin filters in B-glass were placed, in 1932, in front of the prism, and the focus was changed by moving the objective between the exposures made in short and long wave lengths. The 1934 polarigraphs were equipped with sliding plateholders for four plates each, as devised by W. H. Wright. The gelatin filters were placed in front of the plates, and the differences in focal length for the various exposures were adjusted in the plateholders. Table 1 gives a summary of the data for the polarigraphs.

The reason for greatly reducing the effective opening of the objectives was to minimize a possible polarization of the incident light by the objectives. The focal length of the polarigraphs was, for the same reason, chosen as great as possible. The settings of the two Wollaston prisms in 1934 differed by 180°, in order to check the influence on the polarization results.

The 1932 polarigraph was mounted on a polar axis and tripod, with a hand guiding mechanism, and was equipped with a guiding telescope. In 1934 both polarigraphs were mounted on a polar axis

equipped with a box, to allow an orientation in declination, developed by W. F. Meyer, of the University of California. A clock drive and guiding telescope lent by the Lick Observatory were in-

TABLE 1

DATA FOR POLARIGRAPHS

	1932	1934—I	1934—II
Objective	Voigtländer Euryscope	Voigtländer Euryscope	Brashear Triple
Diameter of the objective	$3\frac{3}{4}''$	$3\frac{3}{4}''$	$2\frac{1}{8}''$
Focal length of the objective in integrated light	$35\frac{1}{4}''$	$35\frac{1}{4}''$	60″
Free aperture of Wollaston prism	18.0 mm	20.0 mm	23.0 mm
Dispersion of Wollaston prism	1°.1	1°.3	1°.1
Free opening of shutter	17.0 mm	19.5 mm	6.7 mm
Size of plates	5×7″	$3\frac{1}{4}\times4\frac{1}{4}''$	$3\frac{1}{4}\times4\frac{1}{4}''$
Number of plates exposed	9	4	4
Diameter of images of moon in integrated light	8.6 mm	8.8 mm	14.8 mm
Distance from center to center of the two corona pictures	16.9 mm	19.7 mm	29.0 mm

stalled.[1, 2] The shutters of the two polarigraphs were operated simultaneously.

III. THE ECLIPSE STATIONS

The 1932 eclipse station was at Gray, Maine; and the 1934 station was at Laol Island of the Losap group in the East Caroline Islands. Data concerning the eclipse stations and the eclipses are presented in Table 2.[3]

Both eclipses were observed under perfect weather conditions.[4] A careful study of the sky immediately following totality and thereafter, both in 1932 and 1934, failed to show any trace of haze or general cloudiness such as may be expected from the cooling of the

[1] W. M. Cohn, *Pub. A.S.P.*, **46**, 177, 1934.

[2] S. A. Mitchell, *Eclipses of the Sun*. 4th ed. New York: Columbia University Press, 1935.

[3] S. Nakano, *Tokyo Astron. Obs. Reports*, **2**, 129, 1934; *Japan. J. Astr. and Geophys.*, **12**, 13, 1935.

[4] W. M. Cohn, "Some Meteorological Observations in Connection with the 1932 and 1934 Total Eclipses" (unpublished).

atmosphere. The good results of the ultraviolet exposures of the Harvard College Observatory party obtained in 1932 at Small's

TABLE 2

ECLIPSE DATA

	Aug. 31, 1932	Feb. 14, 1934
Location	Small's Farm, Gray, Maine	Laol Island
Longitude	70°21′ W.*	−152°44′16″ E.†
Latitude	43°53′ N.	6°53′29″ N.
Elevation (approx.)	370 ft.	3 ft.
Apparent altitude of sun at mid-totality	60°40′	57°55′
Time of totality:		
Calculated	88ˢ	130ˢ‡
Observed	86ˢ	124ˢ
Apparent semidiameter (at time of second contact)—		
Of moon	975″.2	1001″.2§
Of sun	951″.0	971″.7
Computed times of second contact	$3^h29^m02^s$ E.S.T.	$10^h16^m20^s$ Local Civil Time‡
Position angles of points of contact on the sun:		
First contact	306°41′.3	236°48′§
Second contact	98°56′.3	15°.31
Third contact	332°33′.9	271°41
Fourth contact	124°37′.6	50°57
Position angle of sun's axis of rotation	+21°.07	−16°.97

* Data obtained through the courtesy of Mr. L. S. Barnes, of the Harvard College Observatory.

† Reduced according to observations by Dr. S. Nakano, of Tokyo Astronomical Observatory (S. Nakano, *Tokyo Astron. Obs. Reports*, **2**, 129, 1934; *Japan. J. Astr. and Geophys.*, **12**, 13, 1935).

‡ Data obtained through the courtesy of Dr. L. Watanabe, of Kyoto Imperial University.

§ Computed by Messrs. C. Swanson and E. C. Bower, of the astronomical department of the University of California.

farm also point against the presence of susceptible amounts of haze during totality.

IV. THE PHOTOMETRIC REDUCTIONS

The photometric reductions were carried out by means of standard marks printed on each eclipse plate. A "neutral" Zeiss wedge was

PLATE VII

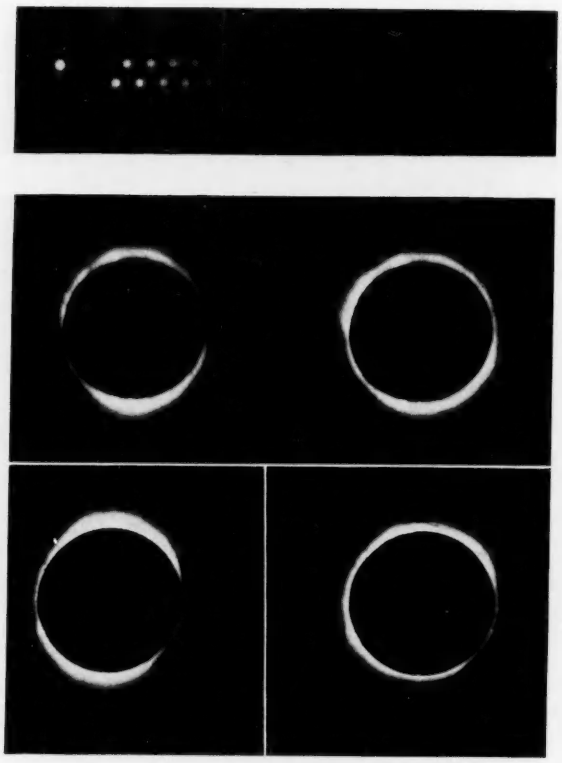

FIG. 1.—Intensity marks, plate SF 209

FIG. 3.—Photographs of the corona. *a* = SF 71-1932; *b* = SF 209-1934. Enlargement 2.2 times.

UNIV. OF MICH.

used, such as was devised by von Klüber (see Pl. VII, Fig. 1).[5, 6] The wedge was calibrated visually by Dr. Dziobek of the Physikalisch-Technische Reichsanstalt of Berlin, using a Brodhun sector photometer. Numbering the holes of the wedge-diaphragm from 2 to 32 the results are shown in curve *a* of Figure 2. The difference between two marks averages 0.3 mag. The wedge was calibrated for the various spectral regions (filter-plate combinations) covered in our work by means of the distance law. Some curves obtained in this reduction are shown in Figure 2.

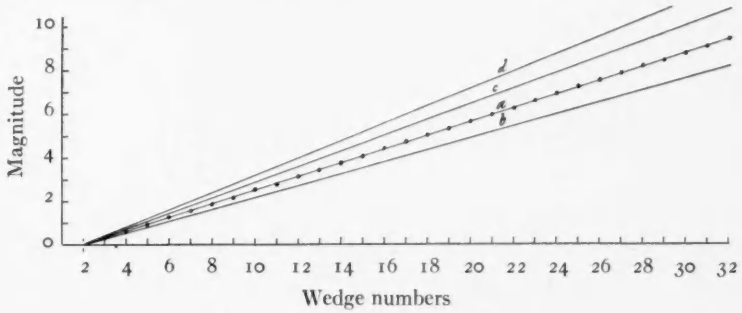

FIG. 2.—Calibration curves for neutral wedge. *a* = visual results (integrated light); *b* = Astro plate plus No. 36 filter; *c* = Astro plate plus No. 47 filter; *d* = Superpan plate plus No. 29 filter.

The original plan was to use sunlight immediately after the eclipses for printing intensity marks on the upper part of each coronal plate left unexposed during totality. Because of cloudiness on the days after the eclipses, standard lamps had to be used. The standard marks were printed with exactly the same exposure-times as the coronal pictures.

A series of exposures for the various filter-wedge-plate combinations was next secured, using plates of the same batches as the coronal plates, on which one set of standard marks was printed by means of a standard lamp and one set by means of sunlight reflected from a chalk plate, the exposure-times being identical (a chalk plate will not, according to von Klüber,[5] change the spectral composition of the incident light). Small differences were found to occur in the

[5] *Zs. f. Ap.*, **2**, 289, 1931. [6] *Ibid.*, **3**, 142, 1931.

characteristic curves obtained with sunlight and with lamplight, and corrections were applied accordingly.[7]

The characteristic curve for each corona plate was derived from microphotometer records through the intensity marks. The characteristic curve was converted into relative intensities, taking into consideration the corrections outlined above. No correction was applied for scattered light caused by the corona itself, because of the lack of data available.[5] This correction must, however, be very small, because the sky was entirely clear during both eclipses.

The 1932 coronal plates received a second set of intensity squares to be used in case absolute intensity values would be required later. A standard lamp was placed in front of the polarigraph. The central portion of the filament was photographed through the same optical system as used in the eclipse, and an auxiliary lens of known absorption values was inserted for focusing. The temperature of the central portion of the filament was measured simultaneously with an optical pyrometer.

Separate investigations were carried out in 1932 and in 1934 in order to find out if a beam of unpolarized light passing through the optical parts of the polarigraphs becomes polarized. Experiments were carried out separately for each objective and for the filters. No polarization was found within the limits of accuracy, and no correction was applied to the values of the coronal polarization. The Wollaston prisms were further tested with regard to complete polarization of the images and were found to be entirely satisfactory, both alone and in the complete optical arrangement of the polarigraphs.

V. PHOTOGRAPHIC PLATES AND FILTERS

Table 3 gives a summary of the plates and filters used in the eclipses. The Agfa Astro and Superpan plates were backed (antihalo). Data for the plates are found in publications by Mees,[8] Stobbe,[9] and von Klüber.[10] The plates for the 1934 eclipse were sealed in airtight tin cans in order to protect them against the high humidity of the tropics. My thanks are due to the California Pack-

[7] W. M. Cohn, *Pub. A.S.P.*, **49**, 245, 1937.

[8] *J. Opt. Soc.*, **21**, 753, 1931; **22**, 204, 1932.

[9] *A.N.*, **251**, 65; 255, 1934.

[10] *Handb. d. Ap.*, **7**, 71, 1936.

ing Corporation of San Francisco for permission to "can" the plates with one of their machines. The cans were kept in refrigerators until shortly before the eclipse.

The 1932 plates were developed in fresh ferrous-oxalate developer, using a camel's hair brush against the Eberhard effect.[11] The 1934 plates were developed in Eastman Tropical developer, in

TABLE 3

PICTURES OF THE CORONA TAKEN IN 1932 AND 1934

Year	Plate No.	Polarigraph No.	Wratten Filter No.	Plate	Maximum Effective Transmission	Effective Transmission Range	Time of Exposure	Seconds after Second Contact
1932	SF 66	I	None	Astro	458 $m\mu$	389–565 $m\mu$	10 sec	5–15
	SF 67	I	None	Astro	.....	.....	1	20–21
	SF 68	I	None	Astro	.....	.....	1/10	26
	SF 69	I	47	Eastman 40	452	383–516	1/10	34
	SF 70	I	47	Astro	446	393–512	1	39–40
	SF 71	I	47	Astro	.....	.....	10	45–55
	SF 72	I	28	Hyperpan	642	569–688	10	63–73
	SF 73	I	28	Hyperpan	.....	.....	1	78–79
	SF 74	I	28	Hyperpan	.....	.....	1/10	84
1934	SF 211	I	29	Superpan	667	614–687	10	18–28
	SF 210	I	75	I-H	481	457–520	20	50–70
	SF 209	I	36	Astro	419	386–463	10	85–95
	SF 208	I	47	Astro	446	393–512	5	103–108
	SF 215	II	29	Superpan	667	614–687	10	18–28
	SF 214	II	75	I-H	481	457–520	20	50–70
	SF 213	II	36	Astro	419	386–463	10	85–95
	SF 212	II	47	Astro	446	393–512	5	103–108

order to prevent abnormal swelling of the gelatin and fogging under tropical conditions. Both in 1932 and 1934 a hardening-bath was used. The developing agents were cooled by ice in 1932. No ice was used in 1934, great care being taken, however, to bring the wash water and all baths to the same temperature. The plates came out very uniformly and free from fog both in 1932 and 1934.

Wratten gelatin filters were chosen with regard to (1) stability, (2) the possibility of using the same filters for photographic and visual

[11] *Ibid.*, **2**, II, 431, 1931.

determinations (in 1932), (3) the narrow range of transmission, and (4) the avoidance of strong coronal lines. The filters were taken to Laol Island in 1934, sealed in tin cans. The transmission of each filter was determined spectrographically before and after the eclipses. A Beaudouin spectrograph lent by Dr. F. G. Keyes, of the Massachusetts Institute of Technology, was used in 1932; and my Hilger grating spectrograph (dispersion 49.4 A/mm), later. The spectra were measured by means of the Zeiss recording microphotometer of the physics department of the University of California. No change was found to occur, within the limits of accuracy, in the transmission values of the filters. Table 3 contains the wave lengths of maximum effective transmission and of effective transmission ranges in sunlight for the filter-plate combinations used.

Filters Nos. 47 and 28 were found most suitable for visual and photographic determinations in the blue and red because of their low absorption values, although their transmission bands are not quite as narrow as those of the 1934 filters. Filter No. 47 was used in 1932 and in 1934 in order to make the results strictly comparable. The reason for taking pictures in integrated (white) light in 1932 was to obtain results comparable with Young's polarization values.[12]

It will be seen that our filter-plate combinations avoid strong coronal lines. If such lines pass through our filters, they will tend to decrease the amount of polarization found in the corona. Line λ 5303 will interfere only in the 1932 exposures in integrated light. Line λ 6374 will influence the 1932 exposures in the red but will have little influence on the 1934 exposures in the red. The fairly strong lines λλ 4231, 4086, and 3986, as well as several weaker corona lines, will pass through our filters; but their intensity seems negligible in comparison with the continuous spectrum of the corona.[13] Lines H and K may interfere in integrated light; they are just at the border line of exposures with filter No. 47, and may play a slightly greater role in exposures with filter No. 36 taken after mid-totality.

No photographs were taken in the range between filters Nos. 75 and 29 because of the very strong line λ 5303. The existence of strong coronal lines in the ultraviolet made it inadvisable to expose

[12] *Lick Obs. Bull.*, **6**, 166, 1911. [13] W. Grotrian, *Zs. f. Ap.*, **7**, 26, 1933.

at shorter wave lengths than that of the combination of filter No. 36 with an Astro plate.

VI. THE ECLIPSE PLATES

Signals for second contact were given by Dr. L. B. Andrews, of the Harvard College Observatory party, in 1932, and by Dr. T. Araki, of the Kyoto Imperial University party, in 1934. Table 3 contains the exposure-times. The time ratio of the 1932 exposures was 1:10:100 in each spectral region, based on test exposures of the full moon. The pictures of the corona showed that such tests are permissible, the actual density of the moon pictures being intermediate between those of the innermost and the medium coronal parts. The 1934 exposures with the Lick camera were planned for obtaining the innermost part, and those with the Harvard camera for the middle part, of the corona. This permits an accurate photometric reduction because of the possibility of working in the straight part of the characteristic curve of all plates. (It was not deemed advisable to reduce over more than 5 mag. on each plate.)

The orientation of the polarigraphs was checked, in 1932, from a plate taken by W. H. Wright and from a paper by Pettit.[14] The 1934 plates were checked by means of a spectroheliogram taken by S. B. Nicholson 17 hours after the eclipse. I am much obliged to Dr. W. H. Wright, of the Lick Observatory, and to Dr. W. S. Adams, of the Mount Wilson Observatory, for placing these plates at my disposal.

Figure 3 of Plate VII shows the photographs of the corona on plates SF 71 and SF 209 of 1932 and 1934. The corona is of the minimum type in both years, with long equatorial streamers and pronounced polar brushes. A streamer appears in the north-northwest in 1932. The shape of the ordinary and extraordinary pictures of the corona on each plate is quite different. The definition of the images on the plates is surprisingly good, and no difference in definition is apparent between the two pictures on each plate. Some difficulties were encountered which resulted from poor guiding of the long exposures in 1932 and from small vibrations in the polar axis apparent in a few

[14] *Pub. A.S.P.*, **45**, 15, 1933.

1934 plates. Plate SF 210 is somewhat underexposed but is still measurable, and Plate SF 214 is underexposed and not measurable. The 1932 plates of 0.″1 exposure and the Lick camera plates of 1934 show only the innermost part of the corona. The dark disk of the moon seems free from scattered coronal light in all pictures.

VII. THE MEASUREMENT AND REDUCTION OF THE ECLIPSE PLATES

The Hartmann microphotometer with rotating table of the Lick Observatory[15] was used for measuring some of the eclipse and test plates. Special wedges were prepared from the same batches as the eclipse plates, by means of a Scheiner sensitometer with a spiral-shaped disk. Mr. J. F. Chappell, of the Lick Observatory, kindly helped in this work.

Points of equal density in the corona were determined by setting the wedge at a certain density and moving the plate (two readings being taken with increasing and decreasing densities of the wedge; cf. Bergstrand[16]). Readings were taken in polar co-ordinates every 10°, counting from the line connecting the centers of the moon's disk in both images of one plate. The intensity marks of the eclipse plates were measured before and after each corona picture. Prominence and background densities were determined. The probable error for these measurements was ±0.1 mag. A set of isophotes was drawn for each corona picture, using directly the several thousand values obtained.

All eclipse and test plates were measured with the recording Zeiss microphotometer of the physics department of the University of California.[17] The light pencil in the plane of the plate was 0.3×0.08 mm. or 0.3×0.12 mm; and the measured area of the plate, 0.08×0.08 mm. or 0.12×0.12 mm.

Photometer records were taken on Eastman Commercial Panchromatic film or on Haloid Special Bromide No. 2 photostat paper, after a series of tests had shown identical results for film and paper records. As a precaution the paper was cut from the roll always in

[15] J. Hartmann, *Ap. J.*, **10**, 321, 1899.

[16] *L'éclipse totale de soleil des 20–21 août 1914*, Part 2, No. 2, Stockholm, 1919.

[17] G. Hansen, *Ann. d. Phys.*, **78**, 558, 1925; *Zs. f. Instrumentenkunde*, **47**, 71, 1927.

the same direction. The maximum shrinkage was found to be 0.4 per cent, this value being checked frequently. No influence of humidity could be detected, within the limits of accuracy.

Records were first taken parallel to the line connecting the centers of the moon's disk. Another set of records was taken perpendicularly to the first tracings. Full blackening was marked on each record. The microphotometer tracings were taken every 0.2 to 0.5 mm on the plate. Before, between, and after each set of photometer tracings records were secured of the intensity marks of the plate. Further records were obtained for determining the density of the background. The measurement and reduction of each plate involved, on an average, 135 microphotometer records.

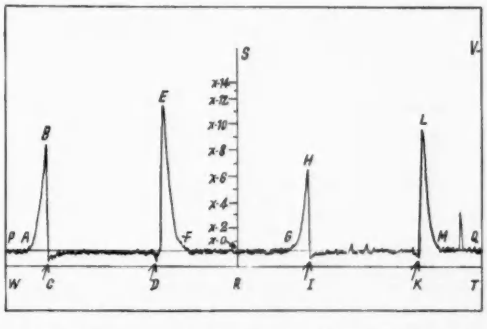

FIG. 4.—Microphotometer record MZ 20927 of SF 209. V = full blackening mark

Figure 4 shows a microphotometer record of plate SF 209 taken through both coronal pictures. *ABCDEF* and *GHIKLM* correspond to the coronal pictures on the plate, *AB*, *EF* and *GH*, *LM* being the corona. *PQ* is the zero line for the skylight background, the true zero line (chemical fog) being *WT*, obtained graphically from the background for the intensity marks of this plate. (The graphical procedure, instead of computation, was used, since the background density was well measurable.)[18] The microphotometer record of Figure 4 shows the dark disks of the moon, *CD* and *IK*, free of scattered coronal light. The slight depressions at *C*, *D*, *I*, and *K* are due to the Eberhard effect. The slope of the curve at the limb of the moon (*BC*, *ED*, *HI*, and *LK*) is almost vertical. This indi-

[18] K. Schwarzschild, *A.N.*, **193**, 81, 1912.

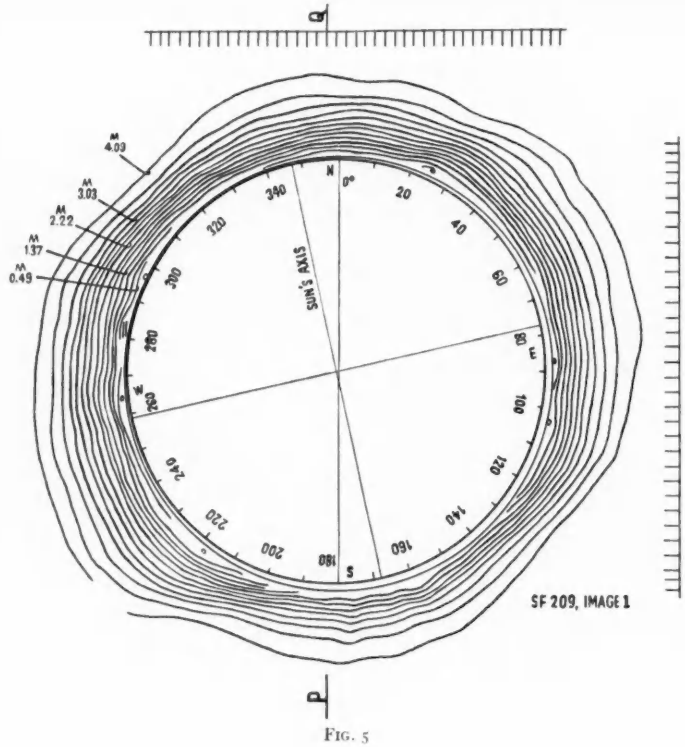

FIG. 5

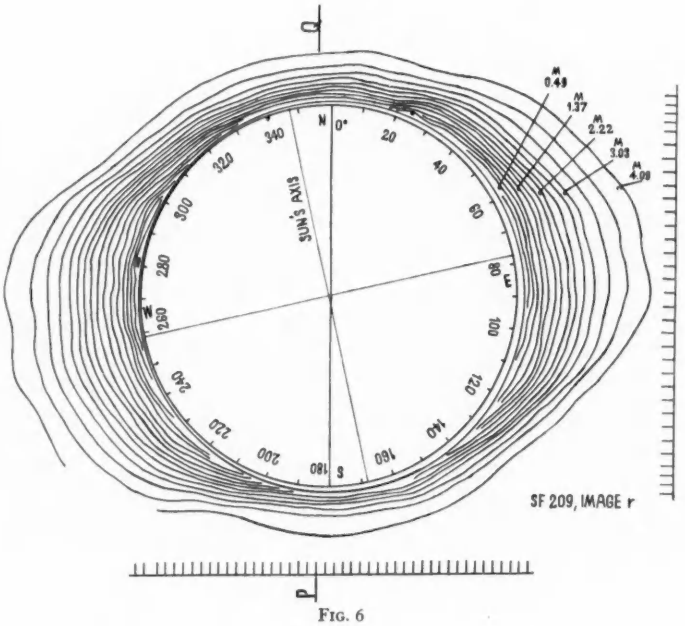

FIG. 6

FIGS. 5 AND 6.—Isophotes for SF 209, images *l* and *r*

cates a very small amount of halation near the areas of the most intense blackening of the plate. It further shows that reflection and diffraction of light within the photographic emulsion, as determined by Mees,[19] are small enough to be negligible.[5] All backed plates of the corona show similar photometer records, whereas the nonbacked plates give not quite so steep a slope.

The blackening of the dark disks of the moon (*CD*, *IK*) is slightly less than that of the skylight background of the plate (*PA*, *FG*, *MQ*). The skylight blackening between and outside of the coronal pictures shows the same amount; it remains constant over the entire width and height of the exposed part of the plate.

Ordinates for drawing isophotes are indicated on *RS* of Figure 4. The first isophote is $x - 0$, the next one $x - 1$, etc., eliminating the skylight background. No effort was made toward obtaining isophotes at 1.0 mag., 2.0 mag., etc., only the greatest possible accuracy in measuring the photometer tracings being considered.

Four sets of isophotes were drawn for each plate of the corona from the Zeiss instrument records, each set comprising, approximately, $\pm 60°$ from north to south and from east to west. The advantage of using the Zeiss microphotometer, compared to the Hartmann microphotometer, is that any number of isophotes may be derived from the records. An advantage of the Hartmann microphotometer was found in the fact that it permits the accurate location and measurement of prominences because of the larger field observed. The Hartmann instrument was used, therefore, mainly in prominence work for the 1934 plates.

Figures 5 and 6 show two sets of isophotes for plate SF 209, obtained from measuring the microphotometer records. At the edge of the figures are shown the co-ordinates along which microphotometer records were taken, *PQ* being the tracing of Figure 4. The relative positions of the sun and the moon are indicated at the middle of this exposure. (The original isophotes were enlarged fourteen times.)

The shape of the isophotes of Figures 5 and 6 is quite different, owing to (1) the flattening of the corona at the sun's poles and (2)

[19] *Ap. J.*, **33**, 81, 1911.

the presence of polarized light in the corona. The outer limits of the corona, curves $x - o$ (points A, F, G, and M of Fig. 4), are less accurately measurable than the remaining points of the corona. All values in which $x - o$ is involved receive less weight in the reduction, and are given in parentheses. It should be mentioned that the isophotes show, in agreement with former investigations of the brightness, only a part of the finer details of the corona which can be detected visually. Dr. S. A. Mitchell[2] has derived, from my values, the ellipticity of the 1934 corona.

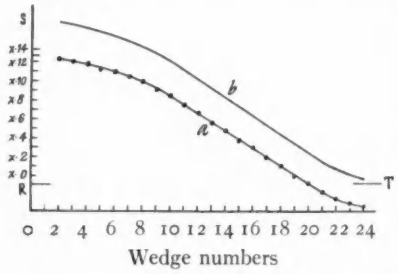

FIG. 7.—a = characteristic curve SF 209, derived from Figure 1; b = curve corrected for the use of lamplight instead of coronal light. (Zero point for curve b is in R.)

Figure 7, curve a, presents the characteristic curve of SF 209 derived from the photometer records of the intensity marks, Figure 1.

TABLE 4

MAGNITUDES FOR ISOPHOTES OF PLATE SF 209

Isophote No.	Point No. of Neutral Wedge	Magnitudes		Log of Relative Intensity
x-14	(8.02)	(1^M60)	(0^M0)	(2.000)
x-13	(8.84).	(1.83)	(0.23)	(1.908)
x-12	(9.74)	(2.09)	(0.49)	(1.804)
x-11	10.84	2.38	0.78	1.688
x-10	12.02	2.70	1.10	1.560
x-9	13.00	2.97	1.37	1.452
x-8	14.04	3.25	1.65	1.340
x-7	15.06	3.53	1.93	1.228
x-6	16.12	3.82	2.22	1.112
x-5	17.02	4.08	2.48	1.008
x-4	18.04	4.36	2.76	0.896
x-3	19.06	4.63	3.03	0.788
x-2	20.10	4.91	3.31	0.676
x-1	21.30	5.23	3.63	0.548
x-0	(22.96)	(5.69)	(4.09)	(0.364)

Curve b is derived from curve a by correcting for use of lamplight instead of coronal light in printing the marks. The ordinates for drawing the isophotes are indicated on RS. Most isophotes are de-

rived within the straight portion of the characteristic curve, values derived from isophotes not within the straight portion receive less weight and are given in parentheses.

The magnitudes for the isophotes are derived in Table 4. Column 2 contains the wedge number for each isophote from curve *b*, Figure 7; column 3 contains the magnitudes from curve *b*, Figure 2. Assuming the isophote of greatest blackening as 0.0 mag., we obtain column 4. The logarithm of the relative intensity is given in column 5. The last line in the table ($x - 0$) refers to the outer limit of the corona.

The table shows that the difference between two isophotes averages about 0.3 mag. only. The entire reduction extends over 4.1 mag. A few more isophotes were determined for maximum blackening at some position angles around 270° (close to the prominences). These isophotes do not exceed more than an additional 1.5 mag., and data derived from them receive less weight.

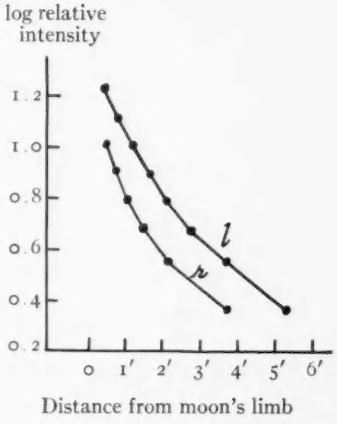

FIG. 8.—Relative intensities for images *l* and *r* as a function of the distance from the moon's limb for SF 209, position angle 180°.

Relative intensities are determined, taking as abscissa the distance from the center of the moon to each isophote, and as ordinate the logarithm of the relative intensity. Curves *r* and *l*, Figure 8, are obtained for the two coronal pictures at position angle 180°. The logarithms of the relative intensity curves are interpolated now for half-minute intervals from the limb of the moon (see Table 5).

The polarization p is computed from

$$p = 100 \cdot \frac{l - r}{l + r} \cdot \frac{1}{1 - 2\sin^2\varphi},$$

l and r being relative intensities of the two coronal pictures, and φ the position angle counted from the line connecting the centers of the two pictures of the moon. In computing p, only those values of Table 5 are used for which intensity curves for both coronal pictures are available.

Intensity curves and polarization values are determined every 10° for the entire corona and for several intermediate angles which seem of interest. Since the correction for the position angle in the polarization formula increases rapidly beyond $0 \pm 20°$, $90 \pm 20°$, etc., no values beyond $0 \pm 20°$, etc., are used for the final data. The polarization values as a function of the distance from the moon's limb are converted to distance from the sun's limb by applying a correction in direction of the radii determined from the relative positions of the sun and the moon at the middle of this exposure. No correction is

TABLE 5

SF 209. COMPUTATION OF POLARIZATION AT POSITION ANGLE 180° AS A FUNCTION OF THE DISTANCE FROM THE MOON'S LIMB

	Distance from Moon's Limb in Minutes of Arc									
	0'.5	1'.0	1'.5	2'.0	2'.5	3'.0	3'.5	4'.0	4'.5	5'.0
log l	1.190	1.040	0.918	0.798	0.702	0.624	0.564	(0.506)	(0.450)	(0.388)
log r	0.992	0.800	0.672	0.546	(0.488)	(0.436)	(0.388)	.....	.....	.....
l	15.488	10.965	8.279	6.281	5.035	4.207	3.664	3.206	2.818	2.443
r	9.818	6.310	4.699	3.516	3.076	2.729	2.443	.....	.....	.....
$l-r$	5.670	4.655	3.580	2.765	1.959	1.478	1.221	.....	.....	.....
$l+r$	25.306	17.275	12.978	9.797	8.111	6.936	6.107	.....	.....	.....
Polarization p in per cent	22.41	26.95	27.59	28.22	(24.15)	(21.31)	(19.97)	.....	.....	.....

applied to the position angles, since the difference amounts to less than 0°.1.

Polarization curves of all eclipse plates obtained in 1932 and 1934 were derived, as shown in Table 5 for SF 209, with the exception of SF 66 and SF 214. No correction was applied for the finite width of the microphotometer slits.[20] Intensity curves obtained from Hartmann and Zeiss microphotometer isophotes were found to give close agreement, the latter receiving higher weight because of the greater number of isophotes. Most details at certain position angles in the isophotes show up distinctly in the polarization curves, even if an irregularity appears in the isophotes for one picture only. Some of the finer details in the pictures could not be measured as accurately as the rest of the corona, such as the transition from polar brushes to the rest of the corona and some tips of prominences appearing in several of the 1932 and 1934 plates.

[20] H. von Klüber, *Zs. f. Phys.*, **44**, 481, 1927.

Polarization values were determined independently for each position angle, using different correction factors according to the formula given above. (This is different from the method of Young,[12] who first computes average values and later applies an average correction factor.) Polarization values were determined only if at least three isophotes were available (this eliminates part of the values for plates showing only the innermost part of the corona).

The probable error at 0°, 90°, etc., amounts to ±0.2 per cent polarization. The accuracy decreases for position angles other than 0°, 90°, etc.; but the probable error does not exceed ±1 per cent for the position angles discussed here.

Polarization values derived from various plates of the same spectral regions were next combined. (On plates SF 71 and 72 only values close to the poles were used, because of poor guiding.) An example for such a combination is shown in Figure 9. Similar results were obtained at other position angles covered by two or three plates. The agreement between the various plates of different times of exposure in 1932 and between the 1934 plates is very satisfactory, particularly since the two sets of 1934 plates (SF 208–211 and SF 212–215) were taken with polarigraphs which were different in all geometrical proportions, and with Wollaston prisms rotated 180° against each other.

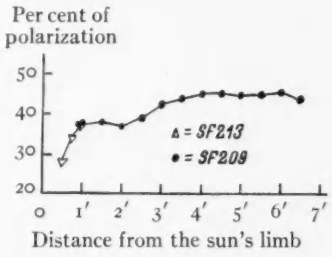

FIG. 9.—Polarization of the corona, position angle 270°, plates SF 209 and 213, obtained with different polarigraphs.

Our reduction eliminates the influence of skylight on the coronal polarization. The selective transmission of the atmosphere is of no influence on our results, since we are concerned only with the relative intensity of the two images on a plate.

VIII. RESULTS OF THE PHOTOGRAPHIC WORK

Table 6 contains the polarization in percentage of the 1932 and 1934 corona as a function of the distance from the sun's limb. The extreme values of the table were measured as close to, and as far from, the limb as possible. They indicate, for instance, the trend of

TABLE 6

POLARIZATION OF THE SOLAR CORONA AS A FUNCTION OF THE DISTANCE FROM THE SUN'S LIMB
1932: PLATES SF 67, SF 68
(No Filter; Agfa Astro Plates)

	Position Angles											
	350°	0°	10°	80°	90°	100°	170°	180°	190°	260°	270°	280°
Extreme values	1′.11 26.4%	1′.08 (34.3)%	1′.03 32.0%	0′.89 19.6%	0′.83 34.7%	0′.75 23.0%	0′.93 32.0%	1′.42 (10.1)%	.....	1′.24 (11.4)%	1′.12 (36.1)%	1′.28 14.1%
1′	.....	.....	.....	(25.4)	33.1	(25.9)	31.3	.....	.....	.....	.....	.....
1.5	26.6%	34.2	30.6	31.8	(34.7)	28.0	27.7	(11.2)	33.0	(20.3)	(37.1)	(28.4)
2	28.4	(36.1)	(35.3)	37.2	(37.5)	29.8	25.4	(18.1)	(36.5)	(38.8)	(40.0)	(45.5)
2.5	28.7	(35.6)	(33.9)	39.6	(36.6)	30.2	(26.3)	.....	.....	(44.8)	(40.3)	(46.7)
3	29.0	.....	.....	39.0	(34.3)	31.2	.....	.....	.....	47.8	(40.7)	(46.3)
3.5	.....	.....	.....	37.0	(35.4)	32.9	.....	.....	.....	51.2	(44.3)	48.5
4	.....	.....	.....	38.4	(39.2)	35.7	.....	.....	.....	(53.0)	(47.1)	49.0
4.5	.....	.....	.....	40.7	(42.4)	38.9	.....	.....	.....	.....	.....	(49.8)
5	.....	.....	.....	(43.3)	(44.3)	(41.5)	.....	.....	.....	.....	.....	.....
5.5	.....	.....	.....	(45.6)	(45.7)	(43.7)	.....	.....	.....	.....	.....	.....
6	.....	.....	.....	(47.3)	(47.8)	.....	.....	.....	.....	.....	.....	.....
Extreme values	.....	2′.80 (36.1)%	2′.72 (33.2)%	.....	6′.19 48.9%	.....	.....	.....	2′.41 (38.1)%	4′.11 (53.5)%	.....	.....

TABLE 6—*Continued*

1932: PLATES SF 69, SF 70, SF 71

(Wratten Filter No. 47; Eastman 40 and Agfa Astro Plates)

	Position Angles											
	350°	0°	10°	80°	90°	100°	170°	180°	190°	260°	270°	280°
Extreme values	1′.22 24.3%	1′.31 18.2%	1′.36 21.5%	0′.54 (0.7)%	0′.59 7.6%	0′.65 8.1%	1′.07 9.0%	0′.86 11.9%	.....	0′.79 43.2%	0′.81 31.8%	1′.30 37.3%
0′.5	.....	.....	.....	.....	.....	.....	.....	.....	13.5	.....	.....	.....
1	.....	.....	.....	4.0	(21.1)	26.1	.....	(15.8)	(17.2)	43.8	34.7	.....
1.5	29.2	19.6	22.6	24.7	37.6	42.6	(24.9)	23.7	18.8	43.9	40.6	38.9
2	(32.3)	24.2	23.3	28.7	41.2	47.1	(27.8)	27.0	22.0	46.0	47.1	45.5
2.5	(35.7)	25.2	22.5	29.4	44.6	53.2	30.7	30.8	26.3	(51.9)	(53.3)	(54.5)
3	(41.7)	20.4	23.2	33.4	47.3	58.5	29.3	32.4	29.7	(55.6)	(51.6)	(58.3)
3.5	(41.0)	18.1	26.6	38.9	49.6	(57.6)	27.8	32.4	33.2	.....	.....	.....
4	41.3	23.1	31.0	(45.1)	(51.4)	(56.7)	29.2	35.1	37.4	.....	.....	.....
4.5	41.5	25.5	32.9	.....	.....	.....	35.0	.....	.....	.....	.....	.....
5	45.5	27.2	(32.9)	.....	.....	.....	.....	.....	.....	.....	.....	.....
5.5	49.9	.....	.....	.....	.....	.....	.....	.....	.....	.....	.....	.....
6	(48.5)	.....	.....	.....	.....	.....	.....	.....	.....	.....	.....	.....
Extreme values	.....	.....	.....	4′.35 (47.2)%	.....	.....	.....	4′.18 36.5%	4′.18 39.6%	3′.29 (57.0)%	3′.31 (52.1)%	3′.30 (57.5)%

TABLE 6—*Continued*

1932: PLATES SF 72, SF 73, SF 74

(Wratten Filter No. 28; Wratten & Wainwright Hypersensitive Panchromatic Plates)

	Position Angles											
	350°	0°	10°	80°	90°	100°	170°	180°	190°	260°	270°	280°
Extreme values	{.....	0′.33 3.0%	.....	1′.21 15.3%	1′.08 −3.0%	1′.26 23.6%	.....	.....	.....	0′.89 21.0%	0′.37 18.4%	1′.29 9.0%
0′.5	14.2	(4.1)	.....	.....	.....	.....	.....	.....	.....	.....	17.8	.....
1	(24.1)	(8.4)	.....	.....	.....	.....	.....	(28.5)	.....	21.1	17.7	.....
1.5	39.6	(13.2)	.....	21.6	2.1	22.4	.....	(33.2)	.....	(24.5)	(23.0)	16.3
2	(44.5)	(21.1)	.....	(15.0)	11.8	23.5	.....	(31.3)	.....	(31.6)	(32.8)	(31.3)
2.5	.....	(31.7)	.....	(20.8)	(15.8)	.....	.....	.....	.....	.....	.....	(39.8)
3	.....	(39.1)	.....	.....	.....	.....	.....	.....	.....	.....	.....	.....
3.5	.....	(42.3)	.....	.....	.....	.....	.....	.....	.....	.....	.....	.....
Extreme values	{2′.44 (56.5)%	.....	.....	.....	2′.93 (40.6)%	.....	.....	2′.45 33.2%	.....	2′.16 (33.5)%	2′.31 (38.3)%	2′.64 (40.5)%

TABLE 6—*Continued*

1934: PLATES SF 208, SF 212

(Wratten Filter No. 47; Agfa Astro Plates)

	Position Angles															
	340°	350°	0°	10°	70°	80°	90°	100°	160°	170°	180°	190°	250°	260°	270°	280°
Extreme values	0′.75 (23.8%)	1′.27 (27.3%)	1′.35 (26.1%)	1′.40 (24.8%)	1′.80 (30.3%)	1′.84 (33.8%)	1′.88 (37.9%)	1′.91 (39.4%)	1′.52 (32.4%)	1′.80 (28.7%)	1′.69 (40.0%)	1′.65 (40.7%)	0′.28 (32.1%)	0′.75 (28.1%)	.....	.....
0′.5	.....	.....	.....	.....	.....	.....	.....	.....	.....	.....	.....	.....	(33.9)	.....	30.7	29.0
1	25.8	.....	.....	.....	.....	.....	.....	.....	.....	.....	.....	.....	(40.1)	(28.9)	34.6	32.5
1.5	30.2	30.6	(28.1)	25.0	.....	.....	.....	.....	.....	.....	.....	.....	45.7	30.1	36.3	34.5
2	34.7	35.2	(32.6)	26.9	31.9	35.2	37.8	38.8	(35.0)	(27.3)	(40.3)	40.4	50.0	33.1	42.8	38.4
2.5	36.3	38.9	(32.5)	29.6	36.6	39.1	37.8	36.6	(35.1)	(27.1)	(42.5)	(42.5)	52.9	38.4	45.3	43.2
3	41.8	43.7	(31.3)	30.9	41.3	41.4	38.1	37.0	(39.6)	(33.8)	.....	(48.4)	55.0	41.2	46.9	50.1
3.5	(46.6)	(44.9)	(31.7)	33.6	42.6	43.8	39.8	37.6	.....	.....	.....	.....	54.7	43.1	48.1	53.8
4	(48.3)	(43.2)	(35.2)	(37.6)	42.3	44.0	41.3	38.9	.....	.....	.....	.....	52.9	44.8	50.3	52.9
4.5	(49.3)	.....	.....	(39.0)	41.7	44.4	42.0	40.4	.....	.....	.....	.....	51.8	48.2	52.3	51.3
5	.....	.....	.....	.....	42.5	44.6	43.6	39.8	.....	.....	.....	.....	51.0	50.9	55.4	52.0
5.5	.....	.....	.....	.....	44.8	45.0	46.2	40.6	.....	.....	.....	.....	50.6	54.0	57.1	53.4
6	.....	.....	.....	.....	47.7	46.6	(49.1)	41.5	.....	.....	.....	.....	52.9	56.9	57.9	55.2
6.5	.....	.....	.....	.....	(50.3)	(48.4)	(51.6)	(42.8)	.....	.....	.....	.....	55.9	(60.3)	(58.8)	(58.1)
7	.....	.....	.....	.....	(51.6)	(50.9)	(52.9)	(47.1)	.....	.....	.....	.....	(58.8)	(62.2)	(59.2)	(60.1)
7.5	.....	.....	.....	.....	(51.2)	(54.0)	.....	.....	.....	.....	.....	.....	(61.7)	(63.2)	(59.7)	(62.2)
8	.....	.....	.....	.....	(50.0)	.....	.....	.....	.....	.....	.....	.....	(64.7)	(64.1)	.....	.....
Extreme values	.....	4′.27 (42.1%)	4′.35 (39.0%)	4′.90 40.3%	8′.30 (49.7%)	7′.84 (55.8%)	.....	7′.41 (50.3%)	3′.34 (41.2%)	3′.30 39.0%	2′.69 43.8%	3′.15 50.5%	8′.29 (64.3%)	.....	.....	.....

TABLE 6—*Continued*

1934: PLATES SF 209, SF 213

(Wratten Filter No. 36; Agfa Astro Plates)

	Position Angles															
	340°	350°	0°	10°	70°	80°	90°	100°	160°	170°	180°	190°	250°	260°	270°	280°
Extreme values	0′.58 20.6%	0′.56 28.4%	0′.81 26.3%	0′.84 26.4%	1′.24 46.6%	1′.10 44.2%	1′.31 43.9%	1′.36 46.8%	1′.52 31.9%	1′.21 27.3%	1′.13 22.4%	....	0′.61 34.7%	.....	0′.51 27.8%	0′.88 (23.8)%
1′	25.3	26.6	28.4	27.2	.....	.....	.....	.....	.....	.....	.....	24.5	37.8	26.5	37.2	(26.2)
1.5	28.7	26.3	(32.9)	29.1	47.2	42.7	43.7	46.2	.....	29.8	25.7	24.9	39.8	30.4	37.9	(35.4)
2	28.2	27.2	(33.8)	30.1	47.1	42.9	43.9	45.3	29.3	31.2	27.8	23.2	39.6	30.8	36.8	(41.9)
2.5	28.2	25.7	(30.0)	28.4	47.3	44.8	44.6	46.7	28.7	30.3	28.3	23.7	40.9	34.5	38.9	43.0
3	26.1	(22.7)	(27.2)	25.5	47.3	45.6	45.1	47.2	(25.5)	(27.9)	(25.3)	(24.3)	43.0	40.8	42.1	44.7
3.5	(22.9)	(21.6)	(26.6)	(24.1)	47.4	45.6	44.7	46.1	(22.1)	(24.8)	(22.1)	(22.8)	45.3	42.9	43.8	46.6
4	(21.1)	(22.7)	(25.4)	(22.8)	48.2	45.6	43.1	44.7	.....	(21.1)	(20.3)	.....	47.6	44.7	44.8	50.3
4.5	(22.8)	.....	.....	.....	47.9	45.0	42.7	44.2	.....	.....	.....	.....	47.1	46.0	44.9	53.3
5	.....	.....	.....	.....	46.4	43.6	43.3	43.1	.....	.....	.....	.....	46.5	45.4	44.4	54.2
5.5	.....	.....	.....	.....	44.9	43.1	(42.6)	(41.9)	.....	.....	.....	.....	47.0	44.3	44.8	50.7
6	.....	.....	.....	.....	(43.2)	(42.6)	(41.8)	(41.6)	.....	.....	.....	.....	46.4	(43.5)	(45.2)	(48.6)
6.5	.....	.....	.....	.....	(41.2)	(39.9)	(41.7)	.....	.....	.....	.....	.....	(46.6)	(43.0)	(43.6)	(47.2)
7	.....	.....	.....	.....	(39.3)	(37.4)	.....	.....	.....	.....	.....	.....	(47.6)	(42.8)	.....	.....
7.5	.....	.....	.....	.....	.....	(36.0)	.....	.....	.....	.....	.....	.....	(47.2)	.....	.....	.....
Extreme values	....	4′.24 (23.6)%	4′.31 (24.1)%	.....	.....	7′.75 (35.3)%	.....	.....	.....	4′.21 (19.8)%	4′.13 (20.0)%	.....	7′.64 (47.1)%	7′.40 (44.0)%	.....	6′.88 (46.5)%

TABLE 6—*Continued*

1934: PLATE SF 210

(Wratten Filter No. 75; Eastman Kodak I-H Plate)

	Position Angles															
	340°	350°	0°	10°	70°	80°	90°	100°	160°	170°	180°	190°	250°	260°	270°	280°
Extreme values	0′.84 19.4%	.....	.....	0′.59 13.2%	1′.14 (43.7)%	1′.22 35.1%	1′.24 32.8%	1′.29 37.5%	1′.35 16.8%	.....	.....	1′.88 (22.9)%	1′.06 34.4%	.....	.....	1′.25 (36.0)%
0′.5	.....	11.7	17.1	.....	.....	.....	.....	.....	.....	.....	.....	.....	.....	.....	.....	.....
1	19.6	15.8	19.7	15.6	.....	.....	.....	.....	.....	(14.5)	(18.0)	22.0	.....	(30.4)	.....	.....
1.5	20.9	17.8	22.3	21.4	(45.7)	35.4	34.5	38.7	15.2	(16.8)	(15.1)	(20.1)	40.1	33.6	40.0	(38.2)
2	(23.8)	(18.0)	(20.3)	(22.9)	50.1	38.6	37.7	41.4	(10.6)	.....	.....	.....	43.1	36.2	38.9	41.5
2.5	.....	(19.9)	(16.2)	(16.4)	53.8	40.2	39.8	42.1	.....	.....	.....	.....	45.2	38.1	38.8	43.0
3	.....	.....	.....	(17.1)	(54.3)	38.2	(39.4)	(41.4)	.....	.....	.....	.....	43.6	41.0	40.4	43.1
3.5	.....	.....	.....	.....	(54.3)	(36.9)	(39.7)	(42.1)	.....	.....	.....	.....	(39.8)	(40.6)	40.0	(43.0)
4	.....	.....	.....	.....	(52.7)	(36.8)	(40.9)	.....	.....	.....	.....	.....	(35.3)	(38.5)	(38.5)	(42.1)
4.5	.....	.....	.....	.....	.....	.....	.....	.....	.....	.....	.....	.....	(33.8)	(37.2)	(38.1)	(40.1)
Extreme values	.....	2′.60 (20.3)%	.....	.....	.....	4′.49 (36.6)%	4′.24 (41.5)%	3′.79 (42.7)%	.....	.....	.....	.....	4′.65 (34.4)%	4′.68 (37.0)%	4′.72 (38.1)%	4′.75 (39.8)%

TABLE 6—*Continued*

1934: PLATES SF 211, SF 215

(Wratten Filter No. 29; Agfa Superpan Plates)

	Position Angles															
	340°	350°	0°	10°	70°	80°	90°	100°	160°	170°	180°	190°	250°	260°	270°	280°
Extreme values	0′.69 6.6%	0′.25 −2.0%	0′.32 3.1%	.....	1′.64 30.7%	1′.38 (25.5)%	.....	.....	.....	1′.05 20.6%	0′.93 21.5%	1′.05 25.2%	1′.84 20.0%	1′.52 19.6%	1′.73 22.4%	.....
0′.5	.....	5.1	6.9	7.2	.....	.....	.....	.....	.....	.....	.....	.....	.....	.....	.....	.....
1	9.6	10.2	9.7	13.1	.....	.....	.....	.....	.....	.....	22.6	.....	.....	.....	.....	.....
1.5	14.4	17.0	14.6	16.2	.....	(25.6)	(21.6)	.....	(34.2)	(26.7)	29.0	(34.0)	.....	.....	.....	.....
2	20.0	23.9	20.5	22.9	31.8	(26.3)	(23.0)	(24.4)	35.3	(29.3)	32.3	(36.9)	20.3	21.7	24.2	(22.7)
2.5	24.2	29.1	28.4	30.6	33.2	(28.3)	(25.4)	(29.5)	37.1	32.8	35.7	36.7	22.3	25.4	26.8	25.1
3	30.2	31.3	34.7	36.9	36.0	31.9	29.0	(32.8)	40.2	38.3	39.1	37.7	28.2	29.0	31.6	29.1
3.5	33.0	33.6	36.2	38.6	42.6	37.5	33.6	(37.6)	44.1	(41.8)	(42.7)	(40.8)	33.6	34.5	37.2	34.7
4	34.5	37.7	35.2	41.5	47.1	44.1	38.2	(41.3)	(46.0)	(43.9)	(46.2)	(44.9)	38.8	39.2	43.8	39.5
4.5	(37.6)	(41.8)	(35.6)	(47.6)	50.7	48.6	44.1	(44.6)	(46.3)	(46.2)	.....	.....	42.9	46.0	49.8	45.4
5	(39.3)	(45.2)	(37.2)	(47.7)	55.4	51.5	49.0	47.5	(45.9)	.....	.....	.....	46.1	51.3	52.8	51.2
5.5	.....	.....	(38.9)	(46.3)	59.3	53.6	53.2	(50.6)	.....	.....	.....	.....	49.4	55.1	54.6	54.7
6	.....	.....	.....	.....	60.9	54.1	57.8	(52.6)	.....	.....	.....	.....	55.2	59.0	55.6	(57.1)
6.5	.....	.....	.....	.....	61.6	56.3	.....	.....	.....	.....	.....	.....	57.2	60.8	58.8	.....
7	.....	.....	.....	.....	.....	.....	.....	.....	.....	.....	.....	.....	58.1	62.4	(62.2)	.....
Extreme values	....	0′.38 0%	....	....	....	....	....	....	5′.20 (35.0)%	4′.73 (47.5)%	....	4′.21 (46.4)%	....	....	....	....
	....	5′.18 (46.2)%	....	5′.68 (46.2)%	....	....	....	....	....	....	....	....	....	....	....	....

the polarization curves close to the limb. (It should be mentioned that no extrapolation has been carried out in any part of this investigation.)

Table 7 presents the means of the polarization as a function of the distance from the sun's limb, giving separate values for the poles and the equator. Figures 10 and 11 show the 1932 and 1934 results in the violet, blue, and red. (Figure 10 gives values for the west only because of the large number of prominences in the east.) Results for unbacked plates—1932 in the red, and 1934 in the green—receive less weight than those derived from backed plates. The following remarks refer to the results obtained.

TABLE 7

POLARIZATION OF THE SOLAR CORONA
1932: MEAN VALUES

Distance from Sun's Limb in Minutes of Arc	SF 67, 68 No Filter	SF 69, 70, 71 No. 47 Filter	SF 72, 73, 74 No. 28 Filter
	North and South		
½	.....	.....	9.2%
1	.....	16.5%	20.3
1½	27.2%	23.1	28.7
2	30.0	26.1	32.3
2½	31.1	28.5	.....
3	.....	29.5	.....
3½	.....	29.9	.....
4	.....	32.9	.....
4½	.....	33.7	.....
5	.....	35.2	.....
	East and West		
1	28.1%	25.7%	.....
1½	30.1	38.1	18.3%
2	38.1	42.6	24.3
2½	39.7	47.8	25.5
3	39.9	50.8	.....
3½	41.6	48.7	.....
4	43.7	51.1	.....
4½	43.0	.....	.....
5	43.0	.....	.....
5½	45.0	.....	.....

TABLE 7—*Continued*

1934: MEAN VALUES

Distance from Sun's Limb in Minutes of Arc	SF 208, 212 No. 47 Filter	SF 209, 213 No. 36 Filter	SF 210 No. 75 Filter	SF 211, 215 No. 29 Filter
	North and South			
½			14.4%	6.4%
1		26.4%	17.9	13.0
1½	28.5%	28.2	18.7	23.3
2	34.1	28.8	19.1	27.6
2½	35.6	27.9	17.5	31.8
3	38.5	25.6		36.1
3½	39.2	23.4		38.9
4	41.1	22.2		41.2
4½	44.2			42.5
5				43.1
5½				42.6
	East and West			
½	31.2%			
1	34.0	31.9%		
1½	36.7	40.4	38.3%	23.6%
2	38.5	41.0	40.9	24.3
2½	41.2	42.6	42.6	27.0
3	43.9	44.5	42.7	31.0
3½	46.7	45.3	42.1	36.4
4	45.9	46.1	40.7	41.5
4½	46.5	46.4	37.3	46.5
5	47.5	45.9		50.6
5½	49.0	44.9		53.8
6	51.0	44.1		56.5
6½	53.3	43.3		58.9
7	55.4	41.8		60.9
7½	58.7	41.6		
8	59.6			

1. *The shape of the polarization curves.*—Exposures at short wave lengths were obtained first, and those at long wave lengths last, in 1932. Because of a possible interference of invisible water vapor which may form in the atmosphere during totality, we took the red exposures first and the blue exposures last in 1934. No systematic

difference is found in the 1932 and 1934 results which might be attributed to the formation of water vapor.

The shape of the polarization curves for short and long wave lengths is quite different The polarization in the integrated light, in

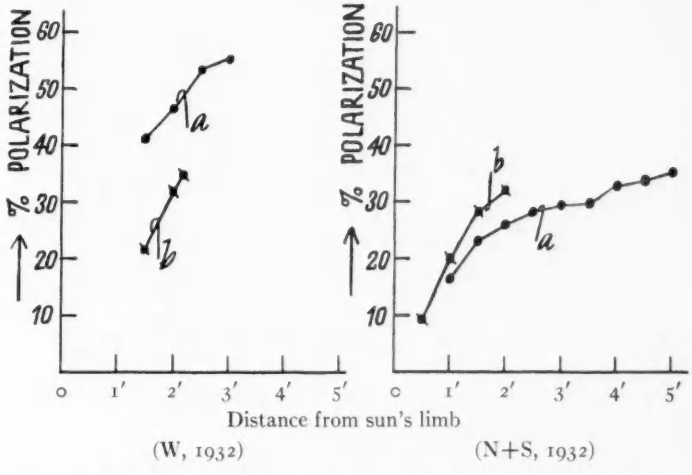

FIG. 10.—Polarization of the 1932 corona. a = blue, b = red curve

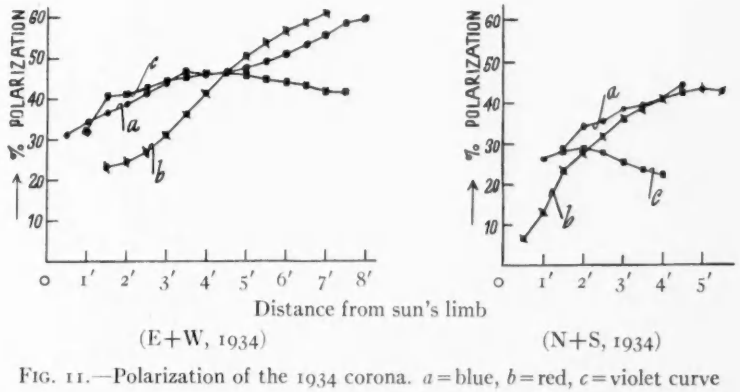

FIG. 11.—Polarization of the 1934 corona. a = blue, b = red, c = violet curve

the blue, and in the red increases steadily from the sun's limb toward the outer corona, whereas it reaches maxima in the violet and in the green, and then decreases again. These differences in the curves for short and long wave lengths are of particular interest.

The shape of the blue polarization curves is very similar in 1932

and 1934, values at the poles for 1934 being somewhat higher than those for 1932. Polarization curves in the violet, blue, and green start, as a rule, with comparatively high polarization values close to the limb. A few low values can be traced to the influence of prominences.

The results of 1932 and 1934 in the red agree quite well, showing considerable steepness of the curves, low polarization values close to the limb, and high values in the middle corona. This agreement is

TABLE 8

COMBINED POLARIZATION VALUES FOR 1932 AND 1934 IN THE BLUE AND RED REGIONS OF THE SPECTRUM

Distance from Sun's Limb in Minutes of Arc	North and South		East and West	
	No. 47 Filter	No. 28/29 Filter	No. 47 Filter	No. 28/29 Filter
½	.....	7.5%	.....	.....
1	19.6%	15.8	29.5%	.....
1½	25.3	24.7	37.5	19.6%
2	30.6	28.9	40.3	24.3
2½	32.6	31.8	44.1	26.6
3	34.3	36.1	46.8	31.0
3½	33.6	38.9	47.2	36.4
4	36.1	41.2	47.3	41.5
4½	37.2	42.5	46.5	46.5
5	35.2	43.1	47.5	50.6
5½	.....	42.6	49.0	53.8
6	.....	.....	51.0	56.5
6½	.....	.....	53.3	58.9
7	.....	.....	55.4	60.9
7½	.....	.....	58.7	.....
8	.....	.....	59.6	.....

very satisfactory because the 1934 plates were backed while the 1932 plates were not backed, and because the filter range was narrower in 1934 than in 1932. Table 8 contains the combined polarization results for 1932 and 1934 in the blue and red.

It should be mentioned that the lack of backing of some of the plates will tend to decrease the polarization values. Further factors tending to decrease the polarization values are: finite width of the microphotometer slits, poor guiding (in 1932), transmission of some weaker corona lines, and scattered light caused by the corona itself.

A very interesting phenomenon appears in many polarization curves. An additional polarization seems superimposed on part of the curves, for instance, in the blue curve of the equatorial corona of 1934 (Fig. 11), in which the superposition starts around $4'.5$. This type of curve seems particularly pronounced in the blue, both in 1932 and 1934, and appears occasionally in the integrated light. The polarization curves in the red do not show this effect; their general trend seems rather to approach a maximum or inversion point at a greater distance from the limb, such as was actually reached in the 1934 polar corona.

2. *Polarization at the poles and the equator.*—The polarization at small wave lengths is, for a certain distance from the limb, smaller at the poles than it is at the equator. The difference in polarization between the polar and the equatorial corona is less in the red than it is at short wave lengths.

The theory by Bergstrand[16, 21] that the polar corona is partly due to coronal streamers originating at low heliographic latitudes means that the superposition of the veil over the corona proper must also influence the polarization in the polar regions. It seems advisable to discuss, mainly, the equatorial parts of the corona where simpler conditions prevail.

3. *The influence of prominences on the polarization of the corona.*—The following position angles of Table 6 are affected by prominences: 80°, 90°, 100°, and 350° in 1932, and 90° and 280° in 1934. Besides these well-pronounced prominences, further tips of strong prominences appear in several 1932 and 1934 pictures. The majority of prominences appear in the red-filter exposures.

The influence of prominences on the isophotes does not exceed $\pm 5°$ from a certain position angle. The polarization values of the corona are greatly depressed close to a strong prominence, such as at 90° in the red and at 80° in the blue 1932 exposures. These strong prominences seem to shift the entire polarization curve to a greater distance from the limb. This will cause, for a certain distance from the limb, smaller polarization values close to a prominence than in the remainder of the corona. Faint prominences, such as at 100° in

[21] *Ark. Mat., Astron., Fys.*, **22**, A, No. 1, 1930; **25**, A, No. 4, 1934; *M.N.*, **95**, 436, 1935.

1932, and at 90° and 280° in 1934, have an influence on the polarization of the corona, not extending farther than 1′.5 from the limb. The polarization curve for a given position angle containing a prominence shows its influence mainly in the wave-length region in which the prominence appears, other spectral regions being not at all, or very slightly, influenced.

TABLE 9

POLARIZATION OF THE 1932 STREAMER, AS A FUNCTION OF THE DISTANCE FROM THE SUN'S LIMB

Distance from Sun's Limb in Minutes of Arc	SF 67, 68 Integrated Light	SF 69, 70, 71 No. 47 Filter	SF 72, 73, 74 No. 28 Filter
Extreme values	1′.58 15.2%	....	0′.25 0.9%
0′.5	.....	.....	8.3
1	.....	12.4%	(16.7)
1.5	.....	15.3	(25.6)
2	18.0	23.2	(34.6)
2.5	20.0	(27.0)	.....
3	22.3	(32.7)	.....
3.5	26.8	(38.7)	.....
4	33.5	(42.2)	.....
4.5	41.2	38.3	.....
5	(44.4)	37.3	.....
5.5	.....	38.2	.....
6	.....	40.1	.....
6.5	.....	42.6	.....
7	.....	46.8	.....
7.5	.....	48.6	.....
8	.....	51.4	.....
8.5	.....	(56.0)	.....
9	.....	(55.2)	.....
9.5	.....	(52.3)	.....

Negative polarization values were obtained in the red, very close to the limb, at 90° in 1932 and at 350° in 1934. These position angles contain a prominence and a very small area of intense blackening (tip of a prominence), respectively. The explanation for the negative values is found in a rotation of the plane of polarization by these prominences. Such rotations have been observed visually by Lyot.[22] (Lyot's measurements were carried out with more sensitive

[22] *C.R.*, **198**, 249, 1934; **202**, 392, 1936.

equipment than ours.) Former investigations by Prazmowski,[23] Dorsey,[24] and Newall[25] indicate very small polarization values of the monochromatic prominence radiations.

4. *The polarization of streamers.*—Streamers appear around position angles 330° of 1932 and 280° of 1934, each of these position angles containing a prominence. The 1932 streamer stands out clearly against the rest of the corona. It could be measured up to 9′.5 from the limb (see Table 9). The polarization curves for this streamer are similar in shape to the 1932 and 1934 coronal curves. The blue curve and the curve in integrated light seem shifted to greater distances from the limb than the corresponding 1932 and 1934 curves, resulting in smaller polarization values than in corresponding parts of the corona. The red curve tends to become negative very close to the limb, but no accurate reduction was possible here because of the great blackening of the plates. The red curve agrees well with the remainder of the 1932 and 1934 values. The 1934 streamer is far less distinct than the 1932 streamer, and no appreciable differences appear in the shape of the polarization curve and in the polarization values, compared with the remainder of the corona.

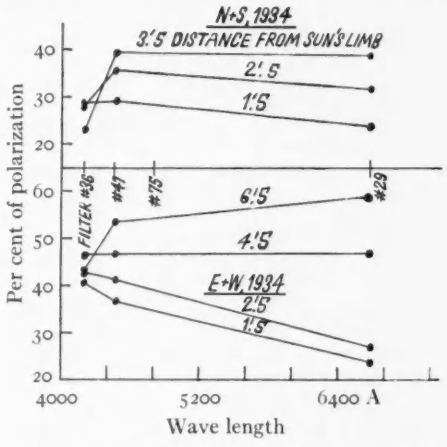

FIG. 12.—Polarization as a function of the wave length, 1934.

5. *Polarization as a function of the wave length.*—Figure 12 shows the mean values of the polarization as a function of the wave length for 1934, taking as abscissa the maximum effective transmission for each filter-plate combination in the violet, blue, and red regions of the spectrum (values in the green of less weight are omitted). The slope of the curves reverses itself from close to the sun's limb to the

[23] *Ibid.*, **51**, 195, 1860.

[24] *Pub. U.S. Naval Obs.*, **4**, IV, D117, 1906. [25] *M.N.*, **66**, 475, 1906.

middle corona. The curve for the equatorial corona is practically parallel to the abscissa at 4′.5 from the limb, indicating the point of intersection of the polarization curves.

6. *The plane of polarization.*—The plane of polarization of the corona was determined by two methods: (*a*) the isophotes for the two pictures of a plate were superimposed on each other, and the points of intersection for corresponding isophotes were determined; (*b*) intensity curves $l - r$ (Table 5) were drawn for a certain distance from the limb (such as 1′.0, 1′.5, etc.); since the values of $l - r$ change from positive to negative and vice versa in the various quadrants, the $l - r$-curves will give the position angle for $l - r = 0$, corresponding to the intersection of the isophotes.

TABLE 10

PLANE OF POLARIZATION

Plate	No Shift	Shift toward Equator	Shift toward Poles
SF 67	SE.	NE.	.....
SF 70	NW., SW.	NE.	SE.
SF 73	.....	NE., NW.	SE.
SF 208	NE., SE.	NW., SW.	.....
SF 209	NE., SE.	NW., SW.	.....
SF 210	.....	SW., SE.	NW., NE.
SF 211	NE.	NW., SW., SE.	.....

The results of this reduction are given in Table 10, which summarizes the large amount of data obtained. Figure 13 shows the results for plate SF 209. The results indicate that the polarization of the corona is not strictly radial. The plane of polarization is shifted frequently toward the equator of the sun, and, in a few cases, toward the poles. Two types of rotation of the plane of polarization occur: (1) the entire width of the corona shows this phenomenon uniformly —for example, the southwestern portion of SF 209, and (2) the region close to the limb shows a stronger rotation than parts of the corona farther away from the limb—for example, the northwestern portion of SF 209.

The rotation toward the equator does not exceed 12° in any plate. Plate SF 210 (of less weight) differs from the remaining 1934 plates,

indicating a shift toward the north. The 1932 plates and SF 208, 209, and 211 of 1934 show no influence of the wave length on the rotation of the plane of polarization, except that values in the red (SF 73, 211) show a slightly greater tendency of rotation toward the equator than the values at smaller wave lengths.

Rotations of the plane of polarization were obtained also by A. W. Wright,[26] Salet,[27] and Young,[12] most values of these authors pointing

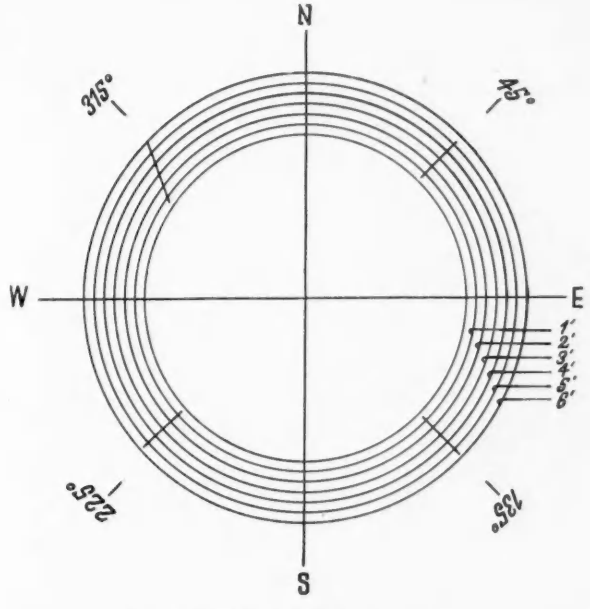

FIG. 13.—Plane of polarization, SF 209

to a rotation toward the equator, with a few exceptions in Young's results. Wright and Young assumed that the rotation was due to accidental errors, or to their optical systems, whereas Salet assumed it to be real and to be caused by the magnetic field of the sun. Since we obtained similar rotations both in 1932 and 1934 (using different optical parts in these eclipses), it seems that we must consider the deviations from radial polarization as real.

Two reasons for the rotation of the plane of polarization of all

[26] *Pub. U.S. Naval Obs.* (for 1876), App. III, 261, 1880.

[27] *Ann. Paris Obs.*, **27**, C1, 1910.

plates (except SF 210) may be offered: (1) the greater amount of polarization at the equator than at the poles will tend to cause a deviation from a strictly radial plane of polarization, and (2) the equatorial parts of a corona of minimum type are brighter than the polar parts; this will also tend to shift the plane of polarization toward the equatorial regions. Similar shifts of the plane of polarization occur in skylight, where the plane of polarization rotates toward the brighter-light source, for example, under the influence of clouds, snow-covered mountains, etc.[28] The shift in the corona will naturally be greatest close to the limb of the sun where the greatest brightness of the corona occurs.

IX. RESULTS OF VISUAL OBSERVATIONS

The photographic work in 1932 was supplemented by visual determinations because many former photographs of the corona are overexposed close to the limb of the sun. The polarization close to the limb was expected to be rather low, and the use of a very sensitive instrument seemed desirable. A Lyot polarimeter[29] was built with two tilting celluloid plates sensitive enough to detect and measure 0.1 per cent of polarized light. Dr. Lyot himself placed one of his polariscope systems at my disposal, additional optical parts being supplied by the Bausch and Lomb Optical Company. The polariscope was attached to a 6-inch Clark refractor of 94 inches focal length, the magnification being one hundred and fifty times. A fine pointer indicated the center of the field for the measurements. The free aperture of the objective was stopped down to 2 inches. The correction was determined for the polarization introduced by the objective, the eyepiece, and the celluloid films (refractive index, 1.5088; thickness, 0.013 mm).

Shortly after second contact, the plane of polarization was determined in integrated light. It showed a rotation of 1°.0 toward the east. The polarization was determined in integrated light and in the red, using the same filter as in the photographic work (Wratten No. 28). Further measurements which were planned for the blue (filter No. 47) were not possible because of lack of time. The results at

[28] C. Dorno, *Veröff. Preuss. Meteorol. Inst.*, **6**, No. 303, 1919.

[29] B. Lyot, "Recherches sur la polarisation de la lumière des planètes et de quelques substances terrestres," Thèses, Faculté des Sciences, Paris, 1929.

position angle 48°, 1'.3 from the sun's limb, are: 5.52 per cent polarization in integrated light and 6.96 per cent in the red.

The rotation of the plane of polarization and the polarization in the red agree well with the photographic results. We will compare later the visual result in integrated light with former work.

It was found, after the 1932 eclipse, that the polarization of the inner corona can be derived from the polarigraph plates, and visual measurements were discontinued in 1934. (Another reason for not recommending the use of the polariscope in 1934 was that the celluloid plates wrinkled at Laol Island, owing to the tropical climate.[30])

X. COMPARISON OF THE RESULTS WITH FORMER WORK

The first photographic polarization results were obtained by A. W. Wright;[26] work was later undertaken by Dorsey,[24] Newall,[25] Perrine (reduced by Young[12]), Lewis,[31] Gilbert,[32] and Fessenkoff.[33] The most complete data are those obtained by Young. Some of his results are presented in Figure 14. Young's plates had a sensitivity range similar to ours, but they were not backed, which tends to decrease the amount of polarization. The shape of Young's individual curves is similar to our own curves. Some of his curves reach maxima, then decrease again, and others show inversion points, with increasing values toward the middle corona. Young's polarization values in integrated light agree quite well with ours, taking into consideration that Young's values refer to distances from the moon's limb and our values to distances from the sun's limb, which is equivalent to a shifting of Young's curves to greater distances from the limb. This agreement between the two investigations is very interesting, since part of Young's

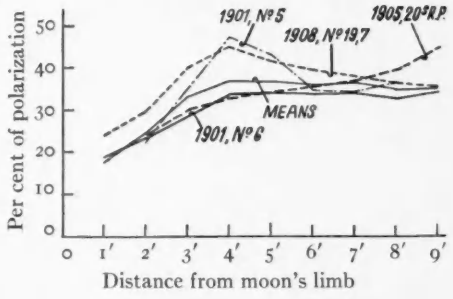

FIG. 14.—Polarization values derived photographically by Young in integrated light.

[30] W. M. Cohn, *Phys. Rev.*, **45**, 848, 1934; *Nature*, **134**, 99, 1934.

[31] *Lick Obs. Bull.*, **10**, 6, 1918.

[32] *Pub. U.S. Naval Obs.*, **10**, B192, 1926. [33] *Russ. Astr. J.*, **12**, 309, 1935.

data were determined from plates taken with the reflecting polarigraph and since difficulties were encountered in his photometric work (no intensity marks were available on the original plates).

Visual measurements by A. W. Wright[26] gave 11.9 per cent polarization for distances from 4′ to 10′ from the moon's limb; Wood[34] found 10 to 15 per cent for the entire corona, and Dorsey[24] 10.7 per cent at 8′ from the moon's limb (for further data see Mitchell[35]). Lyot's determinations without an eclipse[36] gave values ranging from 0.7 to 2.5 per cent at 1′20″ from the sun's limb. The most complete visual data of the polarization as a function of the distance from the moon's limb are those by Johnson,[37] who measured five points in 1934. Figure 15 contains the visual results by Dorsey, Lyot (mean value), Johnson, and our own visual result in integrated light. Johnson's curve shows an inversion point similar to our 1934 curves in that region. Lyot's values at a distance of 1′20″ from the sun's limb are higher at the equator than at the poles; this agrees with our own photographic results for small wave lengths. Lyot's mean visual value and our own visual value are in close agreement, showing a rather steep polarization curve close to the sun's limb.

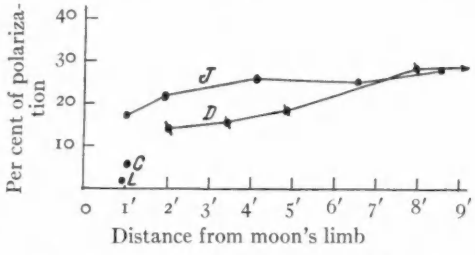

FIG. 15.—Polarization of the corona derived by the following authors: J = Johnson; D = Dufay and Grouiller, corrected for skylight; L = Lyot, without an eclipse; C = W. M. Cohn, visual value in integrated light.

Dufay and Grouiller[38] obtained polarization values spectographically in 1932. Figure 15 presents their results in the coronal region covered by Young's work and ours. Their polarization curves are identical between 4000 A and 5700 A. The shape of the polarization curve of Dufay and Grouiller, its numerical values, and the

[34] *Pub. U.S. Naval Obs.*, **4**, IV, D112, 1906.

[35] *Handb. d. Astrophys.*, **4**, 231, 1929.

[36] *C.R.*, **191**, 834, 1930; *Bull. Soc. Astr. France*, 1931, 248; *Zs. f. Ap.*, **5**, 73, 1932.

[37] *Pub. A.S.P.*, **46**, 226, 1934.

[38] *C.R.*, **196**, 1574, 1933; **203**, 453, 1936; *J. de Phys. et le Rad.*, **7**, 481, 1936.

spectral distribution are so different from those of all other investigators that the question arises if Dufay and Grouiller's results may not be influenced by scattering, etc., in their instrument, or by the presence of slight haze at their location, since only a small part of the sky seemed clear (every eclipse-observer knows how difficult it is to notice a slight amount of cloudiness or haze if only part of the sky becomes clear just before or during totality). Any scattering in the instrument or haze will decrease the polarization found. The only way to find out about haze during totality seems to be a special investigation, such as taking ultraviolet pictures.

XI. POLARIZATION OF SKYLIGHT CLOSE TO THE CORONA

Let us designate the skylight outside the shadow cone L_s, the skylight in the shadow cone L_m, and the earth shine L_e. The blackening of *CD* in Figure 4 represents L_s for image *GHIKLM* plus L_m for *ABCDEF* plus L_e for *ABCDEF*. (The illumination by coronal light is so small as to be negligible, and the shape of the coronal curves excludes the possibility of an influence of the outer corona on *CD* and *IK*.)

The amount of blackening of the ordinary and extraordinary images *CD* and *IK* is, within the limits of accuracy, identical. Since L_e would cause polarized light, we conclude that L_e is negligible. L_m is due to secondary or multiple scattering of sunlight (and, perhaps, self-luminescence of the atmosphere), which is assumed to be unpolarized. The polarization of L_s is determined as follows: The center line of *CD* corresponds to position angle 180°, and that of *IK* to 0° (with reference to *GHIKLM* and *ABCDEF*). *CD* and *IK* extend in 1932 from 0°.55 to 1°.09 from the sun's limb, and in 1934 from 0°.69 to 1°.25, the average being 0°.9. We can determine the polarization of L_s if we know the relative intensity of L_s at a distance of 0°.9, in position angles 0° and 180° (outside the corona).

Microphotometer measurements show that the background of all plates (*PA*, *FG*, *MQ*, of Fig. 4) is uniform over the entire field covered (8°.1×7°.3 and 4°.8×4°.6, respectively), with the exception of SF 74 and SF 210. This means that the sum of the ordinary and extraordinary images of L_s remains, as a rule, the same over the entire field. It seems unlikely that the blackening of one sky image

decreases exactly by the same amount by which that of the second image increases. The assumption seems more justified that both sky images remain of constant relative intensity. Making use of this assumption for an average distance of 0°.9 from the sun's limb, we use CD and IK for determining the polarization of L_s.

The blackening of CD and IK can be determined (against the chemical fog of the plate) for SF 67, 70, 71, 72, 208, 209, and 211. The result is that the blackening of CD and IK is, within the limits of accuracy, equal for the ordinary and extraordinary images of a plate. The conclusion is drawn that the entire skylight close to the corona is, between 42′ and 65′ from the limb, unpolarized in integrated light and in the violet, blue, and red spectral regions covered in our work. Further data are presented elsewhere.[39]

Attempts were made to measure visually, during the 1932 totality, the polarization of the dark disk of the moon. The 6-inch refractor with a Lyot polariscope (see Sec. IX) and a Martens polarization photometer, used for measurements of skylight polarization at a greater distance from the sun,[30] were directed toward the dark disk of the moon; but no polarization could be determined. This is in agreement with the photographic results.

XII. DISCUSSION OF THE RESULTS

1. The polarization values obtained for short and long wave lengths permit conclusions with regard to the *distribution of particle sizes* in the corona. Experimental and theoretical work by Tyndall,[40] Rayleigh,[41] von Helmholtz,[42] Mie,[43] Debye,[44] and others shows that scattering of unpolarized light produces (perpendicularly to the incident beam) the same polarization for all wave lengths if infinitely small particles are present. Schwarzschild[45] showed that the polarization is uniform over the entire spectrum for free electrons or molecules with infrared oscillations.

The polarization decreases from short toward long wave lengths

[39] W. M. Cohn, "Polarization of Skylight Close to the Sun" (unpublished).

[40] *Proc. R. Soc. London*, **17**, 92, 223, 317, 1868–69; *Phil. Mag.*, **37**, 241, 384, 1869.

[41] *Ibid.*, **41**, 107, 274, 1871; **47**, 375, 1899.

[42] *Wiedem. Ann.*, **32**, 1, 1887.

[43] *Ann. d. Phys.*, **25**, 377, 1908.

[44] *Ibid.*, **30**, 57, 1909.

[45] *Astron. Mitt. Göttingen*, **13**, 1906.

as long as the particles obey, over the entire spectrum, the relation $(2\pi r/\lambda) < 1$, r being the radius of the scattering particles.

The addition of larger particles reverses the slope of the polarization curve, and the polarization at long wave lengths becomes higher than that at short wave lengths (see the experiments by Pernter,[46] von Hauer,[47] Laski,[48] and others).

There exists a distribution of particle sizes, between the extremes of maximum polarization at short and long wave lengths, for which the polarization is uniform over the entire spectrum. Such conditions have occasionally been observed by Nichols,[49] Raman and Seshagiri,[50] and Kalitin.[51]

Our polarization results, which are most complete for the 1934 equatorial corona, show, close to the limb, the largest amount of polarized light for short wave lengths; the polarization becomes uniform at $4'.5$; and at greater distances the polarization is highest for long wave lengths. The conclusion is drawn that the *average particle size in the corona increases from close to the limb toward the outer corona*. A rough calculation shows that close to the limb the average particle diameter amounts to less than 100 $m\mu$; and beyond $4'.5$, to less than 170 $m\mu$. The latter value is small compared with long wave lengths but large compared with short ones. (Lack of data for the refractive index of coronal matter prevents the use of the tables by Blumer.[52]) These dimensions are of similar magnitude to those derived by Schoenberg and Jung[53] for interstellar material, and by J. Rudnick[54] for certain B-type stars. We are not in a position to decide whether the scattering is due to metallic or dielectric particles, since both types will cause, for diameters of about 170 $m\mu$, a greater polarization in the red than in the blue (Mie's theory). Our results do not indicate whether the coronal particles are neutral or ionized. Taking into consideration high temperature, ultraviolet emission, emission lines of the corona, etc., we conclude that at least

[46] *Denkschr. K. Akad. Wiss. Wien*, **73**, 301, 1901.

[47] *Ann. d. Phys.*, **57**, 145, 1918.

[48] *Phys. Zs.*, **19**, 369, 1918.

[49] *Phys. Rev.*, **26**, 497, 1908.

[50] *Phil. Mag.*, **46**, 426, 1923.

[51] *Meteorol. Zs.*, **43**, 132, 1926.

[52] *Zs. f. Phys.*, **32**, 119, 1925; **38**, 304, 1926.

[53] *A.N.*, **253**, 261, 1934.

[54] *Ap. J.*, **83**, 394, 1936.

part of the coronal particles are composed of ions which should be in equilibrium with free electrons.

It seems most likely that free electrons and small and large particles are found in the entire corona and that only their relative number changes in the various parts of the corona. Our result that the coronal polarization is independent of the wave length at $4'.5$ seems rather due to the transition between two distributions of particle sizes than to the presence of free electrons only at this distance from the limb. One may readily assume that the observed increase of average particle size will finally lead to a prevalence of large particles, according to Grotrian's theory.[55]

The increase of average particle size as a function of the distance from the limb explains the appearance of sharp Fraunhofer lines at about $5'$ from the limb, observed by Moore[56] and others: A sufficient number of particles of less than 170 $m\mu$ will reflect sunlight of short wave length, whereas the light of long wave length is scattered, according to Rayleigh's law. We are led to expect here Fraunhofer lines at short, but not at long, wave lengths. Obervations have been made, so far, with plates sensitive to short wave lengths. It will be interesting to see if Fraunhofer lines appear in the red with increasing distance from the limb.

The particle size in the middle corona is close to 200 $m\mu$, a value derived under simplifying assumptions by Schwarzschild,[57] Arrhenius,[58] and Mitchell,[59] for which gravitation and radiation pressure will compensate each other, keeping the particles in equilibrium. Most of the particles close to the limb are of such size that they should move away from the sun. Such a movement of coronal matter was actually observed by Moore[60] in the middle corona. This seems due, then, to the action of radiation pressure on the small particles which we find in the inner corona. It will be seen that the combined action of gravitation and radiation pressure in the corona is similar to that found by Trumpler[61] for nebular matter.

[55] *Zs. f. Ap.*, **8**, 124, 1934. [56] *Pub. A.S.P.*, **35**, 59, 1923; **46**, 298, 1934.

[57] *Sitz.-Ber. Akad. Wiss. München, math.-nat. Kl.*, **31**, 293, 1901.

[58] *Ap. J.*, **20**, 224, 1904; *Lick Obs. Bull.*, **2**, 188, 1904.

[59] *Ap. J.*, **20**, 63, 1904. [60] *Pub. A.S.P.*, **35**, 333, 1923. [61] *Ibid.*, **42**, 214, 1930.

The presence of small particles in the inner corona leads one to expect a shift of the maximum of the coronal emission toward the blue as compared to the continuous emission of the sun. Such a shift exists, as shown in the accurate measurements by Grotrian and Ludendorff,[62] although it is small and is just within the limits of accuracy given by Grotrian. We are led to assume that the reason for the small shift in the inner corona is the presence of larger particles, as suggested by Struve, Elvey, and Keenan[63] for certain nebulae, and the emission of light by the corona itself.

Grotrian found in the middle corona the same shift toward the blue. We find in the middle corona a preponderance of greater particle sizes, which should cause a shift toward the red. It is difficult to explain this fact unless one assumes an additional emission of the corona proper, which is relatively greater at short wave lengths than the emission of the sun. We have suggested[64] that such an emission may be due to a luminescence radiation with continuous spectrum (caused by electron impact on coronal particles) superimposed on the temperature radiation. This type of luminescence radiation has also been observed, in the meantime, for slow electrons, by Lossev[65] and Claus.[66]

Unpolarized light scattered perpendicularly to the incident beam by particles infinitely small compared to the wave length will be completely polarized. The incomplete polarization of the corona may be caused by three factors: (*a*) increasing particle size; (*b*) deviations from spherical shape of the particles; and (*c*) emission of the corona proper, which may be temperature or luminescence radiation. A calculation shows that factors (*a*) and (*b*) alone cannot account for the polarization values obtained. Factor (*c*) seems of great importance and will be discussed presently.

2. An attempt was made to compute the emission proper of the 1934 corona, following Schuster,[67] Young,[12] and Minnaert.[68] Let J_t and J_r be the tangential and radial components of the scattered

[62] *Zs. f. Ap.*, **3**, 199, 1931.
[63] *Ap. J.*, **77**, 275, 1933.
[64] W. M. Cohn, *A.N.*, **245**, 378, 1932.
[65] *Phil. Mag.*, **6**, 1024, 1928; *Phys. Zs.*, **32**, 692, 1931.
[66] *Phys. Zs.*, **31**, 360, 1930; *Ann. d. Phys.*, **11**, 331, 1931.
[67] *M.N.*, **40**, 35, 1879.
[68] *Zs. f. Ap.*, **1**, 209, 1930.

light, and $2A$ the emission proper of the corona; then the polarization is

$$p = (\pm 1) \cdot \frac{J_t - J_r}{J_t + J_r + 2A}.$$

(The factor ± 1 enters because of the position-angle correction, positive values being used around 0° and 180°, and negative values around 90° and 270°.)

Table 11 contains $J_t + J_r + 2A$, equal to the sum of the relative

TABLE 11

ANALYSIS OF RESULTS

$\lambda = 4460$ A, $U = 0.79$

Distance from Sun's Limb in Minutes of Arc	Observed Values			Calculated Values		
	J_t+J_r+2A	p	J_t-J_r	J_t-J_r	J_t+J_r	$2A$
	SF 208, North					
1½	368.5	0.285	104.9	105	295	74
2	249.0	.324	80.6	79	213	36
2½	175.5	.343	60.2	60	166	10
3	121.5	.369	44.9	45	119	3
3½	87.0	.392	34.1	35	90	−3
4	62.0	.411	25.5	25	62	0
4½	47.0	0.442	20.8	20	41	6
	SF 208, East and West					
1	1754.7	0.310	544.0	546	1742	3497
1½	1219.8	.367	447.7	432	1170	2390
2	803.4	.385	309.3	327	909	1712
2½	587.6	.412	242.1	250	752	1340
3	454.0	.439	199.3	195	561	1015
3½	353.5	.467	165.1	156	437	791
4	274.4	.459	125.9	119	336	610
4½	214.4	.465	99.7	106	246	460
5	172.5	.475	81.9	90	200	373
5½	139.4	.490	68.3	60	182	321
6	114.6	.510	58.4	61	146	261
6½	93.6	.533	49.9	49	152	246
7	78.8	.554	43.7	42	128	207
7½	68.7	.587	40.3	41	140	209
8	56.7	0.596	33.8	33	134	191

TABLE 11—*Continued*

$\lambda = 4190$ A, $U = 0.83$

Distance from Sun's Limb in Minutes of Arc	Observed Values			Calculated Values		
	J_t+J_r+2A	p	J_t-J_r	J_t-J_r	J_t+J_r	$2A$
	SF 209, North					
1	416.5	0.269	112.0	112	310	107
1½	272.5	.293	79.7	81	194	79
2	191.5	.298	57.1	56	141	51
2½	141.0	.281	39.6	40	136	5
3	108.5	.254	27.5	28	108	1
3½	86.5	.238	20.6	21	93	−6
4	72.0	0.230	16.6	16	73	−1
	SF 209, East and West					
1	1512.7	0.320	484.1	489	1526	3039
1½	989.0	.404	399.6	383	1048	2037
2	702.5	.410	288.0	298	808	1511
2½	525.5	.426	223.9	233	652	1178
3	411.4	.445	183.1	181	491	902
3½	323.0	.453	146.3	143	390	713
4	259.0	.461	119.4	113	293	552
4½	209.8	.464	97.3	98	213	423
5	173.5	.459	79.6	81	172	346
5½	142.0	.449	63.8	65	156	298
6	118.5	.441	52.3	55	126	245
6½	104.3	.433	45.2	41	127	231
7	91.5	.418	38.2	37	108	200
7½	79.0	0.416	32.9	37	117	196

$\lambda = 4810$ A, $U = 0.74$

Distance from Sun's Limb in Minutes of Arc	Observed Values			Calculated Values		
	J_t+J_r+2A	p	J_t-J_r	J_t-J_r	J_t+J_r	$2A$
	SF 210, East and West					
1½	1093.3	0.383	418.7	420	1313	2406
2	852.8	.409	348.8	348	993	1846
2½	672.3	.426	286.4	288	730	1402
3	546.8	.427	233.5	231	552	1099
3½	447.0	.421	188.2	189	408	855
4	369.7	.407	150.5	148	267	637
4½	313.5	0.373	116.9	120	207	521

TABLE 11—*Continued*

$\lambda = 6670$ A; $U = 0.47$

Distance from Sun's Limb in Minutes of Arc	Observed Values			Calculated Values		
	J_t+J_r+2A	p	J_t-J_r	J_t-J_r	J_t+J_r	$2A$
	SF 211, North and South					
1	1258.8	0.130	163.6	163	520	739
1½	859.3	.233	200.2	201	578	281
2	632.5	.276	174.6	174	431	202
2½	458.8	.318	145.9	146	326	133
3	331.0	.361	119.5	120	272	59
3½	222.5	.389	86.6	86	183	40
4	167.0	.412	68.8	70	139	28
4½	134.3	.425	57.1	56	109	25
5	102.8	.431	44.3	45	90	13
5½	85.0	0.426	36.2	36	58	27
	SF 211, East and West					
1½	1590.0	0.236	375.2	374	977	2567
2	1409.5	.243	342.5	344	883	2293
2½	1224.3	.270	330.6	330	753	1977
3	1052.3	.310	326.2	326	736	1788
3½	893.8	.364	325.3	326	671	1565
4	750.3	.415	311.4	310	591	1341
4½	620.5	.465	288.5	289	571	1192
5	501.8	.506	253.9	253	424	926
5½	407.3	.538	219.1	219	381	788
6	329.3	.565	186.1	186	310	639
6½	275.2	.589	162.1	163	244	519
7	228.0	0.609	138.9	139	231	459

intensities of both coronal pictures on a plate. Separate data are given for the polar and the equatorial corona. (No data are presented for the polar corona of SF 210 and for the south portion of SF 208 and 209, because of the small number of data available.) Column 4 gives $J_t - J_r$, as observed.

Assuming a decrease of the coronal density according to r^{-4}, r^{-6}, and r^{-8}, we have computed, for our wave lengths, theoretical values for $J_t - J_r$ and J_t; the darkening at the sun's limb was taken into consideration by applying Minnaert's U-values. Equations were de-

rived, using the method of least squares and solving by means of determinants for $J_t - J_r$ (col. 5 of Table 11) and J_t, which leads to J_r, $J_t + J_r$, and $2A$.

The agreement between the observed and calculated values of $J_t - J_r$ was rather close for SF 208, 209, and 210 but was less satisfactory for SF 211. SF 211 was recalculated, using the trial-and-error method of Minnaert. I am very grateful to Dr. Minnaert for computing part of the values for SF 211. The agreement between

TABLE 12

EMISSION PROPER OF THE 1934 EQUATORIAL CORONA, $2A$, REDUCED TO $2' = 100$

Distance from Sun's Limb in Minutes of Arc	SF 208	SF 209	SF 210	SF 211
1	204	201	.....	.....
1½	140	135	130	112
2	100	100	100	100
2½	78	78	76	86
3	59	60	60	78
3½	46	47	46	68
4	36	37	35	58
4½	27	28	28	52
5	22	23	.....	40
5½	19	20	.....	34
6	15	16	.....	28
6½	14	15	.....	23
7	12	13	.....	20
7½	12	13	.....	.....
8	11	.....	.....	.....

the observed and the calculated values of $J_t - J_r$ is now very satisfactory (Table 11). The possible presence of the veil superimposed on the corona proper, according to Bergstrand, makes it difficult to interpret the values of the polar corona.

The emission proper of the equatorial corona is presented in Table 12 in which the emission at $2'$ is arbitrarily set equal to 100. The emission of the corona decreases, at all wave lengths, from the limb toward the middle corona. The emissions in the violet, blue, and green coincide very closely. This is very interesting, since the polarization curves of SF 208 and 209 show considerable differences, par-

ticularly beyond 4′.5 from the limb (Fig. 11). The coronal emission at great wave lengths differs considerably from that at small wave lengths. The coronal emission derived by Minnaert from Young's values is in close agreement with our curves for short wave lengths.

TABLE 13

RELATIVE INTENSITY, POLARIZATION, AND EMISSION PROPER PER VOLUME ELEMENT OF THE 1934 EQUATORIAL CORONA

Distance from Sun's Limb in Minutes of Arc	Values per Volume Element Reduced from Observation			Calculated Values		
	$(J_t+J_r+2A)_I$	p_I	$(J_t-J_r)_I$	$(J_t-J_r)_I$	$(J_t+J_r)_I$	$2A_I$
	SF 208, East and West					
1	2087	0.277	578.1	578	1492	3579
2	847	.349	295.7	296	704	1551
3	435	.426	185.3	186	349	784
4	245	.443	108.5	108	199	444
5	145	.451	65.4	65	113	258
6	98	0.498	48.8	49	75	173
	SF 209, East and West					
2	765	0.400	306.0	306	716	1481
3	376	.438	164.7	165	331	707
4	215	.476	102.3	102	192	407
5	136	0.478	65.0	65	109	245
	SF 211, East and West					
2	1123	0.115	129.1	129	247	1370
3	797	.175	139.5	139	284	1081
4	604	.302	182.4	183	360	964
5	427	.439	187.5	188	348	775
6	(266)	(0.558)	(148.4)	(148)	(260)	(526)

The emission proper of the corona close to the limb is relatively greater at short than at long wave lengths, this ratio being reversed beyond 4′.5. The result seems to indicate a coronal radiation of a temperature gradually decreasing up to 4′.5 from the limb and then slightly increasing again, or a corresponding combination of temperature and luminescence radiation.

3. A coronal picture represents the projection of a spherical shell on the celestial sphere, the central part of which is obscured by the moon. An attempt was made to determine the polarization per volume element, p_I, of the 1934 equatorial corona. The problem is similar to determining the space-distribution law of stars in globular clusters, as discussed by von Zeipel,[69] Plummer,[70] Trumpler,[71] and Wallenquist.[72]

The equatorial corona was assumed to be of globular symmetry. Taking the outmost radius of the corona equal to 100, we obtained a number of successive spherical shells by dividing 100 by the number of minutes of the corona counted from the moon's center. Separate equations were derived for the tangentially and radially polarized images of each plate, and relative intensities per volume element were computed. The equations followed Wallenquist's work, which is quite similar to the method used by Trumpler. It was necessary to carry out computations also for those parts of the outer corona which were not used in the original calculations, since they influence the inner corona (such as image *l*, Table 5, values for distances $> 3'.5$).

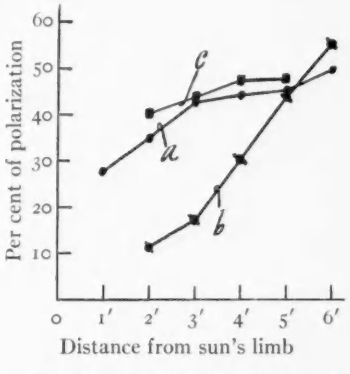

FIG. 16.—Polarization per volume element of the 1934 equatorial corona. *a* = blue, *b* = red, *c* = violet curve.

Intensities and polarization values per volume element were determined for individual position angles of the equatorial corona of SF 208, 209, and 211 (SF 210 contains too small a number of points for obtaining a curve). The results are presented, as a function of the distance from the sun's limb, in columns 2 and 3 of Table 13. No values are given close to the outer limits of the corona because of the uncertainty of determining the exact limits of the outermost shell. Figure 16 presents the p_I-curves.

[69] *Ann. Paris Obs.*, **25**, F1, 1908.

[70] *M.N.*, **71**, 460, 1911.

[71] *Lick Obs. Bull.*, **12**, 10, 1925. [72] *Ann. Bosscha Sterrenw. Lembang*, **4**, 47, 1933.

The general trend of the p- and p_I-curves is the same, the point of intersection of the curves being shifted from $4'.5$ to $5'.2$. This means that our former conclusions regarding the distribution of particle sizes in the corona remain, essentially, the same.

The p_I-values are, as a rule, smaller than the corresponding p-values, with the exception of the violet curve. The explanation of this result is that the observed p-values of SF 208 and 211 are higher in the middle than in the inner corona, and those of SF 209 decrease in the middle corona. It should be noted that the decrease of p_I against p in the red is most pronounced, and an extrapolation of the p_I-curve points to zero polarization at the limb.

TABLE 14

EMISSION PROPER, PER VOLUME ELEMENT, OF THE 1934 EQUATORIAL CORONA, $2A_I$, REDUCED TO $2' = 100$

Distance from Sun's Limb in Minutes of Arc	SF 208	SF 209	SF 211
1	231	.....	.....
2	100	100	100
3	51	48	79
4	29	27	70
5	17	17	57
6	11	.....	(38)

4. Table 13 contains, furthermore, the emission proper per volume element, $2A_I$. The trial-and-error method gave the most satisfactory agreement between the observed and the calculated values of $(J_t - J_r)_I$. $2A_I$ shows curves similar to those obtained for $2A$. Table 14 presents data for the emission proper reduced again for $2'$ equal to 100. We find a close agreement between the $2A_I$-values for SF 208 and 209 and a different curve for SF 211. The $2A_I$-curves for small wave lengths are somewhat steeper than those for $2A$, and the difference between short and long wave lengths is greater for $2A_I$ than it is for $2A$. This seems to indicate a decrease in the temperature (or temperature *plus* luminescence) radiation per volume element of the corona up to $6'$ from the limb. The decrease

is slightly steeper than was concluded from the data of 2*A* in the preceding reduction.

In concluding, I wish to acknowledge the help I have received from many sources. Grants were made, in 1932, by the Rumford Fund, and, in 1932 and 1937, by the Permanent Science Fund of the American Academy of Arts and Sciences. Director Harlow Shapley, of the Harvard College Observatory; Directors R. G. Aitken and W. H. Wright, of the Lick Observatory; Professor L. Campbell, of the Harvard College Observatory; the A.A.V.S.O.; and Professor A. C. Hardy, of the Massachusetts Institute of Technology, placed at my disposal equipment for building the apparatus used. Dr. B. Lyot, of Meudon, provided optical parts for the polariscope; Mr. C. W. Elmer, of the Custer Observatory, loaned the refractor in 1932; Dr. W. E. Forsythe, of Nela Park, Cleveland, Ohio, calibrated the standard lamp and placed an optical pyrometer at my disposal. Dr. A. D. Little, of Cambridge, Massachusetts, and Mr. Charles S. Ash, of San Francisco, California, permitted the use of their workshops. Messrs. C. A. Mayer, of Cambridge, Massachusetts, and J. E. Dimick and A. Schaar, of Berkeley, California, helped in building the instruments and the equipment.

Mr. and Mrs. A. J. Small, of Gray, Maine, made our stay at their farm in 1932 pleasant and profitable; the imperial Japanese government provided transportation to the Losap Islands by the cruiser H.I.J.M.S. "Kasuga" in 1934; the National Research Council of Japan helped the expedition in many ways; and the South Seas government provided the facilities for work in the tropical islands.

Professors A. O. Leuschner and C. D. Shane, of the astronomical department of the University of California, helped with many suggestions in this work. Professor R. T. Birge, chairman of the physics department of the University of California, permitted the use of the Zeiss microphotometer. Professor W. F. Meyer, of the astronomy department of the University of California, suggested the polar-axis assembly of 1934. I am much obliged to Drs. J. H. Moore and R. J. Trumpler, of the Lick Observatory, and to Dr. M. Minnaert, of Utrecht, for helpful discussions of this work.

Among the many others to whom I am indebted, I must name Professors K. Hirayama, K. Sotome, and J. Ueta, and Commander T. Akiyosi, I.J.N., of Japan; my assistants at Gray, Maine, Mrs. Margaret Walton Mayall, Mr. R. N. Mayall, Mr. R. Leary, and Mrs. Sibylla Tolksdorf Cohn; and my assistants at the Losap Islands, Mr. T. Hirai, of the Astronomical Institute, Kyoto Imperial University, and Mr. Schmidt. To all of these, and to many other friends who so generously helped me in this work, I wish to express my heartiest thanks.

BERKELEY, CALIFORNIA
June 1937

ATOMIC LINES IN THE SPECTRUM OF ANTARES

DOROTHY N. DAVIS

ABSTRACT

A complete study of the spectrum of Antares ($1^{M}22$, cM1) involves the identification of both atomic and molecular lines. A detailed study has been made of all atomic lines found on high-dispersion plates. When atomic lines had been eliminated, a preliminary investigation of the molecular bands was undertaken. Comparisons have been made throughout with the behavior of lines in the spectra of the Sun and Arcturus ($0^{M}24$, K0).

A table of 3625 wave lengths, estimated intensities, and identifications in the spectrum of Antares for the region λλ 3600–6600 has been compiled. A study of the atomic lines has yielded definite evidence for the presence of 29 elements: *H*, *Na*, *Mg*, *Al*, *Si*, *Ca*, Ca^+, *Sc*, Sc^+, *Ti*, Ti^+, *V*, V^+, *Cr*, Cr^+, *Mn*, *Fe*, Fe^+, *Co*, *Ni*, *Cu*, *Zn*, *Sr*, Sr^+, *Y*, Y^+, *Zr*, Zr^+, *Ru*, Ba^+, La^+, Ce^+, Pr^+, Nd^+, Sa^+, Eu^+, Gd^+, and Dy^+. The identification of 16 elements is questionable. For 10 elements the stellar data are insufficient, mainly because the ultimate lines lie beyond the limits of the plates available. For 6 elements laboratory data are insufficient. Of the remaining 31 elements which are apparently absent, 5 are not expected to be detectable because of low abundance and large atomic weight, and 20 have inaccessible ultimate lines. In the latter group are 5 elements—*B*, *C*, *N*, *O*, and *F*—whose presence is established by molecular evidence.

Details of identifications are discussed for 68 atomic spectra, but details for molecular spectra have not been included in the present paper. As expected, there is abundant evidence to indicate that the temperature of Antares is lower than that of Arcturus.

The hydrogen lines are excessively strong. Yttrium lines, which are very weak in the spectrum of Arcturus, are strong in Antares. The *H* and *K* lines are doubly reversed and are the strongest lines in the spectrum. The unusual strength of the Ca^+, Ba^+, and Sr^+ lines must be largely due to the exceedingly low surface gravity and the great extent of the Antares atmosphere.

Antares ($1^{M}22$, cM1) is trigonometrically a giant but spectroscopically a supergiant.[1] Interferometer measures have shown that the radius of this star is 480 times that of the sun. The extremely low surface gravity, about 1/7600th that of the sun, must exert a large influence upon the character of the spectrum. The temperature of Antares has been determined by several methods, which have yielded values ranging from 2620° K to 3100° K.

The variable radial velocity of Antares was confirmed in 1906 by W. H. Wright.[2] The velocity varies in a semiregular period of 7.4 years, with a small amplitude of about 6 km/sec. Antares has been treated as a spectroscopic binary,[3] but Dr. J. H. Moore[4] has chosen

[1] F. Schlesinger, *Second General Catalogue of Stellar Parallaxes*, 1935; J. A. Hynek, *Pub. A.S.P.*, **48**, 260, 1936.

[2] *Lick Obs. Bull.*, **4**, 98, 1906. [3] *M.N.*, **88**, 669, 1928. [4] *Lick Obs. Bull.*, **18**, 1, 1936.

to regard Antares as a single star of variable velocity, and has eliminated it from his catalogue of spectroscopic binaries. Because of the unusual strength of the hydrogen lines, the spectrum of Antares has been described as "composite."[5] There are, however, good reasons for believing that the spectrum described here is due to a single star in which unusual conditions prevail.

THE OBSERVATIONAL MATERIAL

The present study is based upon 4644 measurements of lines and bands found on 14 plates which were carefully selected from the ex-

TABLE 1

DATA FOR PLATES MEASURED

Plate	Region	Dispersion (A/Mm)	Date	Number of Measurements	Spectrograph Note	Radial Velocity
1096	λλ 3585–4270	5.58–10.0	1936 Aug. 5	460	1	+0.30
1400[1]	4035–4274	3.08	1937 June 26	515	2	−2.60
1400[2]	4318–4526	3.09	1937 June 26	515	2	−3.51
654	4181–4466	8.02–12.41	1905 Mar. 22	330	3	+0.42
12[1]	4305–4571	2.86– 3.61	1926 June 30	290	4	.....
12[2]	4580–4984	3.74– 5.09	1926 June 30	410	4	−5.6
9378	4395–4623	9.65–12.85	1917 Aug. 3	300	5	−2.17
17374	4527–4623	11.19–12.78	1930 June 20	85	5	.....
633[1]	4966–5367	5.61	1933 Apr. 11	450	6	−4.91
650[2]	5358–5373	5.72	1933 May 3	15	6	.....
654[2]	5371–5778	5.67	1933 May 4	450	6	−3.98
650[3]	5775–6183	5.69	1933 May 3	412	6	−5.14
633[3]	6168–6197	5.66	1933 Apr. 11	27	6	.....
654[4]	6192–6597	5.67	1933 May 4	385	6	−3.79
Total...	.....	.....	.....	4644	.....	.....

NOTES TO TABLE 1

1. Nine-foot ultraviolet prism (Mount Wilson).
2. Nine-foot grating, second order (Mount Wilson).
3. Three-prism Southern Mills (Chile).
4. Fifteen-foot prism (Mount Wilson).
5. Three-prism Mills (Lick).
6. Nine-foot grating, first order (Mount Wilson).

cellent collections of plates at the Mount Wilson and Lick observatories. The data for these plates are contained in Table 1. Most of the columns need no explanation. In the third column the dispersion

[5] A. C. Maury, *Harvard Ann.*, **28**, 189, n. 212, 1897.

is given for each end of the prism plates. For the grating plates the average dispersion is quoted.

The plates were measured and reduced in the usual manner. Radial velocities ranging from -5.6 to $+0.42$ km/sec were obtained. From a study of 902 unblended lines, it was found that the average residual in wave length (taken without regard to sign) for a given plate does not exceed ± 0.025 A.

Systematic displacements of a few lines were observed as follows: *Ca*$^+$, -11.3 km/sec; *Na*, -4.86 km/sec; *H*, -6.0 km/sec. A preliminary study of the lines of other elements has shown that relative shifts are small or unsystematic.

The intensities of the lines were estimated visually at the time of measurement. The meaning of the numbers in the arbitrary intensity scale is as follows: 0–2, faint; 2–5, moderately faint; 6–8, moderately strong; 9–15, strong; 16 and greater, very strong.

Identifications were assigned when possible. An important basis for assigning identifications was provided by the behavior of lines in multiplets and the theoretical intensities of multiplet lines. For this work, Dr. C. E. Moore's *Multiplet Table* was of the utmost utility. Before proceeding with the final identifications, a comparison of the behavior of unblended Antares lines in the solar, the sun-spot, and the Arcturus[6] spectra was made for many of the elements. This work formed the basis for making decisions about blended lines, which outnumber the unblended lines by more than three to one.

A table of 3625 wave lengths, intensities, and identifications in the region λλ 3600–6600 has been compiled. Because of the expense of printing, the list cannot be published at this time. Anyone desiring a copy may obtain one upon application to the writer.

A study of the molecular lines and bands has also been made; but the results cannot be included in the present paper, which will deal solely with the atomic lines.

DISCUSSION OF ATOMIC SPECTRA

A few notes on identifications for 68 spectra are contained in the following pages, where the elements are discussed in the order of atomic number. Since no discussion is possible for elements lacking

[6] S. G. Hacker, *Princeton Obs. Pub.*, No. 16, 1935; *Ap. J.*, **83**, 140, 1936.

strong lines in the observed region, lines of Co^{+}, *Rh*, *Pd*, *Cd*, and others are not discussed below.

H.—The hydrogen lines are second only to the calcium lines in strength. The absorption in *Hα* and *Hβ* is complete for the widths quoted in Table 2, and these lines apparently have no wings. A direct comparison of Arcturus and Antares spectrograms taken with the same spectrograph shows that the intensity of *Hα* is only slightly greater in Antares. The smaller value, given by Dr. Hacker, may be due to the relatively low dispersion of the prism plate at *Hα*. No direct comparisons of the other hydrogen lines could be made. The unsatisfactory nature of the identification of the *Hδ* blend is due to

TABLE 2

DATA FOR HYDROGEN LINES

	Arcturus (i)	Antares		Identification
		i	Width	
Hα	50	150	1.59 A	*H*
Hβ	50	100	1.44	**H** *Cr*
Hγ	40	25rv	.....	**H** *Cr*
Hδ	.....	10h	.....	*Fe H In?*

the fact that there is no good way to judge the relative contribution of iron to this line. The iron line in question belongs to an intercombination multiplet, other members of which are also blended in Antares.

Li.—A copy of Plate 1406[2] (obtained in the second order of the 9-foot Coudé grating spectrograph) was searched carefully for lines near the *Li* doublet, λ 6707.79 and λ 6707.94. In Table 3, measurements in the Antares spectrum are compared with lines observed in the spectrum of the Sun and Arcturus.

A line has also been found at λ 6707.43 (2) in Aldebaran (K5).[7] Two other strong *Li* lines, λ 4071.93 and λ 4602.99, coincide closely with stellar lines which are otherwise easily accounted for. Although *Li* has been found in the Sun,[8] there appears to be little evidence for concluding that it is present in Arcturus, Aldebaran, or Antares.

[7] F. E. Roach, *Ap. J.*, **80**, 239, 1934. [8] C. E. Moore, *ibid.*, **85**, 81, 1937.

C.—The lowest excitation potential of 17 carbon lines[9] in the region λλ 4677–6587 is 7.45 volts. One line, λ 4932.00 (5), coincides with a stellar line which may be attributed to vanadium. Apparently the evidence for the presence of carbon must rest upon molecular lines.

Na.—Members of the diffuse and sharp series, as well as the principal series, are present. All lines are somewhat stronger than in the spectrum of Arcturus.

Mg.—All magnesium lines are weakened or unchanged in the spectrum of Antares. The lines are so widely separated that a comparison of estimated intensities of lines in the same star is unsatisfactory. Statements made here are based upon a study of enlargements. The green triplet is definitely weaker in Antares than in Arcturus. The ultimate line at λ 4571 appears to be practically unchanged. The diffuse series is apparently strengthened with respect to the sharp series.

TABLE 3

THE λ 6707 REGION

Sun	Intensity		Antares		Arcturus	
	Disk	Spot	λ	*i*	λ	*i*
.....	.....	.....	06.33	0wH	.....	.....
6707.458.....	−2	.....	07.48	1h	07.45	1 (unidentified)
07.83 } *Li*.....	−3	4	.....	.....	.....	.....
07.939 }			.....	.....	.....	.....
.....	.....	.....	08.19?	1h	.....	.....
08.989.....	−3N	.....	09.00	0?	.....	.....

Al.—The strong lines at λ 3944 and λ 3961 have about the same intensity in Antares as in Arcturus.

Si.—The *Si* lines are definitely weaker in Antares than in Arcturus, but a larger percentage of lines was found than in the Sun or Arcturus.

Si+.—No trace of the *Si*+ lines could be found.

K.—The main basis for suspecting this element in Antares is provided by the line λ 4044.14 (8R), which is apparently blended in a

[9] C. E. Moore, unpublished material.

complicated manner with several lines. The region around this line is greatly disturbed by the wing of a strong iron line at λ 4045.85, which has an intensity of 33?W in the sun. It must be admitted that the evidence for identifying *K* in Antares is inconclusive. Unfortunately, the first member of the principal series lies beyond the red limit of plates available.

Ca.—The *Ca* spectrum contributes a larger proportion of lines to the Arcturus and Antares spectra than to the solar spectrum. All *Ca* lines are strengthened in Antares, and the ultimate line at λ 4226 has extensive wings. The intensities of λ 4226 and *H*a are comparable, but their relative intensities can only be guessed. The difference in the dispersion and quality of the plates for these two regions and the great difference in the appearance of the lines makes it very difficult to compare them visually.

Ca+.—The *H* and *K* lines are the strongest and most unusual lines in the spectrum of Antares. They are apparently *twice* self-reversed and have very extensive wings. It is difficult to tell whether they are stronger or fainter in Arcturus.

Sc.—Although scandium is relatively rare on the earth, it seems to be well represented in the stars. A large proportion of the lines are unblended in the spectrum of Antares. All lines are greatly strengthened in Antares. Two higher-level multiplets, $z^4F^o - e^4D$ and $z^4F^o - e^4F$, are present, though faint. These were not observed in Arcturus.

Sc+.—The *Sc*+ lines are also well represented and are of nearly the same intensity as in Arcturus. For example, a line at λ 4246.83 (100), which has intensity 30 in Arcturus and 20 in Antares, appears about the same on the enlargements.

Ti.—The spectrum of *Ti* is very well developed in Antares. The lines of *Ti* are, more than lines of any other element, noticeably increased both in intensity and percentage contribution to the spectrum on passing from the Sun to Arcturus and Antares. More than half the lines identified in Antares belong to the triplet system, while 8 per cent belong to the singlet system. The remainder belong to the quintet and intercombination systems. The strongest lines arise from the a^5F and a^3F levels.

Class I lines[10] are strengthened most. Lines of Classes IV and V are about the same as in Arcturus, or weaker. A study of the unblended lines has shown that, on the average, increase over sun-spot intensities varies directly with the sun-spot intensities. A similar effect was noted for the increase in intensity on passing from disk to spot.

When the theoretical intensities for 50 lines in seven supermultiplets were plotted against the observed intensities, some correlation was found.

Ti+.—The *Ti*+ spectrum is less completely developed than in Arcturus. The lines are weaker than in Arcturus.

V.—The *V* spectrum is well developed in Antares, although it contributes a smaller percentage of lines than in the solar and Arcturus spectra. The increase over Arcturus intensities is less than for *Ti*. Lines which are greatly strengthened in the spot spectrum are strengthened least in Arcturus and Antares. Class I lines are strengthened most in both cases. The few unblended Class III lines are apparently unchanged in Antares.

The strongest lines arise from the a^4F level. A comparison of theoretical and observed intensities was less satisfactory than for *Ti*.

V+.—The intensities are about the same in Antares as in Arcturus, but fewer lines were found.

Cr.—The development of the *Cr* spectrum parallels that observed in Arcturus. Lines of Classes III and IV are of about the same intensity as in Arcturus, while Class I lines are markedly strengthened in Antares. The strongest lines arise in the a^7S, a^5S, and a^5D levels. Most of the unclassified lines in the observed region are present.

Cr+.—The lowest excitation potential of *Cr*+ lines is 2.41 volts. Few *Cr*+ lines are observed in Antares, and these are definitely weaker than in Arcturus.

Mn.—The *Mn* spectrum is well developed in Antares. Even the lines arising from the relatively high level, 3.06 volts, are moderately strong, or about the same as in Arcturus. Low-level Class I lines (e.g., $a^6S - z^8P^o$) are markedly strengthened, while higher-level

[10] Here, as in other places, the term "Class" refers to the temperature class assigned by King.

Class I lines (e.g., $z^8P^o - e^8S$) are nearly the same or are weaker in Antares. A few unclassified lines are present.

Mn$^+$.—All the classified lines lie beyond λ 3498. A faint line, λ 4419.78 (2), is apparently blended with vanadium lines at λ 4419.94 (12). The two strongest *Mn*$^+$ lines in Arcturus, λ 4253.02 (2) and λ 4365.29 (1), fall in regions where unmeasurable structures were noticed in the spectrum of Antares. It appears that no decision can be made.

Fe.—A careful study of the unblended lines has shown that (1) Class V lines are, on the average, weakened in Antares; (2) lines of Classes II, III, and IV are about the same or are weaker in Antares; and (3) Class I lines are markedly strengthened in Antares.[11] Because of the numerous departures from *LS* coupling observed in the *Fe* spectrum, it was considered unprofitable to compare theoretical intensities with observed intensities.

Fe$^+$.—Fewer *Fe*$^+$ lines were found in Antares than in Arcturus, but the intensities show little change, on the average. The only unblended line which seems fainter in Antares is λ 5425.269 (2), excitation potential 3.19 volts. A line of excitation potential 3.88 volts at λ 6416.925 (predicted) appears about the same on the enlargements.

Co.—Lines of Classes III, IV, and V are about the same or are weaker in Antares. Most of the Class I and II lines are stronger in Antares.

Ni.—The strongest lines are in the ultraviolet and account for many lines on the low-dispersion plates.[12] A line at λ 3380.6 (80R) has an intensity of 50W in Antares. The lines of lowest excitation potential are strengthened most. Most Class V lines are weakened. No suitable Class IV lines are available for comparison in the region common to Antares and Arcturus.

Ni$^+$. The strongest lines lie beyond λ 3408. A line at λ 4244.81 (1) falls near a hazy stellar line which may be attributed wholly to *Sa*$^+$. Hence, the identification of *Ni*$^+$ in Antares is questionable.

[11] It will be understood that, unless otherwise stated, comparisons are made with respect to the Arcturus spectrum.

[12] The writer has measured down to λ 3300 on low-dispersion plates obtained with the Crossley reflector of the Lick Observatory by Professor C. D. Shane and Mr. D. M. Popper.

Cu.—The ultimate lines are near λ 3250. Two unblended *Cu* lines at λ 5105.54 (8n), E.P. 1.38 volts, and λ 5153.24 (8n), E.P. 3.77 volts, appear about the same in both stars.

Zn.—The ultimate line is at λ 3075. Of three lines found in Arcturus, one at λ 4810.53 (10R), E.P. 4.06 volts, falls near a stellar line at λ 4810.61 (3h). The only other possibility for this line is an unclassified faint *Cr* line, λ 4810.74, of Class III*A* and intensity −1 in the spot spectrum. There is only one *Zn* line in the region λλ 4800–6300; so the observed coincidence is probably real.

Ga.—The two strongest lines, λ 4033.03 (30R) and λ 4172.06 (30R), fall very close to stellar lines which are otherwise easily accounted for. The other lines are completely obscured; so the identification of *Ga* is questionable.

Ga$^+$.—The strongest line, λ 4262.05 (10), may account for λ 4262.04 (10WH) in Arcturus, but it is completely obscured in Antares by a *Cr* line at λ 4262.17 (6). Other lines are completely obscured or absent; so the identification of *Ga*$^+$ is doubtful.

Ge.—One strong line is completely obscured by the great *Ca* line at λ 4226. The other accessible line, λ 4685.85 (2), coincides with a faint Arcturus line and may possibly be blended in Antares with a *Ni* line at λ 4686.22 (5) and a *Ti* line at λ 4686.57 (4), neither of which satisfactorily explains the stellar line at λ 4686.02 (7W), so far as wave length is concerned. The identification of *Ge* must remain doubtful.

Sr.—The strongest line, λ 4607.33 (600R), is unblended and appears the same in Antares as in Arcturus. All the other lines are blended or masked.

Sr$^+$.—The strong line, λ 4215.54 (300r), is strengthened in Antares. Other lines are blended.

Y.—The *Y* spectrum is well developed in Antares, whereas Dr. Hacker found little evidence for *Y* in Arcturus. Ten multiplets are represented. The greatest strengthening is shown by λ 6435.02 (500 in laboratory), which is hardly visible in the Arcturus spectrum and has an intensity of 7 in the Antares spectrum.

Y$^+$.—The *Y*$^+$ spectrum is also well developed in Antares. There seems to be no diminution in intensity on passing from Arcturus to

Antares; in fact, the line at λ 4883.69 (200) appears stronger in Antares.

Zr.—Lines of all temperature classes are strengthened about the same amount in Antares, and several lines not observed in Arcturus appear in Antares. Lines common to the two spectra are considerably stronger in Antares. An interesting Class V line at λ 5046.55 (10) is stronger in Antares; in fact, no line was measured at this position by Dr. Hacker. This line is barely distinguishable on an enlargement of a grating spectrogram for Arcturus.

Zr^+.—Few Zr^+ lines common to both spectra are unblended in Antares. Several strong lines appear in the ultraviolet, the strongest being λ 3614.78 (18), which has an intensity of 10 in Antares. Since Plate 1096 was considerably underexposed in this region, it is very possible that the estimated intensity is too high. An unblended line at λ 4208.98 (30) has been assigned intensity 8 in both Arcturus and Antares. It may be tentatively concluded that Zr^+ is about the same in both stars.

Cb.—The strongest lines, λ 4058.99 (2000) and λ 4079.73 (1000), are completely obscured by *Mn* and *Ti* lines. Four strong lines, λ4100.916 (600), λ 4152.602 (600), λ 4164.65 (400), and λ 4168.122 (200), may possibly be present in blends. Although Dr. Hacker concluded that the evidence favors the identification of *Cb* in Arcturus, and there are more coincidences than could be expected by chance alone, the writer feels that the evidence is not sufficiently convincing to make a definite decision for either star.

Mo.—The three strongest lines, λ 3798.26 (50R), λ 3864.11 (50R), and λ 3902.97 (50R), are masked by moderately strong lines of *Fe*, *Ti*, and *Cr*. Only two lines, λ 5533.03 (30R) and λ 5570.399 (25R), fall close enough to stellar lines to be of interest. Both stellar lines are difficult to explain without supposing that *Mo* contributes a little. In the absence of unblended lines, nothing further can be said.

Mo^+.—All the Mo^+ lines suspected in the solar spectrum have excitation potentials of about 2.9 volts. There are no close coincidences with stellar lines. It may be concluded that Mo^+ contributes nothing to the Antares spectrum.

Ru.—One line, λ 4584.44 (30), appears to be present and un-

blended. In both stars the line has been given an intensity 1. Other lines of *Ru* are blended or masked.

Ag.—The leading lines of the principal series are at λ 3280 and λ 3382. No coincidences have been observed with the first members of the diffuse series at λ 5209, λ 5465, and λ 5471.

In.—The resonance line at λ 4101 is masked by *Hδ* and an *Fe* line. The data for two other lines are given in Table 4. The first of these lines is of particular interest since it coincides with a bright line observed in long-period variables. In view of the questionable identification of *In* in Antares, it is apparent that some unusual process must be responsible for the λ 4511 line in long-period vari-

TABLE 4

INDIUM LINES

Laboratory		Sun				Arcturus			Antares		
λ	*i*	I.A.	Intensity		Identification	λ	*i*	Ident.	λ	*i*	Ident.
			Disk	Spot							
4511.27	8R	11.31	.....	−1	*In*	11.17	1n	*Ti*	11.22	1h	*ZrO Ti In?*
5253.97	3	54.04	−1	0	*Fe*	.....	.....	.....	54.06	1	*Zr TiO? In?*

ables. A resonance mechanism has been suggested by A. D. Thackeray.[13]

Sn.—The only accessible line is λ 3801.027 (30R), which does not coincide with a stellar line. Stronger lines lie beyond the ultraviolet limit of the plates.

Ba.—Just as in Arcturus, the strongest line at λ 5535.48 (1000R) may possibly contribute to a stellar line at λ 5535.40 (11). There is little basis for judging how much the unclassified *Fe* line, λ 5535.42 (2), contributes to this line. Two other strong *Ba* lines are at λ 3501.11 (200R) and λ 7059.95 (400r). A number of the strongest lines given by Kayser[14] were looked up, but no suggestive coincidences were found.

Ba$^+$.—The ultimate line at λ 4554 (1000R) is greatly strengthened in Antares. This is of considerable interest, since one of the outstanding characteristics of *S*-type spectra is the unusual strength

[13] *Ap. J.*, **81**, 467, 1935. [14] *Handbuch der Spectroscopie*, **7**, 80, 1924.

of this line. An unblended line at λ 6496.90 (600r) is also greatly strengthened in Antares. The strong line at λ 4934.04 (700R) is about one-half as wide as Hβ.

La+.—The *La*+ lines are nearly the same or are slightly fainter in Antares than in Arcturus. There are too few unblended lines to form a basis for further statements.

TABLE 5

COMPARISON OF CHANCE AND OBSERVED COINCIDENCES FOR LINES OF *Pr*+, *Gd*+, and *Dy*+

	Pr+			*Gd*+			*Dy*+			
		$x = 0.05$ A, $i \geqslant 100$			$x = 0.06$ A, $i \geqslant 100$			$i \geqslant 60$		
X	*M*	*C*	*O*	*M*	*C*	*O*	*M*	*x*	*C*	*O*
λλ 4000–4200	7	1.3	5	14	3.0	5	13	0.03 A	1.5	3
4200–4400	6	1.0	3	15	2.9	2	6	0.08	1.6	2
4400–4600	6	1.0	3	4	0.7	2	2	0.05	0.3	2
4600–4800	2	0.2	0	1	0.1	0	.....	.....	.....	.....
4800–5000	3	0.3	1	.....	.....	.....	.....	.....	.....	.....

NOTES TO TABLE 5

C = the number of chance coincidences = $N[1 - \exp(-2Mx/X)]$
where N = number of lines in stellar spectrum in the interval X (in angstroms),
M = number of lines in laboratory spectrum having intensity greater than or equal to i (quoted in Table 5 at top of columns) and lying in the interval X,
and x = coincidence limit (in angstroms) within which line must fall in order to be considered a coincidence.
O = observed number of coincidences with stellar lines.

Ce+.—There can be no doubt that the presence of *Ce*+ in Antares is well established. Intensities are about the same as in Arcturus.

Pr+.—A comparison of predicted chance coincidences[15] with observed coincidences gave the results contained in Table 5.

Nd+.—The strongest lines are present, and there are numerous cases where *Nd*+ will alone account for an observed stellar line. The lines are stronger in Antares than in Arcturus.

Sa+.—The relatively great increase in the number of *Sa*+ lines

[15] According to theory of Russell and Bowen, *Ap. J.*, **69**, 202, 1929.

found in Antares must be largely due to the fact that the wave lengths in the complete spectrum were not published until recently.[16] In addition, it is possible that the writer may have been a little overzealous in attributing lines to Sa^+. The strongest lines occur around λ 3600, where the resolving-power of the Antares plate is very low. Of the remaining lines, the strongest ones appear to contribute to the spectrum of Antares. Even a few lines fainter than 150 in the arc are present. For $x = 0.04$ A, the value of C found for the region λλ 4200–4400 was 4.9, while 10 coincidences were actually observed. Seven of these coincidences fall within ±0.02 A. This result seems sufficiently convincing without considering the 145 remaining strong lines in the spectrum of Sa^+. The intensities are about the same as in Arcturus.

Eu^+.—Two of the strongest lines, λ 4129.73 (500R) and λ 4205.05 (600R), coincide very closely with stellar lines. Most of the 10 lines stronger than 200R coincide closely with stellar lines or are completely masked by strong atomic lines. The intensities are about the same as in Arcturus.

Gd^+.—Most of the Gd^+ lines are completely masked in the spectrum of Antares. Lines at λ 4191.06 (200) and λ 4342.18 (300) are unblended in Arcturus but appear to be slightly blended in Antares. The observed coincidences exceed the computed chance coincidences by a small amount (see Table 5); so there is a little doubt about considering Gd^+ definitely identified in Antares.

Tb^+.—Two lines, λ 4144.47 (100) and λ 4278.54 (200), are the only ones sufficiently free from serious blending to be suitable for discussion. The former is absent from the Arcturus spectrum but may be blended in Antares with a solar line identified as $Ce^+ - Ti$. The latter may be responsible for an unidentified Arcturus line at λ 4278.48 (3WH), while this Arcturus line and another at λ 4278.22 (20WV) have apparently blended together to form a line at λ 4278.38 (6) in Antares. Nothing definite can therefore be said about Tb^+.

Dy^+.—The strongest line, λ 4211.72 (1200), unfortunately falls near a stellar line, λ 4211.92 (12), for which several contributors have already been established. The line at λ 4186.81 (600) appears

[16] A. S. King, *ibid.*, **82**, 140, 1935.

to be missing, while a less intense line, λ 4103.31 (500), is present and apparently unblended. The differences between computed and observed coincidences are small in the region λλ 4400–4600. It is doubtful that the line λ 4449.70 (60) is strong enough to contribute to a near-by stellar line, but there seems to be no doubt about the line λ 4589.37 (150). Although Dy^+ lines have not previously been recognized in Arcturus, it appears that at least two lines, λ 4221.08 (1) and λ 4589.32 (6n), should be identified with Dy^+.

Ho.—A strong line at λ 4163.03 (100) falls very near a line of intensity 3 in Antares and a line of intensity 5WV in Arcturus, where the stellar line has been attributed to *CN*. This may be only a chance coincidence. A stronger line at λ 4053.92 (400) is masked by a Ti^+ line. No discussion seems possible.

Ho^+.—Only two lines have an intensity greater than 100 in the arc. One is masked, and the other is absent.

Tm^+.—Although some of the strongest lines are accessible, no coincidences could be found with stellar lines.

Yb.—Only two lines are available for discussion, both of which are in the solar spectrum. Both lines fall near stellar lines which can be otherwise accounted for.

Yb^+.—One of the two strong lines, λ 3684.20 (200), falls nearer a stellar line at λ 3684.17 than an iron line which probably is largely responsible for the stellar line. No decision can be made about Yb^+.

Lu^+.—Two lines, λ 4184.26 (100) and λ 5983.90 (100), fall near stellar lines. The second appears to be blended with an iron line, but the first is completely masked by Ti^+ and Gd^+ lines. Other strong lines do not appear at all; so the identification of Lu^+ in Antares is questionable.

Hf.—Since this element is just below *Zr* and *Ti* in the periodic table, it should be of interest. Only one strong line, λ 4093.16, coincides with a stellar line which is otherwise unidentified. There are two unidentified solar lines near by, so there is little evidence for identifying *Hf* in Antares.

Hf^+.—Most of the stronger lines which coincide with stellar lines lie beyond λ 3600. The only possibility seems to be a line at λ 5311.63 (25), which may be blended with a Zr^+ line in Antares. No decision can be made.

Ta.—Three lines have recently been identified in the Sun.[17] The faintest, λ 5939.75 (20b), coincides with a stellar line at λ 5939.82 (0), which is otherwise unaccounted for. Since the other two lines appear to be absent, and all are absent from the Arcturus spectrum, there is no basis for making a decision.

W.—The two strongest lines are masked. A line at λ 4079.34 (6) which is strongest in the Sun coincides with a stellar line at λ 4074.35 (5), which is otherwise unaccounted for. There appears to be no way to test the significance of this coincidence.

Os.—Three of the strongest lines fall near stellar lines. In view of the fact that there are only three other lines in the region λλ 4000–4600, this appears to be a large number of coincidences. It seems more than likely, however, that one line, λ 4135.75 (5) in Antares, is really a band line which is intensified in the stars. There are so many possibilities for the other lines that identification of *Os* in Arcturus and Antares must remain questionable.

Ir.—The strongest lines fall beyond λ 3600, and some have recently been identified in the Sun.[18] Coincidences with Antares lines are not very close, and there seems to be no basis for making a decision.

Pb.—Two strong lines, λ 3639.45 (500R) and λ 3683.09 (1000R) are obscured in the Antares spectrum by strong lines of *Cr*, *Fe*, and *V*. Nothing definite can therefore be said about the presence of *Pb* in Antares.

SUMMARY AND CONCLUSIONS

The 92 elements may be classified into five groups, according to the nature of the spectroscopic evidence for their presence in the stars. Table 6 contains a comparison of the data for the Sun, Arcturus, and Antares. Of the 27 elements considered present in the Sun but classified otherwise in Antares, only *Li* and *Be* appear to be definitely absent from the spectrum of Antares. For five elements, *B*, *C*, *N*, *O*, and *F*, the evidence in Arcturus and Antares is based solely upon molecular data.

The data for elements present in Antares are summarized in Table 7. The second and third columns give the number of un-

[17] C. E. Moore, *ibid.*, **85**, 86, 1937. [18] *Ibid.*

blended (U) and blended (B) lines representing each element in Antares, and the fourth column contains the total number ($T = U + B$) of lines for each element. These figures include 90 predicted lines, due mostly to *Fe*, *Cr*, and *Ti*.

TABLE 6

OCCURRENCE OF ELEMENTS IN SUN, ARCTURUS, AND ANTARES

	Sun	Arcturus	Antares
Present	61	33	34
Questionable	3	10	16
Insufficient stellar data	2	15	10
Insufficient laboratory data	7	6	6
Absent	19	28	26

The last three columns of Table 7 contain the intensities of the strongest lines of each element in the Sun, Arcturus, and Antares.

TABLE 7

LINE-COUNTS AND MAXIMUM INTENSITIES

	Number of Lines			Maximum Intensities				Number of Lines			Maximum Intensities		
	U	B	T	⊙	α Boo	α Sco		U	B	T	⊙	α Boo	α Sco
H	1	3	4	40	50	150?	*Cu*	1	4	5	10	10	15
Na	5	8	13	30	40	50	*Zn*	0	1	1	3	3	(3)
Mg	9	7	16	30	30	20	*Sr*	1	8	9	− 1	5	5
Al	2	2	4	20	12	10	Sr^+	1	1	2	8	(20)	(20)
Si	6	10	16	12	2	3	*Y*	8	29	37	0	(0)	7
Ca	30	49	79	40*	100?	300?	Y^+	10	20	30	3	15	8
Ca^+	2	1	3	200	800?	900?	*Zr*	31	58	89	− 1	3	11
Sc	19	37	56	2	7	17	Zr^+	5	17	22	2	4	10
Sc^+	7	24	31	5	30	12	*Ru*	1	2	3	0	1	1
Ti	185	349	534	7	40	30	Ba^+	5	4	9	8	20	50
Ti^+	24	48	72	12	20	10	La^+	5	37	42	1	11	4
V	92	191	283	4	40	30	Ce^+	14	22	36	0	4	4
V^+	1	5	6	5	4	6	Pr^+	2	10	12	− 1	3	3
Cr	72	250	322	5	50	40	Nd^+	12	23	35	0	10	8
Cr^+	1	5	6	5	3	7	Sa^+	14	84	98	− 1	6	9
Mn	33	66	99	7	15	30	Eu^+	1	6	7	1	15.	12
Fe	431	775	1206	40	60	50	Gd^+	0	13	13	0	3	(8)
Fe^+	12	16	28	6	12	6	Dy^+	2	3	5	0	(6)	6
Co	31	103	134	6	5	10							
Ni	52	122	174	20	12	10	Total	1128	2413	3541	.....	.....	.....

* Intensity in spot.

For lines of unusual strength the intensity estimates in Antares are untrustworthy. Such intensities are indicated by question marks. The intensities given for *Al* in Arcturus and for *Ca* and Ca^+ lines in both Arcturus and Antares were estimated from enlargements of the

spectra. For Sr^+ the given intensities are inclosed in parentheses because the λ 4215 line may possibly be disturbed by a faint *Fe* line. Other intensities inclosed in parentheses correspond to blended lines, there being no unblended lines available.

Evidence that the temperature of Antares is lower than that of Arcturus may be summarized as follows: (1) the percentage of ionized lines is less in Antares than in Arcturus; (2) lines of lowest temperature classes are noticeably stronger in Antares; (3) lines of Classes IV and V are about the same, or slightly weaker, in Antares. A determination of the exact difference in temperature is not obtainable from the present material.

It is a pleasure to thank Dr. W. H. Wright and Dr. Walter S. Adams for giving the writer an opportunity to select plates for this study and for extending many other courtesies. Without the cooperation of the Lick and Mount Wilson observatories this study could not have been made. To Professor C. D. Shane and Professor F. A. Jenkins the writer is especially indebted for advice and helpful criticism. Finally, the writer wishes to express her gratitude to Professor Henry Norris Russell and to Dr. Charlotte E. Moore, who have encouraged the writer and supplied her with unpublished spectroscopic material.

VASSAR COLLEGE OBSERVATORY
September 1937

INVESTIGATION OF STANDARDS OF MAGNITUDE WITH A WEDGE PHOTOMETER

ALICE H. FARNSWORTH

ABSTRACT

A condensed account is given of extensive work by Professor Parkhurst using a wedge photometer on telescopes of aperture 6, 12, and 40 inches for the measurement of 435 stars in groups, at 7, 9.5, 12, and 15 mag.

The scale of the 6-inch reflector between 7^m and 9^m5 is similar to that of *Harvard Annals*, **45** and **74**. Between 9^m5 and 12^m the ratio of the interval as given by *Harvard Annals*, **74**, to that of the 12-inch refractor is 1.38, indicating marked scale divergence. Three more recent investigations of a portion of the fields: remeasurement with the photometer on the 12-inch, photovisual determinations with a grating on the 24-inch reflector, and photovisual polar comparisons with the 12-inch Metcalf telescope at Harvard Observatory, concur in reducing the divergence, by 41, 67, and 90 per cent, respectively (the last is of relatively low weight). Tentatively a scale 1.25 times that of the early wedge on the 12-inch is suggested as being near the truth.

In 1900 Professor E. C. Pickering proposed a co-operative plan for the measurement of faint stars with wedge photometers, at a number of different observatories. The share of work undertaken at the Yerkes Observatory and carried out by Professor J. A. Parkhurst, largely between 1903 and 1905, involved the determination of the magnitudes of two groups of stars near the twelfth and fifteenth magnitudes in twenty-four fields surrounding variable stars in the northern sky, the so-called Rumford fields. The photometer was used for this purpose on the 40-inch telescope. The results for these stars were published in connection with the report on the entire plan made by Dr. S. A. Mitchell in 1923.[1] The Yerkes magnitudes appear reduced to the zero point adopted for that report, namely, the mean magnitude of the stars near the twelfth magnitude as given in *Harvard Annals*, **74**.

Mr. Parkhurst greatly extended his program of observation and used the photometer on three different telescopes to determine the magnitudes of four groups of stars in each field, as follows: with his 6-inch reflector, stars of the seventh and ninth magnitudes; with the 12-inch refractor, stars of the ninth and twelfth; and with the 40-

[1] *Mem. Amer. Acad. Arts and Sci.*, **14**, No. IV, 215, 1923.

inch refractor, stars of the twelfth and fifteenth.[2] Thus the revised Yerkes magnitudes of the 1923 report, based on measures with the 40-inch telescope only, represent but a small portion of the entire work. The measures with the 12-inch exhibited a large scale-difference from the Harvard magnitudes of the same stars; for this reason Mr. Parkhurst was all the more desirous that the entire work be published in detail. Since this has never been done, it seems desirable even at this date to summarize the original data and to add the results of later checks carried out by Mr. Parkhurst and others.

A description of the instrument, the reduction curve of the wedge, and the methods by which it was calibrated are given in the report[3] already cited; the somewhat modified curve adopted for the 6-inch reflector has also been published.[4] These curves translate the mean wedge readings into relative magnitudes which are changed into actual magnitudes by the addition of a constant. This zero-point constant was furnished for the three telescopes as follows:

6-inch: Mean magnitude of 3 or 4 stars in Group I, from *Harvard Annals*, **45**

12-inch: Mean magnitude of 5 stars in Group II, from measures with the 6-inch telescope

40-inch: Mean magnitude of 5 stars in Group III, from measures with the 12-inch telescope

The mean magnitude of the fainter group measured with each telescope thus becomes, in turn, the zero point for the pair of groups measured with the next larger telescope.

As a sample, results are tabulated for one field, S Piscium (Table 1). Designations in the successive groups are BD numbers, Hagen numbers,[5] and the letters which appear on the reproductions of the star fields found in Plates I–VI of the 1923 report. The mean magnitude from measures made with each instrument on from three to six nights is given for each star. Results from each telescope are in a vertical column directly below its designation. Means used for zero point are indicated. The final column shows differences in magnitude between *Harvard Annals*, **45** or **74**, and Parkhurst's measures

[2] As a matter of fact, the stars measured average $7^{m}1$, $9^{m}6$, $12^{m}2$ and $15^{m}0$ on the zero point of the Harvard catalogues. For brevity these will be referred to as Groups I–IV.

[3] Mitchell, *op. cit.*, pp. 229 ff.

[4] Parkhurst, *Researches in Stellar Photometry*, *Carnegie Pub.*, No. 33, 8, 1906.

[5] I. G. Hagen, S.I., *Atlas stellarum variabilium*, Ser. II, 1899.

with the 6-inch or the 12-inch, as indicated in subscripts of column headings.

The precision of the results is given by the quantity: twice the range divided by three times the number of observations, averaged

TABLE 1

S. PISCIUM

GROUP	STAR	6-INCH	12-INCH	Δ MAG.
				$H.A._{.45} - P_6$
I	+9° 138	6m62	.....	+0m03
	142	7.12	.....	− .02
	158	7.50	.....	−0.03
				$H.A._{.74} - P_{12}$
II	2	8.10	7.98	+0.22
	4	9.65	9.66	− .09
	8	10.09	10.14	+ .13
	9	10.20	10.28	+ .24
	10	10.38	10.34	+0.60
Mean	.....	9.68	9.68	+0.22
Range	.....	3.24	3.44	4.04
		40-INCH		
III	A	10.62	10.72	+0.50
	13	10.98	10.70	.89
	C	11.05	11.26	.49
	D	11.14	11.12	.84
	E	11.66	11.66	+0.84
Mean	.....	11.09	11.09	+0.71
Range	.....	1.24	1.53	1.70
IV	Q	13.75	.....	.....
	R	14.00	.....	.....
	S	14.01	.....	.....
	T	14.54	.....	.....
	U	14.99	.....	.....

for each group of stars with each instrument. For the brighter and fainter groups, respectively, the averages are: for the 6-inch, $\pm 0^m03$ and 0^m04; for the 12-inch, $\pm 0^m03$ and 0^m05; for the 40-inch, $\pm 0^m04$ and 0^m06. Thus there is for each instrument a slight advantage for the brighter group of stars, and for the overlapping groups of stars there is a slight advantage in favor of the larger telescope.

A comparison of the scales of the three telescopes, within the narrow limits of a single group of stars, is based on values of the range (defined as the sum of the differences, without regard to sign, of the individual magnitudes in the group from the mean). Its value in a given field is fortuitous (see values given in Table 1), but the ratio of the ranges obtained for the same group of stars from two different telescopes may be significant. These ratios for 6-inch to 12-inch, and 40-inch to 12-inch, which are plotted as dots and crosses in the upper section of Figure 1, average 0.86 and 0.87, respectively. This suggests that the scale of the 6-inch (near the ninth magnitude) agrees with that of the 40-inch (near the twelfth magnitude) in being less extended than that of the 12-inch by about 13 per cent. Judged in the same manner, the Harvard scale is more extended than the 12-inch by 15 per cent at the ninth, and 20 per cent at the twelfth, magnitude. The method is of limited value, as accidental errors enter with full weight and the magnitude limits are narrow.

A comparison with the Harvard system is most easily effected by a study of differences such as are recorded in the last column of Table 1. Obviously these must average zero for Group I in each field, since *Harvard Annals*, **45**, furnished the zero point. That the differences for Group II also average practically zero is shown by the behavior of the circles, in the second section of Figure 1, which represent mean magnitude differences: *Harvard Annals*, **74**, *minus* Parkhurst 12-inch for Group II in the twenty-four fields. Evidently the scale of the 6-inch between 7 and 9.5 mag. is in substantial agreement with that of *Harvard Annals*, **45** and **74**.

The mean differences—Group III *minus* Group II—on the other hand, are large and systematic. Table 1 furnishes the value $+0^{m}.49$, for example, as the amount by which the interval as given by *Harvard Annals*, **74**, exceeds measures with the 12-inch. Values in all the fields are shown graphically in the lower part of Figure 1. The series of dots gives the 12-inch values in order of increasing Δ mag.; thus the form of this curve is arbitrary. The Harvard Δ mag. are shown by crosses, and a heavy line has been drawn to represent their average behavior. Unfortunately, only 70 of the 120 stars measured in Group II are given in *Harvard Annals*, **74**. Those values of Δ mag. which depend on less than three stars in Group II are

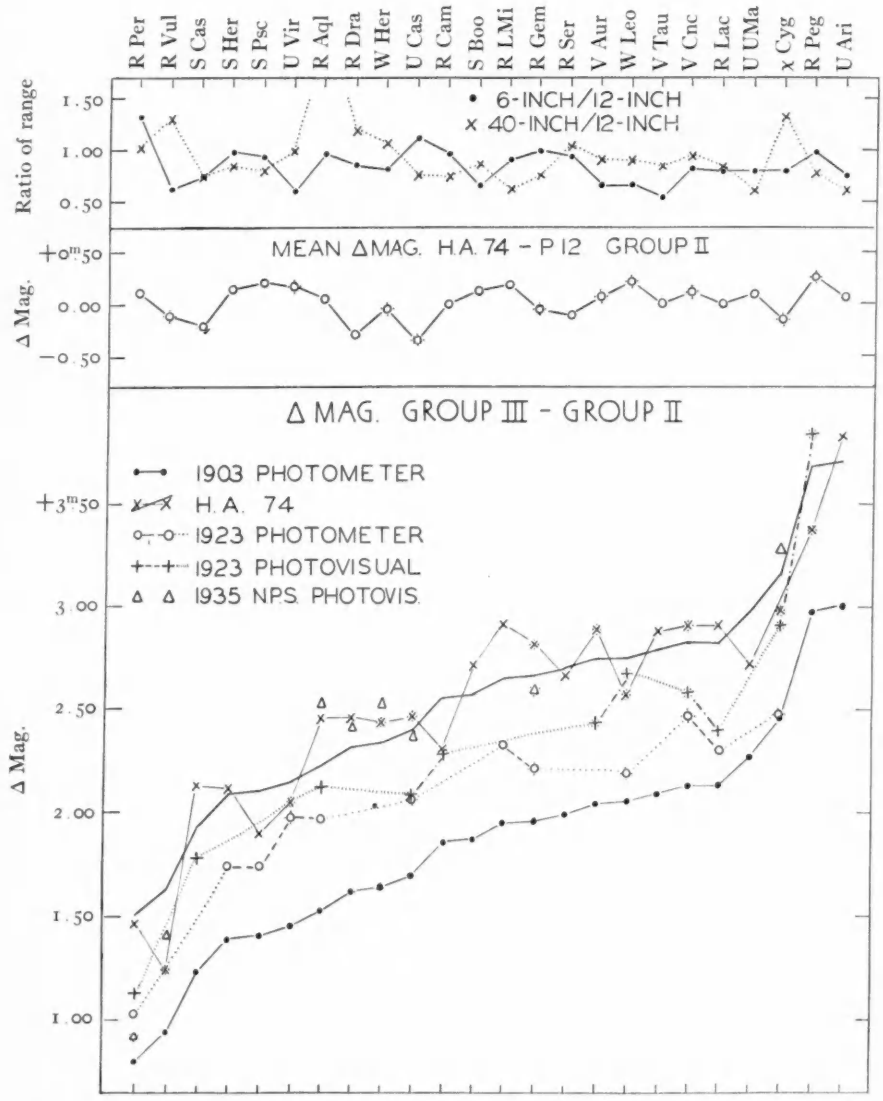

FIG. 1.—Points surrounded by dots are entitled to less weight. In the lowest section of the figure the upper heavy line without points is drawn parallel to the lowest curve at a distance $0^m.70$ above it.

surrounded by dots. The weighted average of all is $+0^m.70$. The average magnitude interval between Groups II and III as measured with the 12-inch is $1^m.85$; in *Harvard Annals*, **74**, it is $2^m.55$; the ratio between the scales is 1.38. When values of this ratio are plotted with the interval as argument, they suggest that the ratio diminishes as fainter stars are approached (1.53 at Harvard $10^m.5$, 1.20 at Harvard $11^m.3$). This is not in line with the evidence from the ratio of ranges given above.

Accidental differences for the stars of Group I from Potsdam magnitudes average $\pm 0^m.07$; from Potsdam corrected[6] for color, $\pm 0^m.10$; and from *Harvard Annals*, **45**, ± 0.11. The fact that the smallest difference is from Potsdam uncorrected may be laid to better agreement in color perception, as shown by a tabulation of the stars with respect to Potsdam color class and Draper spectral type. The tabular differences from Potsdam uncorrected are small and without system; differences from Potsdam corrected and from Harvard both show a marked divergence, in that the measures with the 6-inch make the red stars appear brighter and the blue stars fainter.

Comparisons based on color indices determined by Miss Parsons[7] and Mr. Parkhurst (1920–1923) show no well-defined color equation between the 12-inch system and *Harvard Annals*, **74** (based on measures with a 12-in. photometer), in Group II; but in Group III there is a slight tendency for Harvard to see the red stars fainter and blue stars brighter. Comparison of Yerkes apertures yields no definite color effect between 12-inch and 40-inch for Group III; for Group II a trend from *minus* to *plus* differences (P_6–P_{12}) is noted with increasing color.

Whatever the cause of the large difference between the measures with the 12-inch and the Harvard scale, between 9 and 12 mag. in Rumford fields, each of three later investigations of the same stars tends to show that the 1903 photometer scale was too contracted. Unfortunately each study has included only part of the fields and has been subject to its own uncertainties. All that will be given here is a brief account of method, addition of the results to Figure 1, and a few final comments.

[6] *Pub. des Astrophysikalischen Observatoriums zu Potsdam*, **17**, XXXIV, 1907.

[7] *Pub. Yerkes Obs.*, **4**, 291, 1921.

In 1923–1924 Mr. Parkhurst repeated the calibration of the wedge and, assisted by Professor A. S. Young, remeasured, with the 12-inch, in twelve fields the stars of Groups II and III. Certain changes were made in the arrangement for producing the artificial star. The same reduction curve was used as in the original reductions of the 12-inch measures. For comparison with *Harvard Annals*, **74**, and the results obtained with the photometer in 1903, circles have been added to Figure 1 showing the Δ mag. between the means of the same stars as were used for the previous comparisons. The average interval in the twelve fields comes out $1^m.98$, as compared with $1^m.68$ in 1903 and the Harvard value $2^m.41$, comparisons involving fewer than three stars in a group being given half-weight.

In eighteen fields photographic and photovisual magnitudes of the stars in question have been determined by Miss Parsons[8] or Mr. Parkhurst. Most of the plates were taken with reduced aperture through a parallel-wire grating on the 24-inch reflector; a few were taken with the 40-inch. Cramer Isochromatic plates behind yellow filter J1[9] furnished the photovisual results with which we are here especially concerned. Measurement was made with an artificial scale in the Hartmann microphotometer. Such of the results as could be put into the form of Figure 1 are shown there by plus signs. The scale of magnitudes is slightly more extended than in the case of the photometer measures of 1923, the average interval in eleven fields, $2^m.25$, lying between the early photometer value $1^m.78$ and the Harvard value $2^m.48$.

Another photographic check was applied in the summer of 1935 when the writer compared eight fields directly with the North Pole and measured two others on previously existing plates. The plates were taken, through the courtesy of Dr. Shapley, at the Harvard College Observatory, in Cambridge, a photographic series (I) with the 8-inch Draper telescope, and a photovisual series (MA) on Cramer Isochromatic Presto plates with the 12-inch Metcalf telescope. A polar comparison consists of three successive plates, field-pole-field, developed together. The guiding is automatic. Measures were made with a scale of images mounted in an eye-piece held in the hand. Magnitudes, corrected for absorption, were interpolated from the

[8] *Ibid.* [9] Parkhurst and Farnsworth, *Ap. J.*, **62**, 180, 1925.

polar curves. It is only fair to say that the material is of poor quality on the average. Too often polar and field images differed in quality. Sometimes one plate of a comparison had to be rejected. Lack of transparency necessitated exposures so long that the images tended to elongate, or in many cases they were too near the plate limit to be reliable. It would not be surprising if the stars in the fainter group were measured too faint, thus tending to make the plotted Δ mag. too large. The results appear as triangles in Figure 1. The average interval in eight fields is $2^m.17$, compared with early photometer $1^m.51$ and *Harvard Annals*, **74**, $2^m.25$. It is interesting that the Harvard data support each other loyally, the photovisual plate and the 12-inch photometer of forty years ago telling approximately the same story.

TABLE 2

RATIOS BETWEEN INTERVALS, GROUP III – GROUP II

SOURCE	NO. OF FIELDS	NO. OF STARS		RATIO
		Gr. II	Gr. III	
Harvard Annals, **74**/1903 photometer	24	70	117	1.36
	24	70	117	1.42
1923 photometer/1903 photometer	12	32	59	1.18
	12	60	68	1.20
1923 photovisual/1903 photometer	11	28	55	1.26
	18	86	79	1.28
1935 photovisual/1903 photometer	8	20	39	1.44
	10	42	43	1.54

Since the results that can be represented in Figure 1 are limited to those stars which are contained in *Harvard Annals*, **74**, they are given in Table 2 in a different form, namely, as ratios of the interval between Groups II and III as determined more recently and in 1903. The upper line in each case shows the data used in Figure 1; the lower line, the more complete data.

Numerous measures of stars in the North Polar Sequence were made by Mr. Parkhurst in 1914–1915 with the photometer on both the 12-inch and the 40-inch telescopes, and several series were made

with the 40-inch telescope in 1924. These indicate: (1) that the scale of the photometer on the 12-inch ($9^m.5$ to $12^m.5$) and on the 40-inch ($10^m.5$ to $15^m.4$) agreed in 1914, (2) that in 1924 the scale (evidence from the 40-inch) was effectively more extended, (3) that the photometer scale in 1914 was 15 per cent less extended than the photovisual scale[10] with which the measures were reduced; in 1924 (a less certain determination), perhaps 4 per cent less extended. The last two points thus confirm findings from the Rumford fields.

An attempt to judge where the truth lies might place it in a scale at least 1.25 times more extended than that of the 1903 photometer, thus making the stars in Group III on the average $0^m.28$ brighter than they are given in *Harvard Annals*, **74**. The reasons are as follows: (1) The quality of the 1935 photovisual comparisons make it likely that the indicated extension of scale is excessive; the check is more fragmentary than the others. (2) The measures of the North Polar Sequence make it appear that in 1923 the photometer scale still needs perhaps 4 per cent extension to reach the photovisual scale[10] generally regarded as reliable (1.20 [Table 2] + 4 per cent = 1.25). (3) Unpublished photovisual magnitudes of the North Polar Sequence determined with the grating on the Yerkes reflector suggest that the scale of the latter is about $2\frac{1}{2}$ per cent more extended than the scale of the *Transactions* (1.28–2.5 per cent = 1.25). Undoubtedly current investigations of the photometric scales employed in *Harvard Annals* will be able to throw light on the foregoing suggestion.

MOUNT HOLYOKE COLLEGE
SOUTH HADLEY, MASSACHUSETTS
August 1937

[10] *Trans. I.A.U.*, **1**, 71, 1922.

A STUDY OF THE GLOBULAR CLUSTER MESSIER 92

J. J. NASSAU

ABSTRACT

The distance modulus of Messier 92 is determined from the bright stars and the mean magnitude of 12 cluster-type variables. From the former, $m - M = 14.93$; and from the latter, 14.94 ± 0.01. Two variables not belonging to the cluster are indicated, as well as two other stars with range in variation of 0.25 mag., which are marked as probable variables.

From star counts, the ratio of the minor to the major axis is found to be 0.85, with a position angle of the major axis of 28°. Sensitometer tracings give 14′ for the diameter of the cluster.

The globular cluster Messier 92 (NGC 6341) lies in the constellation Hercules at α 17^h14^m1 (1900), δ $+43°15'$ (1900), some eleven degrees from the great cluster of Hercules (M 13). Its corresponding galactic co-ordinates are l 36° and b $+35°$. The cluster has an integrated photographic magnitude of 5.1[1] and a diameter of 8′.3.[2] It is somewhat elliptical (the ratio of minor to major axis equals 0.8), with a position angle of the major axis of 25°.[2] The classification of the cluster is given as IV by Shapley and Sawyer.[2] Their determination of the distance, 10,860 parsecs,[3] is based mainly on the magnitudes of the bright stars of the cluster. Miss Cannon[4] gives G5? for its spectral class. The color excess of the cluster is given by Stebbins and Whitford[5] as −0.02 mag.

In 1922 Miss Woods announced[6] the discovery of one variable in this cluster, and a brief statement by Guthnick and Prager[7] gives 13 more. In a summary report Hachenberg[8] attributes to the group one W Ursae Majoris type variable and 13 cluster-type variables, one having an amplitude of only 0.15 mag. The eclipsing variable probably does not belong to the cluster.

The observational program for the present investigation was made with the reflector at the Perkins Observatory during the summer of

[1] Sawyer and Shapley, *Harvard Bull.*, No. 848, 1927.

[2] Shapley and Sawyer, *ibid.*, No. 852, 1927.

[3] Shapley and Sawyer, *ibid.*, No. 869, 1929.

[4] *Ibid.*, No. 868, 1929.

[5] *Ap. J.*, **84**, 132, 1936.

[6] *Harvard Bull.*, No. 773, 1922.

[7] *Sitz. d. Preuss, Akad. d. Wiss.*, **27**, 508, 1925.

[8] *Viert. der Astr. Ges.*, **72**, 160, 1937.

1936 and on two nights in June, 1937. The mirror was stopped down to 60 inches to accommodate the existing Newtonian flat. The exposures ranged from six minutes to one hour (one plate only). The majority of the plates were exposed fifteen minutes. Nearly all plates were Eastman 40 and received the same treatment.

TABLE 1

VARIABLE STARS IN M 92

Heliocentric Julian Time	1	2	3	4	5	6	7	8	9	10	11	12	13	14
2428														
362.6410	14.9	15.0	15.3	15.1	14.1	15.0	15.3	15.0	15.1	14.8	15.0	14.0	15.1	15.0
.7813	14.9	.....	14.5	15.2	14.3	14.5	14.5	14.4	14.8	14.8	14.8	14.0	14.8	15.0
.8035	.....	.....	14.6	.....	14.3	14.4	14.5	14.7	15.1	14.9	14.9	14.0	14.8	14.9
363.7111	14.8	.....	15.2	14.8	13.9	15.1	14.9	15.0	15.1	15.1	14.7	14.0	14.8	15.0
.7285	14.8	15.1	15.3	14.6	13.9	15.2	14.9	15.0	15.2	15.2	14.7	14.0	15.0	15.0
366.6861	14.3	.....	14.4	15.1	14.3	14.8	15.2	14.8	15.1	14.9	15.0	14.0	14.8	15.0
371.6623	14.9	14.9	15.2	15.3	14.7	14.8	15.2	14.7	15.1	14.8	14.8	14.0	14.8	15.1
.6755	14.9	15.0	15.3	15.4	14.4	14.9	15.1	14.8	15.1	14.8	14.8	14.0	15.0	15.1
.7102	14.9	.....	15.2	15.5	14.4	14.8	15.1	14.7	15.1	14.6	14.8	14.0	15.0	15.1
374.6769	14.8	15.0	15.2	15.0	14.4	14.8	14.7	14.3	15.1	14.9	15.2	14.0	15.1	15.1
.6880	14.9	15.2	15.3	14.9	14.4	14.8	14.6	14.4	14.9	15.0	15.1	14.0	15.0	15.1
389.6245	14.3	15.4	15.3	15.1	14.8	14.8	14.7	15.0	14.9	15.0	14.8	14.2	14.8	15.0
.7044	14.6	.....	15.3	15.0	14.8	15.0	14.9	14.8	15.1	14.8	15.0	14.1	14.8	14.9
390.6091	14.8	.....	14.7	15.0	14.6	15.2	15.2	14.8	15.2	14.8	14.8	14.0	15.0	15.0
.6883	15.6	.....	15.2	14.8	14.7	14.5	15.2	.....	14.6	14.9	15.0	14.0	14.8	15.0
391.5918	14.5	14.3	15.3	15.0	14.5	14.9	14.5	14.6	15.2	15.1	15.0	14.0	14.8	15.1
.6314	14.6	14.3	15.2	15.2	14.4	14.8	14.5	14.3	15.2	15.0	15.1	14.1	15.0	15.0
392.5904	14.9	15.2	14.8	15.2	14.4	14.6	15.1	15.1	14.6	14.8	15.2	14.2	14.7	15.1
.6223	14.9	15.1	14.8	15.1	14.4	14.7	15.1	15.0	14.7	14.7	14.8	14.2	14.8	15.1
.7147	15.5	.....	15.3	14.6	14.8	14.9	15.3	14.8	15.0	15.0	14.6	14.0	14.7	15.0
.7331	14.9	.....	15.2	14.6	14.4	15.0	15.3	14.8	15.0	.....	14.7	14.0	14.8	15.0
399.6105	14.9	14.8	14.9	14.9	14.3	15.0	15.0	15.0	15.2	14.7	15.0	14.2	15.1	15.0
.6621	14.9	15.2	14.7	15.0	14.0	15.1	15.2	15.0	15.2	14.9	15.1	14.2	15.0	15.0
.6850	14.9	15.3	14.7	15.0	14.1	15.0	15.2	15.0	15.2	14.8	15.0	14.2	15.0	15.0
400.6159	14.7	14.6	15.3	15.3	14.6	14.4	15.3	14.8	15.0	15.0	15.0	14.1	14.8	14.9
.6603	14.8	14.6	15.2	15.3	14.3	14.7	14.9	14.9	15.0	15.2	14.7	14.2	14.8	14.9
.6721	14.6	14.6	15.3	15.3	14.4	14.7	14.6	14.9	15.0	15.1	14.7	14.2	14.9	14.9
401.6221	15.5	15.3	15.2	14.7	14.7	15.0	14.7	15.0	15.0	14.7	14.7	14.1	14.8	14.9
.6999	14.5	15.3	15.2	15.1	14.3	15.1	15.1	14.5	14.5	14.9	14.8	14.0	14.7	15.1
402.6076	14.8	14.8	15.3	15.2	14.7	14.9	15.2	15.0	15.1	15.0	14.8	14.1	15.0	15.1
.6194	14.8	14.8	15.3	15.2	14.5	15.0	15.2	15.0	15.2	15.0	14.8	14.0	15.0	15.1
696.7065	15.3	15.3	15.4	15.4	14.8	15.1	14.6	14.6	15.2	15.0	15.0	14.3	14.8	15.0
.7745	15.3	15.0	15.4	15.4	14.5	14.8	14.7	14.8	15.0	14.8	14.7	14.1	14.8	14.9
.8287	15.3	.....	15.4	15.3	14.2	14.5	14.9	14.8	14.7	14.9	14.8	14.4	14.8	15.0
697.5704	14.7	14.7	14.7	14.6	14.9	14.8	15.2	14.9	15.2	14.9	14.8	14.5	15.0	15.0
.6995	14.7	14.7	14.7	14.5	14.6	15.1	14.7	14.9	15.1	14.9	14.7	14.2	15.1	15.0
.7773	15.2	14.8	14.8	14.5	14.8	15.2	14.9	15.0	15.2	15.1	14.8	14.2	15.0	15.0
.8204	15.2	14.8	15.0	14.8	14.5	15.1	15.0	15.0	15.1	15.1	15.0	14.0	14.8	15.1
Av.	14.89	14.93	15.08	15.02	14.45	14.87	14.95	14.81	15.03	14.92	14.87	14.10	14.89	15.01

THE VARIABLES

The search for variables was made by examining more than 850 stars on six plates; the magnitude of the faintest star examined was 16.60. Estimates of magnitude were made with a graduated scale of images.

The total number of probable variables found was 16, of which 13 yielded a range of variation between 0.4 and 1.2 mag. and were accepted as variables. Star 14 of our list was found to have a range of

PLATE VIII

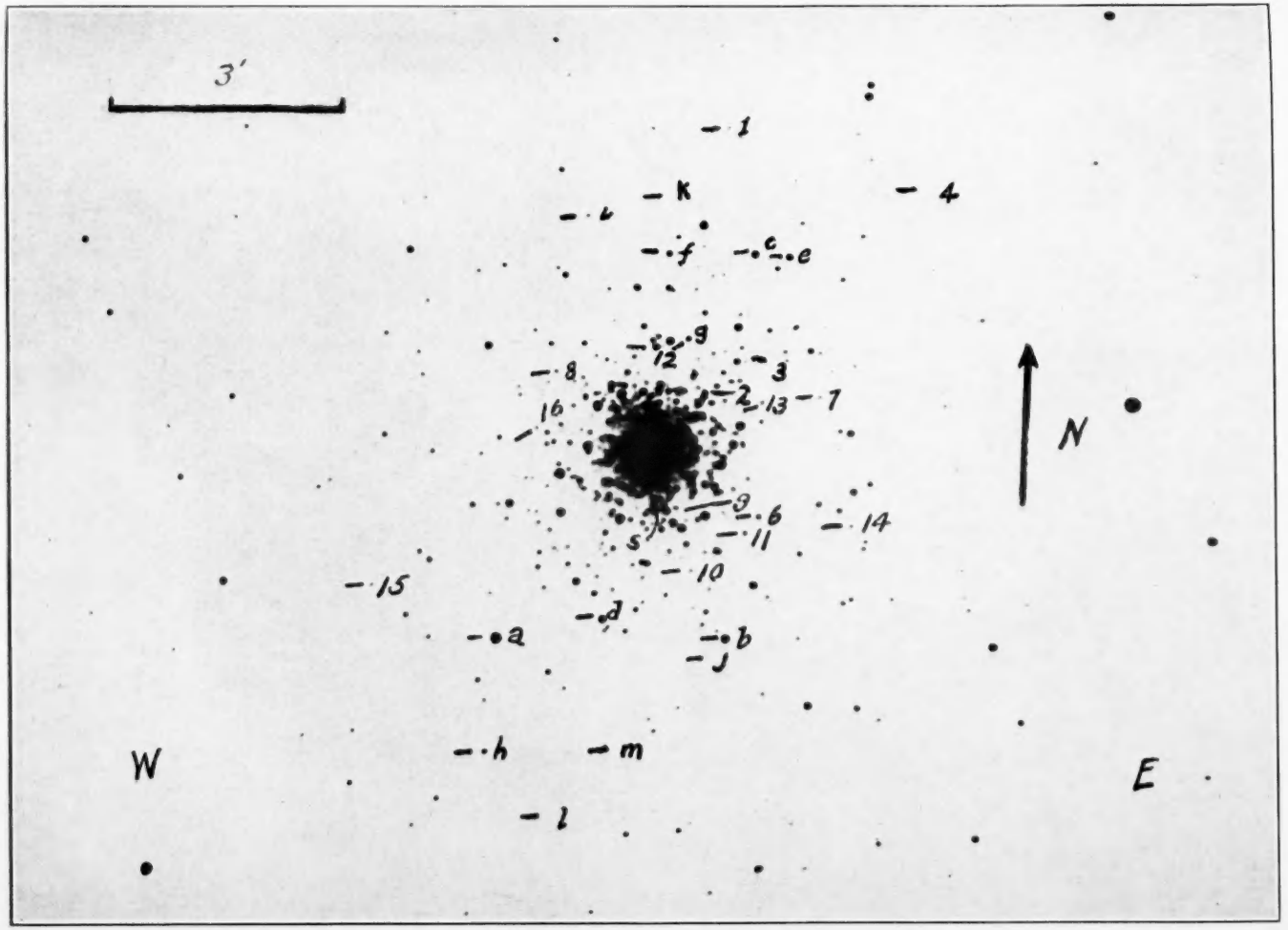

THE GLOBULAR CLUSTER MESSIER 92, MADE FROM AN ENLARGEMENT OF A PLATE TAKEN WITH THE 69-INCH TELESCOPE OF THE PERKINS OBSERVATORY

Comparison stars are lettered *a* to *m;* variables and suspected variables, 1 to 16. Scale: 1 mm = 5″.7

UNIV. OF MICH.

variation of 0.3 mag.; and since Guthnick and Prager[7] listed it as a suspected variable and we have independently found it to be such, it was thought safe to include it among the variables. The two others having a range of 0.25 mag. each were considered as suspected variables. On the foregoing basis Messier 92 may be classified as a cluster relatively poor in variables.

Table 1 gives the individual determination (average of two estimates) of magnitude for the variables on the 38 plates available. The Julian day given is in Greenwich Heliocentric Time of the middle of each exposure.

The last line shows the average magnitude for each star. The averages are about the same, and in all probability these stars are cluster-type variables with the exception of stars 5 and 12. Star 5 is, on the average, 0.49 mag., and star 12 is 0.83 mag., brighter than the average of the 12 variables. These two stars are presumably foreground stars. Judging from the behavior of their variation, we may preclude the probability of their being long-period variables and belonging in the cluster.

TABLE 2

SUSPECTED VARIABLES

Star	Average Magnitude	Range of Variation
15	14.94	0.25
16	14.95	0.25

THE DISTANCE MODULUS

The results obtained for the magnitudes of the bright stars within 7′ of the center of the cluster follow. The region within 25″ of the center of the cluster was not considered.

Magnitude of sixth star	13.42
Magnitude of thirtieth star	13.87
Average magnitude of 25 brightest stars	13.61

To reduce these to the median magnitude of cluster-type variables, we add,[9] respectively, 1.68, 0.95, and 1.30. The weighted mean of the moduli thus obtained (weights 1, 1, and 2, respectively) is

[9] Shapley, *Star Clusters*, p. 160, 1930.

14.93. The average of all the magnitudes of the 12 variables in Table 1 is 14.94 ± 0.01; for reasons given above, stars 5 and 12 were not included.

Assuming a weight of 2 for the modulus of the bright stars and 3 for that of the variables, we obtain for the final modulus 14.94. The distance of Messier 92 as computed from this, adopting zero as the absolute photographic magnitude for cluster-type Cepheids and without regard to the absorption of light in space, is 9730 parsecs. The high galactic latitude of the cluster and its small color excess practically preclude any very great absorption. The effect of general

TABLE 3

SEQUENCE OF STARS IN CLUSTER

Star	Mag.	Star	Mag.	Star	Mag.
a	12.12	f	14.07	k	15.67
b	13.44	g	14.39	l	15.98
c	13.57	h	14.52	m	16.30
d	13.74	i	14.91	.....	.....
e	13.88	j	15.22	.....	.....

absorption should be around 0.1 mag., which would reduce the distance by only 440 parsecs. The distribution of external galaxies in this region supports this assumption.[5]

From the bright stars alone, Shapley[10] obtained for the modulus of M 92, 15.18. Essentially, the discrepancy is due to the zero-point of the determination of magnitudes. In the present discussion a standard magnitude sequence for the cluster was established by taking a series of eleven double-exposure plates, one exposure on the cluster and the other on Selected Area 38.[11] The angular distance between the two fields was found to be 16°. The probable error of the mean adopted magnitude for each star ranged from 0.03 to 0.07 mag., 0.05 being the average. Although the standard stars of the cluster and those of the area were all within 2 cm of the center of the plate, a thorough examination was made for a possible distance correction in the magnitudes. Further examination of this effect was made with the thermoelectric photometer, using seven of the area

[10] *Ibid.*, p. 158, 1930.

[11] Seares, Kapteyn, and van Rhijn, *Mount Wilson Catalogue of Selected Areas*, 1930.

stars which were selected at different distances from the center of the plate. Five plates were thus measured. No correction for the distance of the star image from the center of the plate was found necessary. The magnitudes of the standard stars of the cluster between 13.50 and 15.00 were also checked with the photometer.

DISTRIBUTION OF STARS IN THE CLUSTER

All stars within a radius of 7′ from the center of the cluster (excluding the central portion of 25″ radius) have been used for a distribution study. The magnitude reached was 16.4, or about 0.3 brighter than the faintest recognizable image. The counts are as shown in the accompanying table. The stars as a whole show an

	Magnitude	Number of Stars
I	13.2–14.6	105
II	14.7–15.6	369
III	15.7–16.4	175
Total	.....	649

elliptical distribution with a ratio of minor to major axis equal to 0.85, and with an inclination of 28° for the major axis from north to east. No marked difference in the eccentricity of the ellipse exists between the different magnitude groups.

DENSITOMETER TRACINGS

Densitometer measures on a plate of one-hour exposure were made, using the Stetson photometer[12] with a light beam of 0.7-mm aperture. Readings were taken as far as 25 mm (scale of plate, 1 mm = 0′.45) from the center of the cluster. Near the center the readings were made 2 mm apart, gradually increasing this distance to 5 mm. The light beam was intercepted only by those star images which were within 6 mm of the center of the cluster. The galvanometer readings were reduced to magnitude differences by means of calibration exposures made through a tube sensitometer.

The elliptical form obtained from star counts was hardly noticeable near the dense central region and was definitely absent from regions at greater distance from the center, which is in general agree-

[12] *Ap. J.*, **43**, 253, 1916.

ment with Shapley's results for other clusters.[13] Symmetry having thus been established, values for six diameters 30° apart in position angle have been averaged and are shown in Figure 1. The abscissae are in minutes from the center of the cluster, and the ordinates are differences in magnitude. The means of six readings are represented by the crosses (×). The greatest deviation of individual values from the smooth curve is less than 0.1 mag. The figure shows that the density of the plate is constant from 9′ to 11′ and that from 7′ to 9′

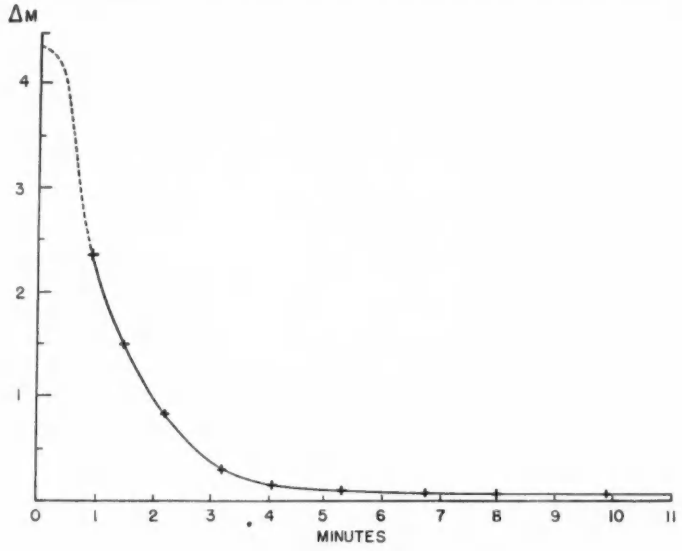

FIG. 1

the density increases linearly. This increase may be due partly to the change of density of the plate. From 7′ to the center of the cluster the change of density due to the cluster is evident. We may conclude that the diameter of the cluster is at least 14′, nearly twice its previous determination.

I wish to express my sincere thanks to Dr. N. T. Bobrovnikoff, director of the Perkins Observatory, for the privilege of the use of the reflector as well as the rest of the facilities of the Observatory.

WARNER AND SWASEY OBSERVATORY
CASE SCHOOL OF APPLIED SCIENCE
November 1937

[13] *Proc. Nat. Acad. Sci.*, **21**, 593, 1935.

REVIEWS

An Introduction to Modern Thermodynamical Principles. By A. R. Ubbelohde. Oxford: Clarendon Press, 1937. Pp. 125. $3.00.

This book is very formal in its attitude toward thermodynamics and appears to be intended for those who wish to be able to handle the methods of thermodynamics to obtain concrete results. No stress whatever is laid on the physical side, though one would have expected that in a book on "modern thermodynamical principles" an approach more in conformity with Carathéodory's axiomatic point of view would have been attempted. As such the book hardly gives any real insight into the fundamentals.

However, the book is useful inasmuch as it includes a variety of modern applications of thermodynamics—e.g., the order-disorder phenomenon discovered by Bragg and Williams in alloys. Particularly interesting is the chapter on the rotational energy of gases, which should be of definite astronomical interest.

S. C.

Elements of Nuclear Physics. By Franco Rasetti. New York: Prentice-Hall, 1936. Pp. xiv+327. Figs. 73 incl. Pls. VIII. $4.50.

This book, belonging to the Prentice-Hall "Physics Series" edited by E. U. Condon, originates as an English edition of a volume *Il Nucleo atomico* (Bologna: Zanichelli, 1936) written for the Italian Consiglio Nazionale delle Ricerche as part of a general treatise on physics, and is intended to give, "in concise form, a survey of the present status of investigation of nuclear phenomena from the experimental as well as the theoretical point of view." This purpose has been achieved, but the requirement of conciseness has prevented the author from any attempt to present the subject, to which his own contributions are well known, in historical order or with complete references, in the text, to early work. The book is of an entirely different character, for example, from the somewhat classical *Radiations from Radioactive Substances* by Rutherford, Chadwick, and Ellis (1930). At that time it was still possible to present a thorough and yet not unwieldy account, in correct historical order, of the subject of nuclear physics. Research has been going on at so rapid a

pace that such a course would now be vastly more difficult, yet the reviewer thinks that the inclusion of a more adequate bibliography, which would not have involved any sacrifice of conciseness in the text of the book, would have made it more useful to physicists.

For astronomers the lack is perhaps not of such great consequence. Read in conjunction with *Radiations from Radioactive Substances*, and with some of the latest papers on nuclear subjects in the physical journals, this book should enable the nonphysicist to become well acquainted with a leading field of contemporary physical investigation, and one that is likely to become of increasing importance to astronomy. Although a knowledge of quantum mechanics is essential to the understanding of those theoretical derivations that are given, usually the results only, like the formula of Klein and Nishina for the scattering of radiation by electrons, are quoted. The nonmathematical reader is thus, so far as most of the theoretical results are concerned, not at any great disadvantage. The clear experimental discussions, combined with the statements of the theoretical results, even if unsupplemented by additional reading, should enable busy astronomers to understand much of nuclear physics, including the problems that nuclear physicists are occupied with, the apparatus they use, and the terms they employ. The final chapter, which astronomers should find of particular interest, is about cosmic radiation. It includes a remarkably concise summary of the evidence, derived from the latitude, azimuthal, altitude, and absorption effects, that bears on the nature of cosmic radiation. The reviewer has no hesitation in recommending this book to astronomers.

T. E. STERNE

HARVARD OBSERVATORY
CAMBRIDGE, MASSACHUSETTS

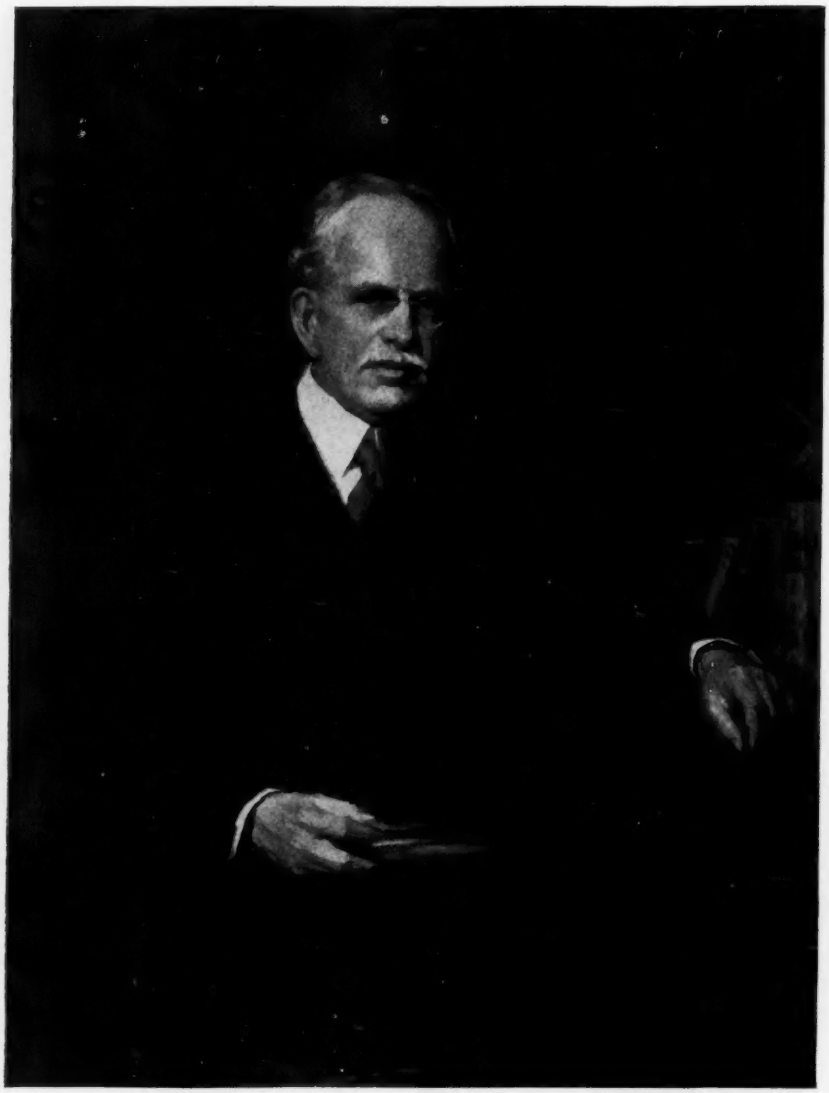

GEORGE ELLERY HALE

1868–1938

From the Portrait by S. Seymour Thomas in the Possession of
the Mount Wilson Observatory

UNIV. OF MICH.